STRUCTURE AND FUNCTION OF SOLUBLE GLYCOPROTEIN G OF VESICULAR STOMATITIS VIRUS

By

RAHUL DAS

A thesis

Submitted to the School of Graduate Studies

in Partial Fulfillment of the Requirement

for the Degree

Master of Science

McMaster University

MASTER OF SCIENCE (2004) **McMaster University**

(Biochemistry) **Hamilton, Ontario**

TITLE: Structure and function of soluble glycoprotein G of vesicular stomatitis virus

AUTHOR: Rahul Das

SUPERVISOR: Professor H.P. Ghosh

NUMBER OF PAGES: XV, 137

Abstract

Membrane fusion plays a crucial role in many biological processes from virus infection to release of neurotransmitters (Hughson 1999). Membrane – bound surface glycoproteins are involved in the fusion process. The enveloped animal virus infection is initiated by interactions between the virus and the cell membrane through the surface glycoproteins called fusion glycoproteins (Eckert and Kim 2001). The fusion glycoproteins are responsible for both receptor binding and membrane fusion activity. The fusion proteins are characterized by a large ectodomain containing fusion peptides, a transmembrane (TM) domain, and a cytoplasimic domain. The viruses can enter cells either at neutral pH or at acidic pH. When exposed to appropriate conditions, the fusion protein undergoes conformational changes, which in turn drives the fusion process.

The fusion glycoproteins can be classified as Class I and Class II fusion proteins (Lescar *et al.* 2001). The Class I fusion proteins are synthesized as a precursor molecule, which then undergoes proteolytic cleavage to generate a mature molecule containing the hydrophobic fusion peptide at the N – terminal. The class II fusion glycoproteins are not synthesized as precursor molecules, and they have internal fusion peptides.

The vesicular stomatitis virus (VSV) glycoprotein G is a class III fusion protein. It has a neutral internal fusion peptide and upon exposure to low pH, the protein undergoes reversible conformational change (Gaudin 2000, Yao *et al.* 2003). A 62kDa soluble ectodomain of VSV G (Gs) has been generated by limited trypsin digestion. The SDS PAGE gel electrophoresis indicates that the trypsin has possibly cleaved near the transmembrane (TM) domain. Liposome binding experiment suggests that Gs can bind to liposomes in a pH dependent manner. Liposome fusion studied by RET assay suggests that the Gs can induce significant amount of hemifusion. However, it failed to induce any content mixing mainly due to considerable amount of membrane leakage activity. This indicates that the binding to the membrane through the TM domain is required for complete membrane fusion. Unlike TBE E soluble ectodomain, Gs can form dimers and trimers at neutral and fusion active pH. Light scattering experiment shows that the aggregation of Gs increases with a decrease in pH. The conformational change with changes in pH was evident from the trypsin sensitivity assay and CD spectroscopy. It was observed that Gs became resistant to trypsin digestion at low pH and α – helicity content of the molecule increased upon lowering the pH. However, the maximum amount of α – helicity was observed at pH 6. The removal of the TM domain also shifts the optimum fusion pH towards more acidic pH in comparison to VSV G. These results indicate that the TM domain is not required for the oligomerization of G protein, but some role has been reserved for the TM domain during membrane fusion.

The CD spectroscopic data also indicated that the G protein undergoes structural rearrangement between pH 7.4 - 6, which could be responsible for the exposure of fusion peptide and subsequent target membrane binding.

ACKNOWLEDGEMENTS

It is the deep sense of gratitude I would like to express and acknowledge the help, assistance and guidance of the following persons without whom the present study would have been impossible.

I am extremely grateful to my supervisor, Dr. H. P. Ghosh for the opportunity to work in his laboratory and supervision.

I am sincerely thankful to my committee members Dr. Richard M. Epand and Dr. Murray Junop for their help and suggestion. I am also grateful to Dr. David Andrews for access to the spectrofluorometer.

I would like to thank Dr. Kakoli Ghosh, Raquel F. Epand and members of Ghosh lab for their help throughout my research.

Also, I would like to thank all my friends for their continuous support and inspiration.

TABLE OF CONTENT

ABSTRACT iv

ACKNOWLEDGEMENTS vii

LIST OF ILLUSTRATIONS xi

LIST OF TABLES xiii

LIST OF ABBREVIATIONS xiv

1. INTRODUCTION 1

1.1 Class I fusion proteins 4

1.1.1 Influenza Virus 4

1.1.2 Crystal structure of Influenza HA in native conformation 8

1.1.3 The Spring – Loaded Model 9

1.1.4 Low pH fusion active structure of HA molecule 10

1.1.5 Proposed mechanism for membrane fusion 11

1.1.6 Other Class I fusion peptide 12

1.2 Class II fusion protein 14

1.2.1 Tick Borne Encephalitis virus (TBE) 14

1.2.2 Vesicular Stomatitis Virus 18

1.2.3 Vesicular stomatitis virus G protein 21

1.2.4 VSV G mediated membrane fusion 23

1.2.5 Conformational state of VSV G 25

2. MATERIAL AND METHODS 38

2.1 Chemicals and Reagents 38

2.2 Enzyme 40

2.3 Multi – Component System 40

2.4 Plasmid , bacterial Strains, Viruses and Cell Line 40

2.5 Growth media and buffers 41

2.6 Antibody 42

2.7 Molecular weight markers 42

2.8 Expression and purification of GST fusion protein 43

2.9 Expression and purification of His-G* 44

2.10 Expression and purification of TEV protease 45

2.11 TEV cleavage 46

2.12 Maintenance of mammalian cell 46

2.13 Virus preparation 47

2.14 G protein purification 48

2.15 Trypsin digestion of VSV G 49

2.16 Digestion of VSV G with other protease 50

2.17 Purification of Gs 50

2.18 Cross linking 51

2.19 SDS – Polyacrylamide gel electrophoresis 51

2.20 Western Blotting 52

2.21 Lipid binding assay 53

2.22 Lipid mixing assay for liposome fusion 54

2.23 Leakage assay 55

2.24 Mixing of aqueous content 56

2.25 Light scattering measurement to determine Gs aggregation 57

2.26 Circular dichroism spectroscopy 58

3. RESULTS 59

3.1 Generation of soluble ectodomain of VSV G 62

3.2 Purification of Gs 73

3.3 Lipid binding assay 80

3.4 Cross linking experiment to determine the oligomeric state of Gs 81

3.5 Aggregation of Gs at low pH 83

3.6 Lipid mixing assay 85

3.7 Leakage assay 94

3.8 Mixing of aqueous content 98

3.9 Change in secondary structure 99

4. DISCUSSION 106

5. REFERANCES 117

6. ADDENDUM 130

6.1 Crystallization of soluble Gs 130

LIST OF ILLUSTRATIONS

Fig.1. Schematic diagram representing different class of fusion glycoprotein 30

Fig.2a. Schematic representation of primary structure of Influenza virus HA 32

Fig.2b. Crystal structure of BHA 32

Fig.2c. The Schematic representation of spring loaded mechanism 32

Fig.3. Crystal structure of TBE E glycoprotein 34

Fig.4a. Schematic representation of Vesicular stomatitis virus 36

Fig.4b. Schematic diagram of primary structure of VSV G glycoprotein 36

Fig.5 SDS polyacrylamide gel of purified fusion protein, GST – G* and His – G* 64

Fig.6a. Generation of soluble ectodomain of VSV G by limited trypsin digestion at pH 7.4 67

Fig.6b. Generation of soluble ectodomain of VSV G by limited trypsin digestion at pH5.4 67

Fig.6c. 8% SDS PAGE of trypsin digestion of VSV at pH 5.4 67

Fig.6d. Trypsin digestion of VSV at pH7.4 on ice 67

Fig.7 SDS polyacrylamide gel electrophoresis of trypsin digested VSV in the presence of 1% octylglucoside 69

Fig.8a. Digestion of VSV with trypsin, chymotrypsin, subtulisin and thermolysin 71

Fig.8b. Digestion of VSV with bromelain 71

Fig.8c Digestion of VSV with pronase 71

Fig.9a. SDS PAGE analysis of purified Gs 74

Fig.9b Sephadex G 200 elution profile of Gs 74

Fig.10 Reversibility of structure of Gs at pH 7.4 76

Fig.11 Liposome binding assay to determine the interaction of G and Gs with lipid vesicles 78

Fig.12 Oligomarization of VSV G and Gs with the crosslinking agent DTSSP at pH 7.4 and pH 5.4 82

Fig.13 Aggregation of Gs at low pH 84

Fig.14a. Lipid mixing by RET assay with VSV 86

Fig.14b. Lipid mixing by RET assay with VSV G 86

Fig.14c. Lipid mixing by RET assay with Gs 86

Fig.15a. Determination of optimum pH of liposome fusion for VSV G 88

Fig.15b. Determination of optimum pH of liposome fusion for Gs 88

Fig.16a Effect of PEG on lipid mixing induced by VSV G 91

Fig.16b. Effect of PEG on lipid mixing induced by Gs 91

Fig.17a. Vesicle leakage induced by VSV G 95

Fig.17b. Vesicle leakage induced by Gs 95

Fig.18 Mixing of aqueous content 97

Fig.19 Trypsin sensitivity assay to determine the structural change of Gs protein at acidic pH 102

Fig.20a. Effect of pH on circular dichroism spectra of Gs in presence of liposome 103

Fig.20b. Effect of pH on circular dichroism spectra of Gs in absence of liposome 103

Fig.21 Effect of pH on α – helix content of Gs protein 105

LIST OF TABLES

Table I. Summary of crystal trial using Sigma Membrane Kit 132

Table II. Summary of crystal trial using Hampton 2 Kit 134

Table III. Summary of crystal trial using Hampton 1 Kit 136

LIST OF ABBREVIATIONS

ANTS	Aminonapthalenetrisulfonic acid
BHA	Bromelain treated hemagglutinin
CD	Circular Dichroism
CS	Calf Serum
DMSO	Dimethyl sulfoxide
DPX	p – xylene bis (pyridinium)bromide
DTT	Dithiothreitol
EDTA	Ethylenediaminetetra acetic acid
FBS	Fetal bovine serum
G*	Cloned ectodomain of G
Gs	Soluble VSV G protein
GSH	Reduced Glutathione
GST	Glutathione – S - transferace
HA	Hemagglutinin
HEPES	N-2-hydroxyethylpiperazine-N'-2-ethanesulfonic acid
HGD	High glucose Dulbecco's medium
HIV	Human immunodeficiency virus
IPTG	Isopropyl β, D-thiogalactopyroside
MES	2-[N-Morpholino]-ethanesulfonic acid
NBD	N[7-nitrobenz-oxa-1,3-diazol-4-yl]-dioleoyl
PC	Phosphatidylcholine
PE	phosphatidylethanolamine
PEG	Poly(ethylene glycol)
PBS	Phosphate buffered saline
PMSF	Phenylmethylsulfonyl fluoride
PS	Phosphatidylserine

1. INTRODUCTION

Membrane fusion is a vital step in many complex biological processes. The cell surface glycoprotein is the only protein involved in membrane fusion. Surface glycoproteins are responsible for unfavorable mergering of two membrane bilayers. Therefore, the study of structure and function relationship of fusion glycoproteins is important to understand the cellular fusion mechanism, which will ultimately answer many unsolved questions and may lead to the development of new drugs.

Enveloped animal virus infections are initiated by interactions between the host and the virus, followed by membrane fusion. The virus surface glycoproteins are responsible for both receptor binding and membrane fusion activity. Predominantly, all viral surface glycoproteins share some common characteristics (Hernandez *et al.*1996). These proteins are integral membrane glycoproteins containing a short transmembrane domain and a cytoplasmic domain. The portion of the protein that remains external to the viral membrane is called the ectodomain. The ectodomain is responsible for receptor binding and membrane fusion activity (Fig 1). Most viral fusion glycoproteins have short hydrophobic sequences, which interact with the target membrane during fusion, and are called fusion peptides (Eckert and Kim 2001). Interaction between the fusion peptide and the membrane during fusion have been proven by mutation,

antibody inhibition studies and hydrophobic photolabeling experiments (Zhang and Ghosh 1994, Harter *et al.*1988, 1989, Durrer *et al.*1995, Skehel *et al.*1982, Gaudin *et al.*1995, Gaudin 2000).

A viral infection starts when the surface glycoprotein binds to the cell surface receptor (Eckert and Kim 2001). Following binding to the receptor, the virus can enter the host either by fusion with the cell surface membrane at neutral pH or by endocytosis through clathrin-coated pits and fusion with the endosomal membrane at the acidic pH of the endosome (Hernandez *et al.*1996). Viruses that interact and fuse with the host cell at neutral pH are retroviruses, paramyxoviruses, herpesviruses and poxviruses. The viruses that require acidic pH for fusion are orthomyxoviruses, togaviruses, rhabdoviruses and flaviviruses.

Most of viral fusion glycoprotein exists in metastable conformation at neutral pH (Gaudin 2000). After binding to the cell surface receptor or exposure to low pH, they undergo a series of conformational changes, which triggers the fusion process (White1992, Kielian 1995, Wiley and Skehel 1987 and Wiley 1998). The conformational change exposes the fusion peptide, which interacts with the target membrane and brings the opposing membranes close enough to each other to fuse.

Surface glycoproteins of animal viruses can also be classified into two classes (class I and class II), depending on the characteristics of the fusion peptide (Lescar *et al.*2001). The class I fusion proteins are synthesized as precursor molecules, which undergo proteolytic cleavage to produce the mature fusion protein. They have a hydrophobic fusion peptide at the N – terminal of the fusion glycoprotein. Orthomyxoviruses (e.g., the influenza virus), retroviruses (HIV), and paramyxoviruses (sendai virus) belong to this class (Fig 1). The class II fusion glycoproteins do not undergo any proteolytic maturation and they have internal fusion peptides. Viruses belonging to this class include togaviruses (Semliki forest virus), flaviviruses (TBE), and rhabdoviruses (VSV). However, recently VSV G protein has been classified as class III fusion protein (Yao *et al.* 2003, Gaudin 2000)

Although all the fusion glycoproteins from different viruses serve the same purpose, there is a distinctive difference in structure and mechanism of fusion between the two classes of fusion peptides (Heinz and Allison 2000). The fusion glycoproteins of orthomyxoviruses, paramyxoviruses and retroviruses show similar structural characteristics and they employ coiled – coil mechanisms for membrane fusion (Eckert and Kim 2001, Bullough *et al.*1994, Han *et al.*2001, Wilson *et al.*1981, Crennell *et al.*2000). In contrast envelope glycoprotein of flaviviruses and alphaviruses share similar structural hallmarks (Lescar *et*

*al.*2001, Rey *et al.*1995). The β - barrel structure is the predominating structure present in the class II fusion peptides.

1.1 Class I fusion proteins

Orthomyxoviruses, retroviruses and paramyxoviruses have class I fusion glycoproteins. They have a hydrophobic fusion peptide at the N – terminal, which is generated by proteolytic maturation of precursor molecules. A spring-loaded mechanism involving a coiled – coil structure has been proposed for pH dependent and independent membrane fusion (Eckert and Kim 2001, Crennell *et al.* 2000). The class I fusion peptide, which has been extensively studied, is the influenza virus hemagglutinin (HA) surface glycoprotein.

1.1.1 Influenza Virus

The influenza virus is a member of the orthomyxovirus family. It has a segmented genome of eight negative stranded RNA (Krug R.M 1989). The viral RNA codes for three P proteins (PB_2, PB_1 and PA), hemagglutinin, nucleoprotein, matrix protein (M_1 and M_2 protein), neuraminidase, NS_1 and NS_2. The PB_1, PB_2 and PA proteins together form a complex that plays a variety of enzymatic roles during viral transcription. The viral neuraminidase is an integral membrane protein, which exists as a homotrimer. This protein acts as a major antigenic determinant

and also removes the sialic acid moiety from the glycoprotein. There are two matrix proteins (M_1 and M_2) required for the structural stability of the virus. The two other proteins (NS_1 and NS_2) are found only in infected cells. Although the exact roles of these proteins are unknown, it has been proposed that NS1 might play an important role in shutting down the host protein synthesis machinery. The viral hemagglutinin (HA) is the major viral spike protein, which has both receptor binding and membrane fusion activity. HA is the major antigenic component of the virus against which neutralizing antibodies are produced.

The influenza virus hemagglutinin fusion glycoprotein is synthesized as the precursor molecule HA_0 (Eckert and Kim 2001), which then undergoes proteolytic cleavage to form two subunits, a 221 amino acid residue transmembrane subunit (HA_2) and a 328 amino acid residue surface subunit (HA_1) (Fig 2). The HA_2 is attached to the membrane through a short hydrophobic residue near its C terminus, which also acts as a stop transfer signal during the translocation of HA across the membrane (Krug 1989). The hydrophobic amino acid signal is cleaved after the insertion of the HA protein into the membrane. The HA_2 subunit has the predicted fusion peptide at its N – terminal. The two subunits HA_1 and HA_2 are linked by a disulphide bond between the C14 residue of HA_1 and the C137 residue of HA_2 (Fig2). The HA_1 subunit is responsible for the recognition and binding to specific cell surface receptors (Hernandez *et al.*1996). In the case of influenza virus, sailic acid acts as the receptor molecule. HA protein exists as a

homotrimer (White 1992, Wilson *et al.*1981). Proteolytic cleavage of the precursor HA molecule (HA_0) results in a metastable conformation, which undergoes a dramatic conformational change upon exposure to low pH to a thermodynamically more stable form (Carr *et al.*1997, Durrer *et al.*1996, Skehel *et al.*1982). Therefore, influenza virus HA can exist in two significantly different conformations, a metastable fusion inactive native form and low pH form that is thermodynamically more stable. The energy released during the irreversible structural change from the metastable conformation to the low pH stable conformation compensates the energetically unfavorable process of membrane fusion (Ruigrok *et al.*1986, Carr *et al.*1997, Gaudin 2000). The evidence of conformational change comes from the fact that, upon exposure to low pH, HA aggregates and can bind to liposomes. Hydrophobicity of the protein is also increased under these conditions (Skehel *et al.*1982). Change in proteolytic sensitivity with change in pH and mutagenesis studies support the existence of the two different conformations (Carr *et al.*1997, Korte *et al.* 2001). The HA fusion protein is resistant to proteinase K digestion at neutral pH, in contrast the protein is digested by proteinase K at fusion active pH. The mutation at E4G, E11G, G1E, E11V and E15V effects the membrane fusion ability of the HA fusion protein (Gething *et al.* 1986, Qiao *et al.* 1999 and Korte *et al.* 2001). Change in antigenicity with change in pH also indicates that structural rearrangement occurs at low pH (Wharton *et al.* 1987, Barbey-Martin *et al.* 2002).

However, same structural conformation (fusion active structure) for HA can also be triggered by exposing the HA fusion protein to high temperatures or denaturants like urea (Ruigrok *et al.*1986, Carr *et al.*1997). The temperature or denaturant induced conformational change is also coincident with the membrane fusion. It has been proposed that the native structure of HA is trapped in a metastable state and the fusion active conformation can be activated by destabilizing the native structure (Ruigrok *et al.*1986, Carr *et al.*1997).

Identification of the N - terminal amino acids in the HA_2 protein as fusion peptides has been confirmed by mutational experiments (Gething *et al.* 1986, Qiao *et al.* 1999 and Korte *et al.* 2001), although the most direct evidence was provided by hydrophobic photolabeling experiments (Harter *et al.*1988, 1989, Stegmann *et al.*1991, Tsurudome *et al.*1992, and Durrer *et al.*1996). This technique is based on the principle that depends upon the ability of photoactiveable lipids to covalently modify those polypeptide segments of proteins that directly contact the membrane hydrophobic core. The experiments revealed that liposome fusion was mediated by the first 20 amino acids near the N – terminal of the HA_2 molecule. It was proposed that upon interacting with the membrane, the fusion peptide adopts the structure of a sided α - helix that may penetrate only a single leaflet of the membrane (Han *et al.*2001).

1.1.2 Crystal structure of Influenza HA in native conformation

In 1981, Wilson *et al.* were the first to resolve the high resolution structure of the influenza virus HA fusion peptide (Fig 2). The structure was resolved by crystallizing the bromelain cleaved soluble HA ectodomain called BHA. The BHA lacks the hydrophobic region that anchors HA to the viral membrane. The HA trimeric structure is an elongated cylinder of 135Å long with a radius of 15 to 45 Å (Fig2). The structure of hemagglutinin can be divided into two regions. One includes both HA_2 and HA_1, which form a 76 Å triple – stranded α – helical coiled – coil structure that extends from the membrane surface. At the top of the structure are three exposed globular head domains consisting of HA_1, and it acts as a framework for the sialic acid receptor binding site (Wilson *et al.*1981). The fusion peptide which is at the amino terminal region of HA_2 remains buried in the native structure. The hemagglutinin trimeric subunit is stabilized by the triple stranded coiled – coil structure formed by the fibrous region (Wilson *et al.*1981). There are many inter- and intra-chain salt bridges that also contribute to the stability of the coiled – coil structure. The carbohydrate side chains are located all along the membrane surface rather than at the distal end. Six oligosaccharides are attached to HA_1 and one oligosaccharide is attached to HA_2 (Wiley and Skehel 1987).

1.1.3 The Spring – Loaded Model

It took nearly a decade to propose a possible fusion mechanism after solving the crystal structure of BHA by Wilson *et al.* in 1981. Studies done with synthetic fusion peptides led to the proposition of a spring – loaded mechanism (Carr and Kim 1993, Carr *et al.*1997). Computational analysis showed that a region between 54 – 81 in the HA_2 subunit has the potential to form a coiled – coil structure, whereas in the native crystal structure of BHA this region forms an extended loop conformation. However, biophysical experiments (circular dichroism spectroscopy) with synthetic fusion peptides corresponding to this region (residue 54-89) confirmed that it forms a coiled – coil in solution (Carr and Kim 1993). Therefore, it was proposed that during conformational change from native structure to fusion active structure at low pH, the residue between 55 – 75 changes from a loop to a coiled – coil structure (Eckert and Kim 2001). These structural rearrangements propel the fusion peptide to the opposing end of the molecule, which allows it to interact with the target membrane (Fig 2). The existence of such a fusion mechanism was confirmed when the fusion active structure of HA was solved in 1994 by X-ray crystallography (Bullough *et al.* in 1994).

1.1.4 Low pH fusion active structure of HA molecule

Influenza virus hemagglutinin is the only fusion peptide for which both the neutral and low pH structures have been reported. The low pH structure was described by Bullough *et al.* in 1994. The structure was solved by crystallization of the soluble HA fragment $TBHA_2$. The $TBHA_2$ was obtained by successive proteolytic cleavage of BHA_2 at pH 5 with trypsin and thermolysin respectively. The $TBHA_2$ monomer contains the whole HA_1 fragment and 38 – 175 residue of the HA_2 fragment, which does not include the hydrophobic fusion peptide region.

The $TBHA_2$ trimer is formed by 100 Å long three stranded α– helical coiled – coil structure with one α – helix contributed from each monomer. A β - hairpin formed by HA_2 131 – 140 residues along with 11-16 residues from HA_1 forms an antiparallel β – sheet (Bullough *et al.*1994). The HA_1 and HA_2 subunits are connected by a disulphide bond between the C14 residue from HA_1 to the C137 residue of HA_2. A comparison of BHA and TBHA structure reveals that the molecule undergoes a dramatic conformational change at a lower pH, which results in a thermodynamically more stable conformation. The central triple stranded α – helical coiled – coil structure of BHA has the same structure as that of TBHA. The N – terminal of the HA_2 fragment was displaced by 100 Å, which is required to propel the fusion peptide by 150 Å. The conformational change from

BHA to TBHA is very extensive that most interactions between HA_1 and HA_2 present in BHA are no longer possible in TBHA (Bullough *et al.*1994).

1.1.5 Proposed mechanism for membrane fusion

In 1996, Hernandez *et al.* first came up with a probable mechanism for membrane fusion. They proposed that there are five steps involved during membrane fusion, and suggested that two conformational intermediates might exist between the native HA and the final low pH conformation.

- The first step involves the pH dependent conformational change. In this step, HA protein undergoes structural rearrangement, which enables the fusion peptide to interact with the target membrane (Bullough *et al.*1994, Carr and Kim 1993, Carr *et al.*1997).
- In the second step, clustering of the HA trimer occurs. This step accounts for the lag phase before the onset of membrane fusion.
- The third step leads to the formation of hemifusion. Here fusion peptides reach a transition state. The fusion peptide, which is attached to both the target membrane and the viral membrane, bends radially outward from the fusion site (Hernandez *et al.*1996). This in turn forces the interacting bilayer to bend, resulting in a hemifusion intermediate.
- The HA trimer in the fourth step imposes tension on the hemifusion diaphragm, which causes the breakage of the hemifusion diaphragm. It

was suggested that the tension is the major driving force in the formation of fusion pores.

- In the last step, HA reaches the stable low fusion conformation, which also results in the irreversible opening of the fusion pores.

1.1.6 Other Class I fusion peptides

Another class I fusion glycoprotein whose structure is known is the human immunodeficiency virus (HIV) envelope glycoprotein (Env). HIV is a member of the retrovirus family. The Env protein is the only glycoprotein of HIV responsible for receptor binding and membrane fusion activity (Eckert and Kim 2001). Like all other class I fusion peptides Env is synthesized as a polyprotein precursor molecule, gp160 (molecular weight of the precursor is 160 kDa), which is then proteolyticaly cleaved to generate a surface subunit, gp 120, and a transmembrane subunit, gp 41 (Freed and Martin 1995). The two subunits remain associated by noncovalent interaction. The intracellular disulphide bonds formed between a series of conserved cystine residues are required for the structural stability (Freed and Martin 1995). The gp120 subunit has receptor binding activity and gp41 has membrane fusion activity (Freed *et al.*1990).

Unlike the influenza virus, HIV induces membrane fusion at neutral pH. The HIV infection is initiated by the binding of gp120 to the cell surface receptor molecule CD4 (Freed and Martin 1995). However involvement of other co – receptors has been reported for the efficient infection of HIV (Hernendez *et al.*1996). Binding of gp120 to the receptor induces a series of conformational changes in both gp120 and gp41. The gp120 exposes the V3 loop required for the interaction with the co – receptor, which ultimately results in shedding of gp120 from the viral surface (Moore *et al.*1990, Chan *et al.*1997). Changes in gp41 antibody binding and protease sensitivity suggest that gp120 and CD4 interaction also induce conformational change in gp41. This conformational change eventually exposes the hydrophobic fusion peptide essential for membrane fusion (Freed and Martin 1995).

The structural information about gp41 was obtained from two stable soluble complexes of N51 and C43 generated by limited proteolysis of gp41 (Lu *et al.*1995). Biophysical experiments suggest that N51 and C43 form a trimeric coiled – coil structure, where C43 is oriented in an anti-parallel manner to the outside of the N45 coiled – coil core (Eckert and Kim 2001). The crystal structure of the thermodynamically stable fragment N36 and C34 of gp41 was solved by Chan *et al.* in 1997. N36 and C34 form a six - helix bundle (Chan *et al.*1997). The central coiled – coil is formed by N36, which wrap around by antiparallel C34

helices. The N36/C34 complex has a structural similarity to the low pH induced conformation of the influenza HA_2 subunit.

1.2 Class II fusion protein

The class II fusion proteins are those which do not undergo any proteolytic maturation, and they have internal fusion peptides (Lescar *et al.*2001). Togaviruses (SFV) and flaviviruses (TBE) belong to this class. TBE and SFV are the only class II fusion peptides whose structure has been reported (Rey *et al.*1995 and Lescar *et al.*2001).

1.2.1 Tick - Borne Encephalitis virus (TBE)

Tick - borne encephalitis virus (TBE) belongs to the family of Flaviviridae. More than 50% of the flaviviruses are associated with human diseases, the most common being the Dengue (DEN) virus, yellow fever (YF) virus, Japanese encephalitis (JE) virus, and TBE virus (Heinz and Allison 2000). The TBE virus genome has a positive – stranded RNA with a single long open reading frame. Viral RNA codes for three proteins: a capsid protein (C), an integral membrane protein (E), and a membrane protein (M). The TBE major surface glycoprotein has both receptor binding and membrane fusion activity (Stiansy *et al.*2002). Like

all other class II fusion peptides, the TBE E protein has an internal hydrophobic fusion peptide. After binding to the cell surface receptor the virus is internalized by endocytosis through a clathrin coated pit, which then fuses with the endosomal membrane at acidic pH. Upon exposure to low pH, the TBE E protein undergoes an irreversible conformational change (Heinz and Allison 2001). This protein exists as a dimer at neutral pH, which then undergoes an irreversible trimerization at fusion active pH. The irreversible dimer to trimer transition leads to the fact that TBE E glycoprotein is metastable at neutral pH, and lowering the pH helps the protein to reach a more stable conformation. Fluorescence spectroscopic analysis suggests that low pH conformation is more stable to thermal shock in comparison to that of neutral pH structure (Stiasny *et al.*2001). The TBE E protein - mediated membrane fusion is extremely fast with no measurable lag phase (Heinz and Allison 2000).

High resolution structure of the TBE E protein was first reported by Rey *et al.*1995 (Fig3). The crystal was obtained from soluble ectodomain (Es) released after restricted trypsin digestion (Heinz *et al.*1991). The soluble ectodomain of E protein folds into three domains:

- β – barrel (Domain I)
- An elongated dimerization region (Domain II).
- C – terminal immunoglobulin - like module (Domain III).

The Es homodimer is arranged in a head to tail and the dimers are oriented parallel to the membrane. Domain I is at the center of the monomer, consisting of eight up and down β – barrels. The axis of the barrel is parallel to the viral membrane. The two β – sheets facing each other result in a hydrophobic interior (Rey *et al.*1995). This domain contains two disulphide bridges. Domain II which is the dimerisation domain, contains extended finger - like structure. The cd loop (residue 98 – 113), located at the tip of the domain II, is made of glycine rich hydrophobic sequences, which are important for the fusogenic activity of the virus (Rey *et al.*1995). The tightly folded conformation of the cd loop is stabilized by the disulphide links. The interaction between domain II, domain I, and domain III stabilizes the dimer structure. The dimer interaction is further stabilized by oligosaccharides attached to domain I. Domain III has IgG like folding, which is attached to domain II through a 15 residue anchor and a disulphide bond. At low pH, the TBE E protein undergoes conformational change, which induces dimer to trimer transition. To accomplish this, either dimer interface must come apart (Rey *et al.* 1995). Antibody binding assay suggest that a substantial structural change occurs at low pH. Domain II stabilized by disulphide bonds, also shows altered antigenicity at low pH, indicating that the molecule swings outward to expose the fusion peptide.

It has been proposed that the dimer – trimer transition occurs in two steps (Stiasny *et al.*1996). The first step is the reversible protonation dependent

monomer formation followed by an irreversible trimerization step. It has been suggested that interaction between E and the membrane occurs after the dissociation step but before the trimerization step. The Es protein cannot form trimers at fusion active pH but dissociates reversibly to a monomer (Allison *et al.*1999). The secondary structure prediction showed that the amino acid sequence between 401 and 413 has the potential to form an α – helix structure (Stiasny *et al.*1996). It was proposed that the stem anchor region (401-413) might be essential for homotrimer formation (Allison *et al.*1999, Stiasny *et al.*1996). However, it has been reported that the Es protein converts irreversibly to a homotrimer in the presence of liposomes (Stiasny *et al.*2002). Therefore, it has been suggested that either the stem anchor region or the membrane is required to facilitate stable trimer formation.

Another class II fusion peptide whose structure has been described is the SFV E_1 glycoprotein (Lescar *et al.*2001). SFV belongs to the family Togaviridae. The SFV has a positive – stranded RNA, which enters the cell through endocytosis followed by fusion with the endosomal membrane at acidic pH (Gibbons and Kielian 2002). The viral membrane fusion glycoprotein is a heterodimer of E_1 and E_2. The E_2 has receptor-binding activity and E_1 has membrane-fusion activity. Occasionally, a third protein, E_3, also binds to the E_1 and E_2 heterodimer by non-covalent interaction (Hernandez *et al.*1996). The crystal structure of the SFV – glycoprotein was reported by Lescar *et al.* in 2001. The crystal was obtained by

crystallizing the soluble ectodomain released after subtilisin digestion of the glycoprotein (Wengler *et al.*1999). The crystal structure of the SFV surface glycoprotein is very similar to that of the TBE E protein, despite the absence of detectable sequence homology. Like the TBE E glycoprotein, the SFV glycoprotein has three domains: domain I, domain II, and domain III (Lescar *et al.*2001). Each domain has a secondary structure consisting almost exclusively of antiparallel β –sheets. The central domain is domain I, which has eight stranded β – sheets. The fusion peptide is located at the tip of domain II forming a loop-like structure, which is stabilized by disulphide bonds. This loop plays a critical role in stabilizing the E_1/E_2 heterodimer. Domain II has an IgG-like topology containing an antiparallel β – barrel, stabilized by three disulphide bridges. The E_1 dimer has a head to tail interaction with the fusion peptide loop, which is buried at the dimer interface. When exposed to low pH, the E_1 protein undergoes an irreversible conformational change along with the formation of an E_1 homotrimer (Gibbons *et al.*2000, Gibbons and Kielian 2002).

1.2.2 Vesicular Stomatitis Virus

The vesicular stomatitis virus (VSV) belongs to the family Rhabdoviridae (Coll 1995). Rhabdoviruses have been classified into two genera, the lyssaviruses and the vesiculoviruses. Rhabdoviruses are widely found in plants and animals (Wagner 1987). In plants, they cause widespread disease, transmitted mainly

through arthropods. In animals, they generally infect insects and arthropods. It has been reported that VSV can also infect cattle. In humans it causes influenza-like symptoms that are rarely fatal and mostly spread through laboratory work and infected animals. The lyssaviruses, like the rabies virus, cause fatal diseases of the central nervous system. Other rhabdoviruses, such as the salmonid rhabdovirus and VSHV, are responsible for huge economical losses, particularly to fish hatcheries.

The term rhabdovirus is derived from the Greek word rhabdos meaning rod-shaped. The infectious virion is bullet shaped, round at one end and flat at the other (Fig. 4) (Wagner 1987). VSV contains a tightly coiled nucleocapsid that is surrounded by a lipid envelope from which spikes project out. The spike proteins can easily be removed by protease treatment. VSV is composed of approximately 74% protein, 20% lipids, 3% carbohydrates, and 3% RNA. The lipid envelope is derived from the host membrane (Wagner 1987).

The vesicular stomatitis virus contains a 11kb negative-strand RNA that codes for 5 – 6 proteins (Coll 1995). VSV possesses two membrane proteins, the 67 kDa integral membrane glycoprotein (G) and the 20 kDa matrix protein (M). VSV capsid protein is composed of three proteins, NS (P), N, and L proteins 33 kDa, 50 kDa, and 200 kDa in size, respectively (Coll 1995). These three proteins, along with the viral RNA, form the nucleocapsid. The N protein is the major

nucleocapsid protein, which tightly complexes with viral RNA. The other nucleocapsid proteins are the RNA-dependent RNA polymerase L and NS (P) proteins, which are highly phosphorylated and required for the RNA polymerase activity. The phosphorylation of the NS (P) protein is carried out by host cell protein kinases. Dissociation of NS (P) and L proteins results in the loss of transcriptase activity and infectivity. The matrix protein is the most abundant protein present in the virus and is highly basic and nonglycosylated. The M protein acts as glue that binds to both the nuclecapsid and the viral membrane. The M protein is also required for stabilization of the G trimer (Wagner 1987).

The life cycle of VSV can be broadly divided into eight events (Wagner 1987). Although each step is not the precursor of successive steps, for simplicity they can be arranged in the order: adsorption, penetration, uncoating, transcription, translation, replication, assembly, and budding. After binding to the cell surface receptor, the virus enters the cell by endocytosis through the clathrin-coated pit. At the acidic pH of the endosome, the virus fuses with the endosomal membrane. The membrane fusion uncoats the virus and permits viral transcription to occur. The N – protein encapsidated genomic RNA serves as a template, and NS (P) and L proteins act as RNA-dependent RNA polymerases, which initiate the transcription for all five monocistronic mRNA in the order of 3' – N – NS – M – G – L – 5' (Ball and White 1976). Translation of mRNA starts immediately after transcription. The proteins then undergo posttranslational modifications like

glycosylation and phosphorylation. The VSV G protein is glycosylated in the ER – Golgi complex, which then migrates to the plasma membrane for insertion into the membrane (Kreis and Lodish 1986, Toneguzzo and Ghosh 1978, Irving *et al* 1979). The viral replication is also coupled with translation. It has been suggested that VSV polymerase serves the dual role of mRNA transcription and replication of the entire VSV genome (Kim *et al.* 2002, Wagner and Rose 1996, Wagner 1987). Viral assembly and budding occurs independently of other viral processes. The newly synthesized N, L, and NS (P) protein binds tightly to the newly synthesized RNA to form the ribonucleocapsid. The M protein has the affinity for binding to the ribonucleocapsid to generate the tightly coiled ribonucleocapsid structure of rhabdoviruses. The matrix protein, which can also interact with phospholipids and G proteins, initiates the budding of the fully formed infectious virion (Schnell *et al.* 1998, Capone and Ghosh 1984, Capone *et al.* 1982).

1.2.3 Vesicular stomatitis virus G protein

Like all other envelope viruses, VSV infection is mediated through its surface glycoprotein G. The 67 kDa VSV G glycoprotein is an integral membrane protein of 495 amino acids. The protein is derived from a nonglycosylated precursor (511 a.a) molecule, from which 16 NH_2 – terminal amino acids are removed and inserted into the membrane (Irving *et al.*1979). The majority of this protein is

located outside the viral membrane that constitutes the ectodomain (Coll 1995). The VSV G protein is responsible for the initial binding of the virus to the host membrane receptor and membrane fusion. VSV does not show any specific requirement for any phospholipids. However, phosphatidylserine (PS) has been found to facilitate the initial binding of the virus particle to the lipid membrane (Carneiro *et al.* 2002, Schlegel *et al.*1983). The VSV G protein has two N – linked glycosylations at Asn 174 and Asn 138 (Bailey *et al.*1989). VSV G bears an internal fusion peptide (Zhang and Ghosh 1994, Fredericksen and Whitt 1996, Durrer *et al.* 1995, Gaudin 2000). The primary structure of the G protein shows a constant region (CR) (a.a 82 – 100), a putative fusion peptide region (H2) (a.a 117 – 137) (Fredericksen and Whitt 1996, Li *et al.*1993, Zhang and Ghosh 1994), a conformation sensitive region (H10/ A4) (a.a 395 – 410) (Shokralla *et al.* 1998), a single transmembrane domain, and a short cytoplasmic domain (Fig 4b). After binding to the cell surface receptor, the virus is internalized by endocytosis through the clathrin coated pits, which then fuses with the endosomal membrane at the acidic pH of the endosome. The optimum fusion pH for VSV is between 5.8 and 5.4 (White *et al.*1981). Upon exposure to low pH, the VSV G protein undergoes a reversible conformational change (Crimmins *et al.* 1982, Blumenthal *et al. 1987,* Puri *et al.* 1988, Gaudin 2000). Reversibility of the structure suggests that the G protein does not exist in a metastable conformation (Yao *et al.*2003). The Trp fluorescence and CD spectroscopy suggests that the G protein is equally thermostable at neutral and acidic pH. The VSV G protein could not

induce membrane fusion when the structure of G protein was destabilized with heat or urea, which indicates that the VSV G induced fusion mechanism is different from the fusion mechanism of fusion proteins involving a coiled – coil motif (Yao *et al.* 2003). VSV G protein exists in dynamic equilibrium between a monomer and a trimer at neutral and fusion active pH, both *in vitro* after detergent solubilization and in membrane anchored form (Crise *et al.*1989, Lyles *et al.*1990, Zagouras and Rose 1993). Chemical cross-linking suggests that the protein exist as monomer and trimer at neutral and acidic pH. However, sedimentation analysis suggests that the stability of the trimer increases at fusion active pH (Doms *et al.* 1987, Crimmins *et al.* 1983).

1.2.4 VSV G mediated membrane fusion

The VSV glycoprotein G was initially classified as class II fusion protein. However, reversibility of the structure at acidic pH and differences with other fusion proteins suggests that VSV G could be classified as class III fusion protein (Crimmins *et al.*1982, Blumenthal *et al.* 1987, Puri *et al.* 1988, Gaudin 2000, Yao *et al.* 2003). It has an internal fusion peptide. Primary sequence analysis of the rhabdovirus glycoprotein does not show any hydrophobic amino acid residues at the fusion peptide region or any homologies with other known class II fusion peptides (Gaudin 2000). It has been suggested that for VSV G, the conserved uncharged amino acid sequence (117 – 136) could play the role of a fusion

peptide (Oshnishi *et al.* 1988). Site directed mutations conducted in our laboratory and in other laboratories showed that mutation in the H2 region (117 – 136) inhibits membrane fusion activity (Fredericksen and Whitt 1996, Li *et al.*1993, Zhang and Ghosh 1994). Replacement of amino acids at G124L, F125A, F125D, F125Y, A113K, E139R, and other positions results in complete inhibition of membrane fusion. Therefore, it has been suggested that this region might be involved in the membrane fusion. Direct involvement of the fusion peptide in membrane fusion has been demonstrated by photolabeling experiments (Durrer *et al.*1995, Pak *et al.*1997). Large unilameller vesicle (LUV) containing [^{125}I]TID – PC/16 was incubated with VSV at different pH. The [^{125}I]TID – PC/16 is a very hydrophobic molecule that is localized only to the hydrophobic membrane phase. Upon UV irradiation it produces a highly reactive carbene that labels the protein fragment, directly interacting with the hydrophobic phase of the membrane. The results showed that VSV G was labeled in a pH dependent manner. Analysis of the labeled protein showed that only amino acid residues between 58 – 221 were labeled.

The synthetic fusion peptide designed against this putative fusion peptide region binds to the liposomal membrane in a pH dependent manner; however, no fusion activity of this peptide has been reported (Hall *et al.*1998). A similar fusion peptide used by Carneiro *et al.* (2003) did not show any fusion activity. This might be due to absence of conserved Pro and Cys residue in their fusion

peptide. Again, the P2-like peptide (a.a 145-168) present in VSV G has been reported to bind phosphatidylserine (Coll 1997). The P2-like peptides are characterized by heptad repeats (abcdefg) of hydrophobic amino acids in positions "a" and "b" followed by any short amino acid stretch containing positively charged amino acids not belonging to the heptad repeats. The peptide designed against this heptad repeat can induce membrane fusion. Modification of conserved His 148 and His 149 by DEPC (Diethyl procarbonate) or substitution of His by Ala completely inhibits the membrane fusion activity of this peptide (Carnerio *et al.*2003). It has been suggested that His protonation is essential for membrane fusion, and P2-like peptides also play an important role during membrane fusion. Therefore, it could be speculated that the whole region between 80 – 168 amino acids possibly interacts with the membrane during fusion.

1.2.5 Conformational state of VSV G

When exposed to low pH, the VSV G protein undergoes a reversible conformational change (Crimmins *et al.* 1982, Puri *et al.* 1988, Blumenthal *et al.* 1987, Gaudin 2000). The change in conformation of the G protein at low pH was evident from:

- Increased resistance of the G protein to trypsin digestion at low pH (Fredericksen and Whitt 1996). The VSV G protein is completely digested

by trypsin at neutral pH, but at low pH VSV G becomes resistant to trypsin digestion. Therefore, it was suggested that VSV G undergoes a conformational change at low pH, because trypsin cleavage sites which were exposed at neutral pH were no longer available at acidic pH.

- CD spectral analysis showed that the G protein undergoes a dramatic conformational change at fusion-active pH (Carneiro *et al.*2001).
- Carneiro *et al.* (2001) also reported that upon lowering the pH, bis – ANS binding to the G protein increases, suggesting that low pH exposes the hydrophobic segment of the protein.

Unlike the influenza virus HA fusion protein, no coiled – coil structure formation has been predicted for VSV G (Gaudin 2000, Zhang and Ghosh 1994). The fusion glycoprotein is anchored to the viral membrane through a single transmembrane domain close to the COOH – terminus (Irving and Ghosh 1982). Studies done by this laboratory suggest that the G protein requires membrane anchoring by any hydrophobic peptide sequence for its fusogenic activity (Odell *et al.*1997).

Previous studies done by this group showed that, the mutation in the H10/A4 region (a.a 395 – 418) of the G protein causes inhibition of membrane fusion (Shokralla *et al.*1999 and 1998). Although this region does not interact directly with the membrane during fusion (Durrer *et al.*1995, Pak *et al.*1997), it was

suggested that the H10/A4 region might play an important structural role during membrane fusion. Some of the double mutants in both H2 (fusion peptide domain a.a 118 - 139) and the H10/ A4 region of the VSV G glycoprotein also cannot induce membrane fusion, and they form relatively less stable trimers at low pH. The double mutation at F125YD411N and D137NG404A results in a less stable trimer at low pH (Shokralla *et al.* 1999). It has been reported that there are some highly conserved Cys residues in the fusion peptide region of the VSV G glycoprotein, which can form disulfide bonds with the neighboring Cys residues (Grigera *et al.*1992, Walker and Kongsuman 1999). It was predicted that C75 – C108 and C84 – C130 in the CR – H2 domain (residue 80 – 139) of VSV G can form disulfide bonds, which will result in a loop-like structure in the fusion peptide domain. Site- directed mutation at this region (C130 and C84) initiated by members of this laboratory suggests that these residues are required for the structural stability of the protein (unpublished). Structural analysis using the PHD program predicts that that for the TBE E protein, amino acid residue between 400 – 450 can form an α – helix structure, and this region is required for trimer stability (Stiasny *et al.*1996, Allison *et al.*1999). A similar helix structure has been predicted in the region between a.a 395 – 482 for the VSV G protein by the PHD program (Gaudin 2000). Therefore, it might be possible that H10/ A4 and the H2 region play an important role in oligomer stability.

Pak *et al.* (1997) suggested a probable conformational state of the VSV G protein during membrane fusion. VSV G undergoes a proton-driven shift from the T (tense) state at neutral pH to either the R (relaxed) state, which is fusion active or to the D (desensitized) state, which is fusion inactive (Clauge *et al.*1990, Puri *et al.*1992, Pak *et al.*1997). It has been reported that the VSV G protein either enters the R state at low pH in the presence of the target membrane or it enters the D state in the absence of the membrane. Insertion of VSV G into the membrane is also reversible, which suggests a Velcro-like attachment with the target membrane (Pak *et al.*1997). The D state formed at fusion active pH is also reversible (Clauge *et al.* 1990). In spite of the fact that VSV G is more hydrophobic in the D state, the G protein does not interact with the membrane in this conformation (Durrer *et al.*1995). Studies done with the rabies virus suggest that the D state is irrelevant to the fusion process, but could play a role in avoiding unspecific fusion during G protein transport through the Golgi complex (Gaudin *et al.*1995). VSV G protein undergoes reversible structural change when exposed to fusion active pH (Crimmins *et al.* 1982, Puri *et al.* 1988, Blumenthal *et al.* 1987, Gaudin 2000, Yao *et al.* 2003). It has been observed that low pH activation of VSV G is reversible. It has been observed that prior treatment of VSV G at pH 5.5 significantly enhance membrane fusion, in contrast the rate of membrane fusion was hindered by raising the pH back to 7.4 (Puri *et al.* 1988). Previous results from this laboratory showed that there is no kinetically trapped high energy state of VSV G at neutral pH (Yao *et al.*2003). The G protein is

equally thermostable at neutral pH and acidic pH, which suggests that the energy barrier between the native and the fusogenic state for the G protein is small. Therefore, it may be possible that a large fusion complex may be necessary to complete the energetically unfavorable process of membrane fusion (Gaudin 2000, Yao *et al.*2003).

Figure 1: Schematic diagram representing different classes of fusion glycoproteins. Fusion glycoproteins of animal virus are classified as Class I and Class II fusion protein. The class I fusion proteins are synthesized as precursor molecule, which undergoes proteolytic cleavage to produce the mature protein. They have hydrophobic fusion peptide at the NH_2 – terminal of the molecule, a single transmembrane domain and a cytoplasmic domain. Fusion glycoprotein of orthomyxovirus, retro virus and paramyxovirus belongs to class I. The class II fusion peptide has internal fusion peptide and they do not undergo any proteolytic maturation. The viruses belongs to this class are togavirus, flavivirus and rhabdovirus (Fig Taken from Hernandez *et. al.* 1996) (Old system of classification).

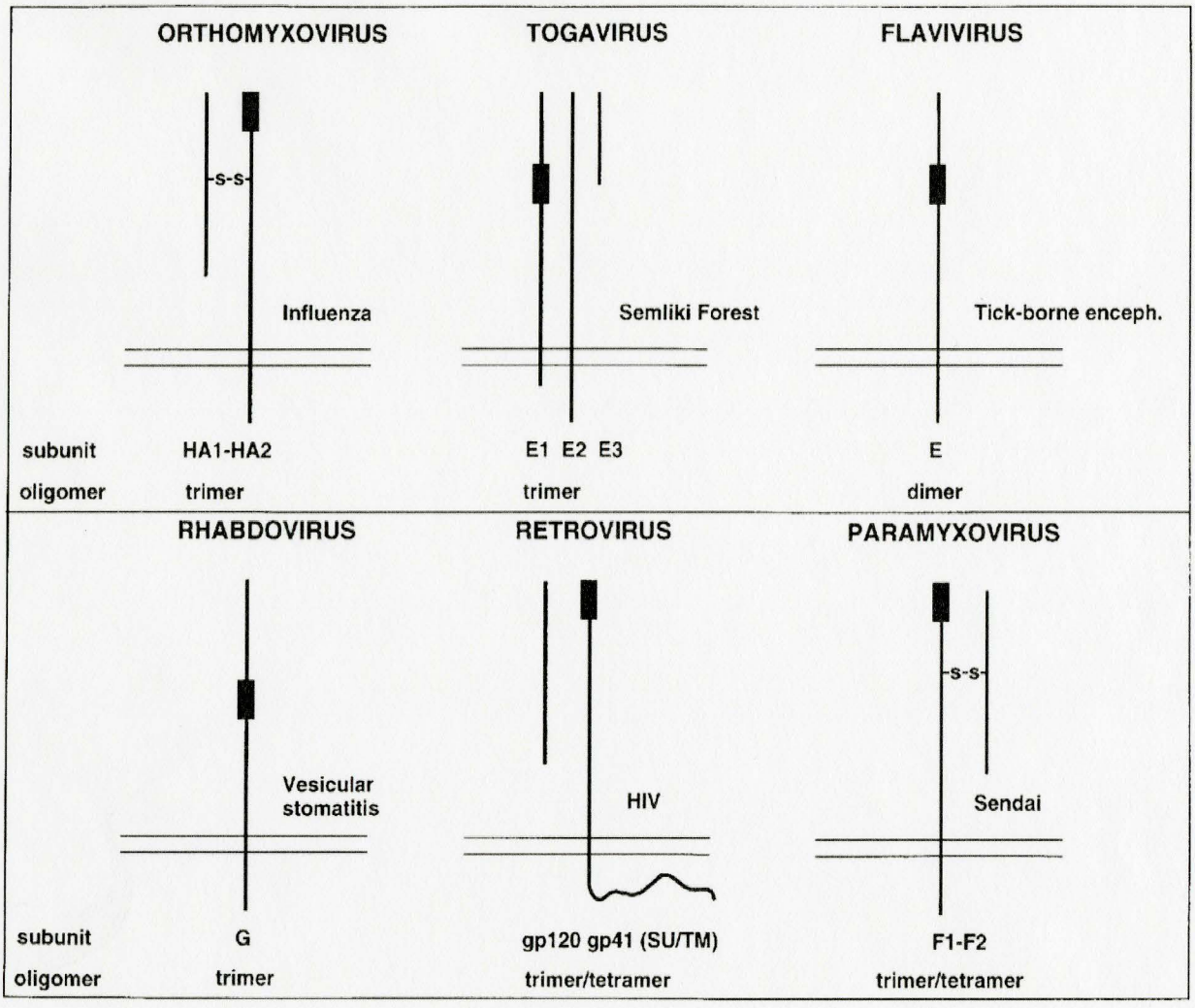
ORTHOMYXOVIRUS
TOGAVIRUS
FLAVIVIRUS
-s-s-
Influenza
Semliki Forest
Tick-borne enceph.
subunit
HA1-HA2
E1 E2 E3
E
oligomer
trimer
trimer
dimer
RHABDOVIRUS
RETROVIRUS
PARAMYXOVIRUS
Vesicular stomatitis
HIV
-s-s-
Sendai
subunit
G
gp120 gp41 (SU/TM)
F1-F2
oligomer
trimer
trimer/tetramer
trimer/tetramer

Figure 2: a) Schematic representation of primary structure of Influenza virus HA fusion peptide. The two subunit of HA fusion peptide HA_1 and HA_2 are linked by disulfide bond. The HA2 has a short hydrophobic fusion peptide (Green color) at the NH_2 – terminal and is attached to the membrane through transmembrane domain (black color) near C – terminal. b) Crystal structure of BHA as reported by Wilson *et al.* in 1981. The HA_1 (yellow) is at the top of the structure form globular domain required for receptor binding. The fusion peptide (green) is buried inside the molecule. The region between amino acid residues 55 – 76 (red) forms coiled – coil structure during membrane fusion. c) The Schematic representation of spring loaded mechanism (Carr and Kim 1993). It was proposed that this structural rearrangement propels the fusion peptide to opposing end of the molecule, allowing it to interact with the target membrane (Fig taken form Eckert and Kim 2001).

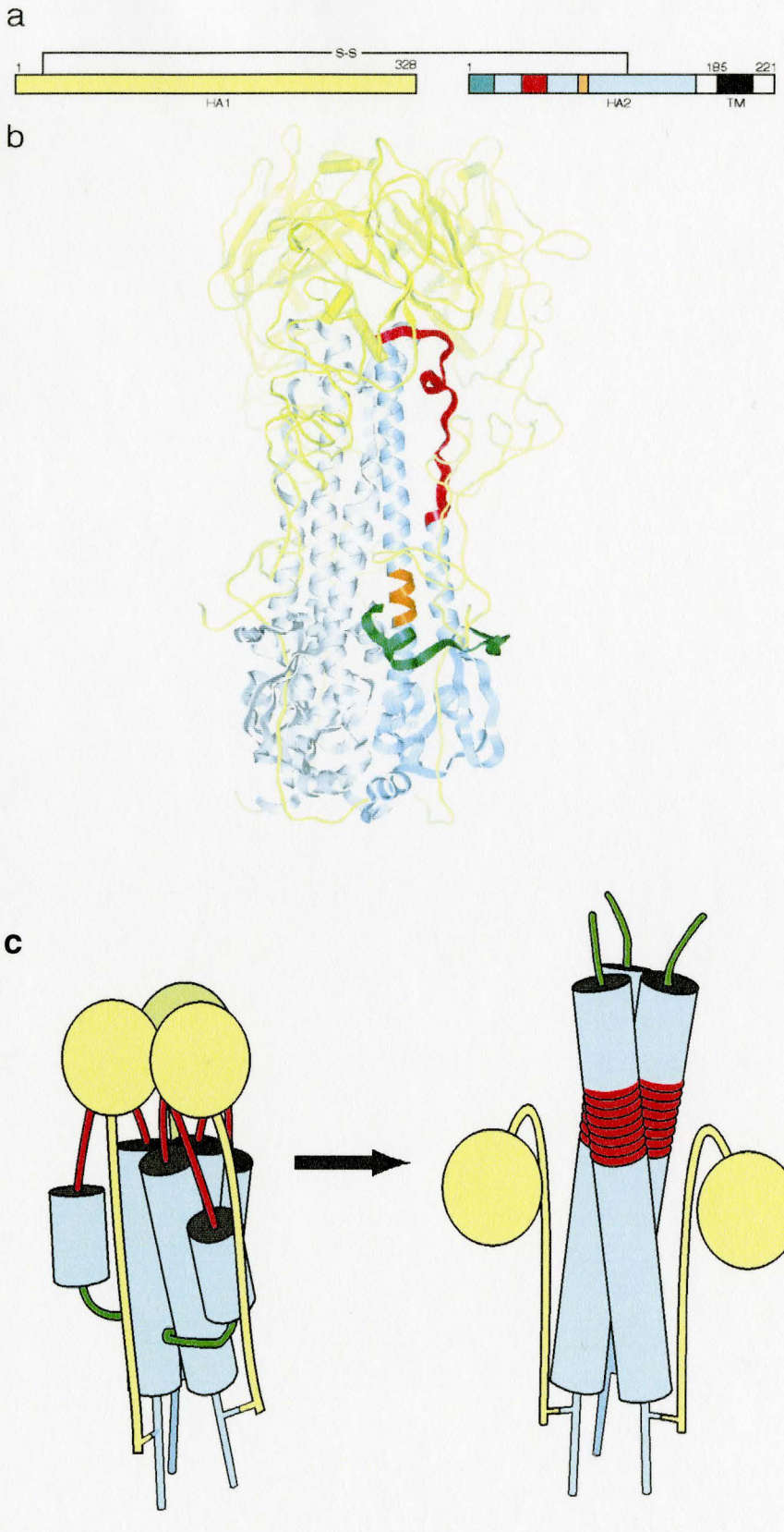
a
S-S
1
328
HA1
1
185
221
HA2
TM
b
c

Figure 3: Crystal structure of TBE E glycoprotein. The crystal was obtained from soluble ectodomain releases after restricted trypsin digestion (Heinz *et. al* 1991). The soluble ectodomain of E protein folds into three domain. The domain I is the β – barrel domain, domain II is the dimerization domain and domain III is the COOH – terminal immunoglobulin like domain. The cd – loop present at the tip of the domain II is believed to be the fusion peptide and domain III is responsible for receptor binding. The tryptophan projection of cd loop interacts with the hydrophobic crevice formed by domain I and domain III, which is responsible for dimer stability (Fig taken form Rey *et. al* 1995).

TBE Virus Surface Glycoprotein E: Top View of the Dimer

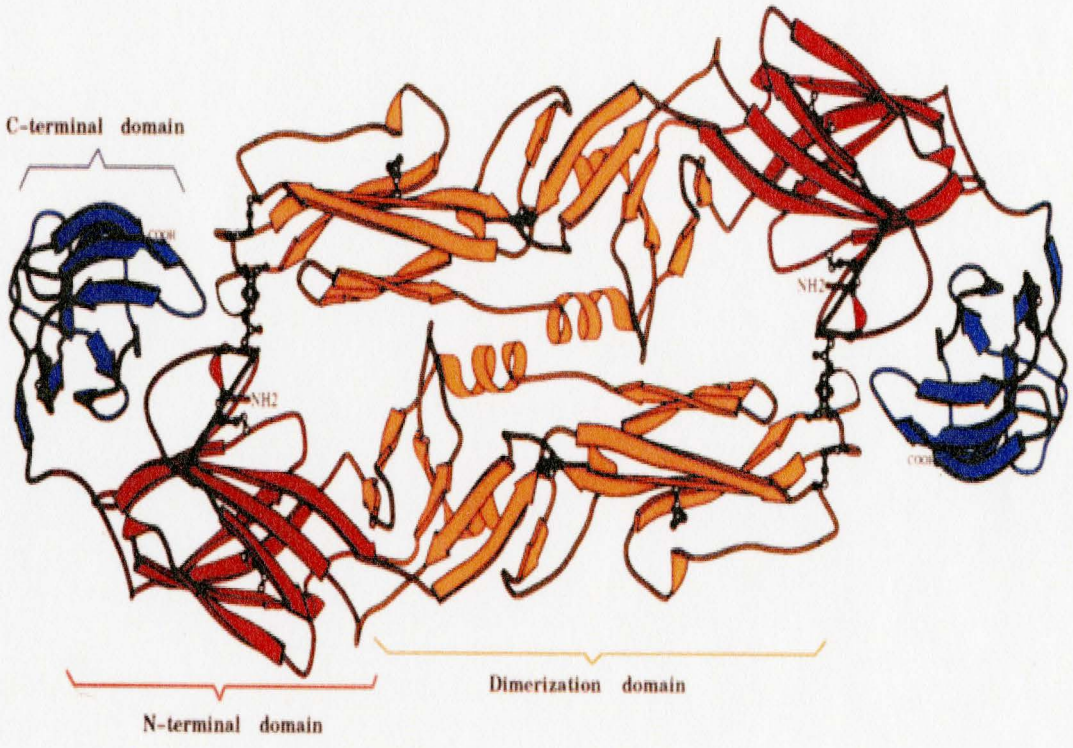

Figure 4: a) Schematic representation of vesicular stomatitis virus (Coll 1995). VSV possess two membrane protein, 67 kDa integral membrane glycoprotein (G) and matrix protein. The nuclecapsid is composed of L, NS (P) and N protein. b) Schematic diagram of primary structure of VSV G glycoprotein. The primary structure of G shows a constant region (CR) at the NH_2 – terminal, a putative fusion peptide region (H2), a conformational sensitive region (H10 / A4), single transmembrane domain and a short cytoplasmic domain (fig taken from Coll 1995).

a

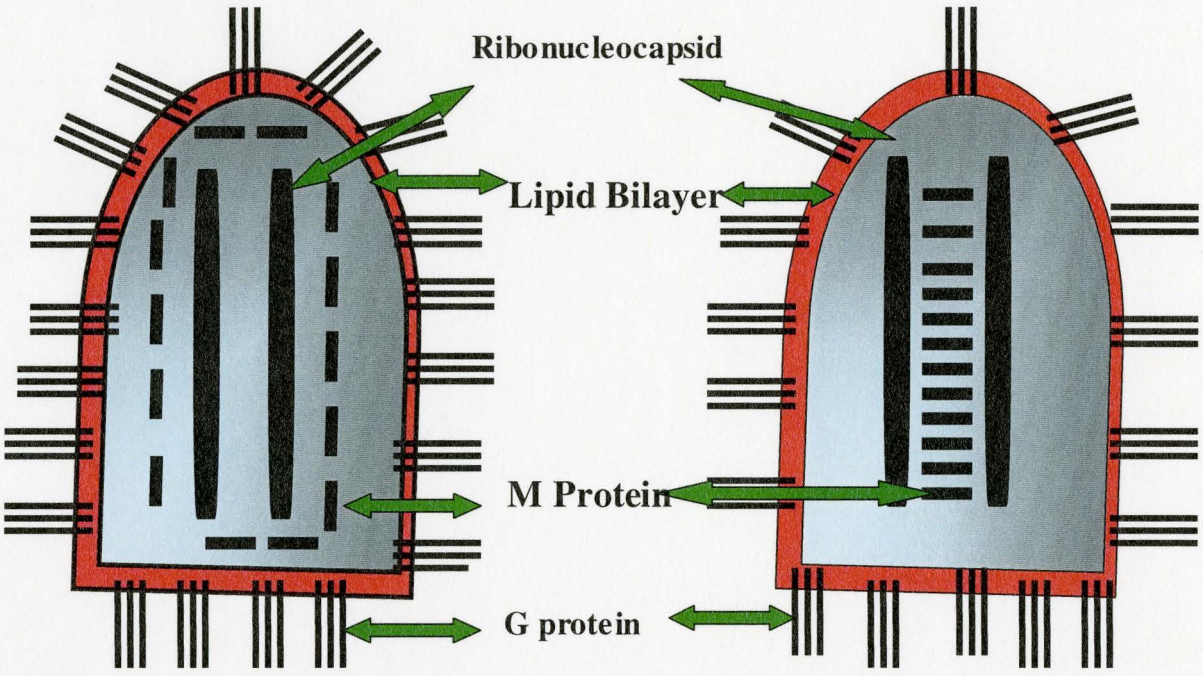
Ribonucleocapsid
Lipid Bilayer
M Protein
G protein

b

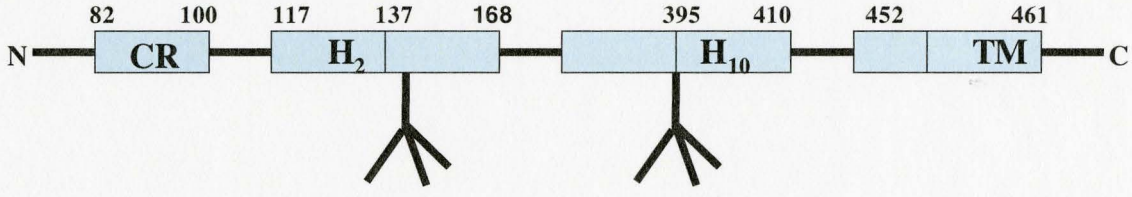
82
100
117
137
168
395
410
452
461
N
CR
H2
H10
TM
C

2. MATERIAL AND METHODS

2.1 Chemicals and Reagents

Chemical	Supplier
Acrylamide	Research Organic Inc.
Ammonium persulfate	BDH
Ampicillin	Sigma
Aminonapthalenetrisulfonic acid (ANTS)	Molecular Probes
Trypticase Peptone	BD Biosciences
Bacto yeast extract	DIFCO
Benzamidine – sepharose	Amersham Pharmacia
Bisacrylamide	Bioshop
Bovine Serum Albumin	Sigma.
β–Mercaptoethanol	BDH
Citric acid	BDH
Calf Serum	GIBCO / BRL
Coomassie brilliant blue stain	GIBCO / BRL
Disodium hydrogen orthophosphate	BDH
DPX	Molecular Probes
DTSSP	Pierce
DTT	Calbiochem
EDTA	Merck
Fetal bovine serum (FBS)	GIBCO / BRL
Glutathione	Sigma
Glycerol	Caledon
Glutathione - Sepharose beads	Amersham Pharmacia
N-2-hydroxyethylpiperazine-N'-2-ethanesulfonic acid (HEPES)	Sigma

Chemical	Supplier
High glucose dulbecco's medium (HGD)	GIBCO / BRL
Imidazole	Sigma
Isopropyl β, D-thiogalactopyroside (IPTG)	Pharmacia
L – Glutamine	GIBCO / BRL
2-[N-Morpholin]-ethanesulfonic acid (MES)	Sigma
NBD – PE (N[7-nitrobenzoxa-1,3-diazol-4-yl]-dioleoyl – phosphatydilethanolamine)	Avantipolar lipids Inc.
Ni – NTA Agarose beads	Amersham Pharmacia
Nonidet P 40	Sigma
NZY media	DIFCO
Octyl β–D-glucopyranoside	Sigma
Penicillin – Streptomycin	GIBCO / BRL
Phosphatidylcholine	Avantipolar lipids Inc.
Phosphatidylserine	Avantipolar lipids Inc.
PMSF	Sigma
Polyethyleneglycol (PEG)	BDH
Potassium chloride	BDH
Potassium dihydrogen orthophosphate	BDH
Rh – PE (Rhodamine – phosphatydilethanolamine)	Avantipolar lipids Inc.
Sarkosyl	Sigma
Sodium Dodecyl Sulfate (SDS)	Bioshop
Sephadex – G 200/ 150/ 75	Amersham Pharmacia
Sodium acetate	BDH
Sodium chloride	Bioshop
Soyabean trypsin inhibitors	Sigma
Sucrose	Merck

NNN'N'N Tetramethylethylenediamine (TEMED)	GIBCO / BRL
Tolylsulfonyl phenylalanyl chloromethyl ketone (TPCK)	Sigma
Tris (hydroxymethyl) – aminomethane (Tris)	Bioshop
Triton X – 100	Sigma
Tween – 20	Sigma

2.2 Enzymes	**Supplier**
Lysozyme	Sigma
Bromelain	Sigma
Chymotrypsin	Worthington Biochemical
Subtilisin	Sigma
TEV protease	Invitrogen
Thermolysin	Sigma
Trypsin (TPCK treated)	Worthington Biochemical

2.3 Multi – Component Systems

BCA* Protein Assay kit	Pierce
Western Lighting kit	Perkin Elmer

2.4 Plasmids , Bacterial Strains, Viruses, and Cell Lines

Bacterial Strain/ Virus/ Cell Line	**Construct**	**Vector**	**Source**
E.coli-BL 21	GST- G*	pGEX-2T TEV	Dr. H.P Ghosh

	Asn_{37} – Ser_{463}		Dr. Y. Yao
E.coli-BL 21	His-G* Asn_{37} – Ser_{463}	pPROEX-HTb	Dr. H.P Ghosh Dr. Y. Yao
BHK 21 Cell Line	-	-	Dr H.P Ghosh
VSV Indiana	-	-	Dr. H.P Ghosh
E.coli-BL 21	His-TEV	pET15b	Dr. H.P Ghosh Dr. F. Sicheri

2.5 Growth Media and Buffers

	Composition
LB Media	1% Bacto – tryptone, 0.5% bacto-yeast extract, 1% NaCl pH 7.2
NZY Media	1% NZ amine, 0.5% Bacto Yeast extract, 1% NaCl pH 7.2
STE Buffer	50mM Tris pH 7.4, 150 mM NaCl, 1mM EDTA
TBS Buffer	50mM Tris pH 8, 450 mM NaCl
TEV Cleavage Buffer	50mM Tris pH 8, 150 mM NaCl, 5mM DTT 0.5mM EDTA
SDS PAGE loading buffer	100mM Tris – HCl pH 6.8, 4% SDS, 0.2% bromophenol blue, 20% glycerol 10% β - mercaptoethanol
PBS	137mM NaCl, 2.68mM KCl, 8.1mMNa_2HPO_4 , 1.5 KH_2PO_4 pH 7
NTE buffer	10mM Tris pH7.2, 1mMEDTA, 150 mM NaCl

2.6 Antibody

The polyclonal antibody against the VSV G glycoprotein was generated by rabbits with a recombinant adenovirus vector expressing G protein (Dr. H. P. Ghosh). The serum-containing antibody was harvested and stored at -20°C. Horse anti-rabbit IgG conjugated to a chemiluminescence marker was purchased from Jackson Immuno Research.

2.7 Molecular weight markers

A high molecular weight marker (188 – 8kDa) was purchased form Invitrogen and contained the following proteins: Myosin (188kDa), phosphorylase B (98kDa), BSA (62kDa), GDH (49kDa), ADH (38kDa), CAH (28kDa), myoglobin (17kda), lysozyme (14kDa), and Aprotenin (6kDa). The low molecular weight protein marker (116 – 14.4) was purchased form MBI Fermentas and contained the following proteins: β–galactosidase (116kDa), BSA (66.2kDa), ovalbumin (45kDa), lactate dehydrogenase (35 kDa), restriction endonuclease (25kDa), β–lactoglobulin (18.4kDa), and lysozyme (14.4kDa).

2.8 Expression and purification of the GST fusion protein

The GST fusion protein was purified according to Frangioni and Neel (1993). Bacteria containing the GST– G* were plated in ampicillin plates from stock cultures stored at -80°C. A single colony was picked and grown in 5 ml LB media containing ampicillin. Expression of GST – G* was checked by IPTG induction. 500 ml of LB media were inoculated with 50 ml of culture grown overnight at 37°C. At 0.6 $OD_{600,}$ inductions were done by adding 0.5 mM IPTG. Induction was carried out for 3-4 hours at 37°C. Bacteria were pelleted down and washed with STE buffer (50 mM Tris pH 7.4, 150 mM NaCl, 1 mM EDTA.). Pellets were resuspended in STE buffer and incubated for 30 min with 100 μg/ml of lysozyme and 1 mM DTT at 4°C. To that 1.5% sarkosyl and 1 mM PMSF were added, and cells were lysed by three cycles of French press at 4°C. After centrifugation at 12,000*g* for 30 min at 4°C, the supernatant was collected and then incubated with GSH beads equilibrated with PBS at 4°C. The beads were then washed with 20 column volumes of PBS. Elution was done with 20 mM GSH in 50 mM Tris pH 7.4, 150 mM NaCl, and 0.5% sarkosyl. Purity of the GST fusion protein was determined by SDS – PAGE, and the protein concentration was estimated by a BCA assay. The purified protein was then stored with 15% glycerol at -20°C.

2.9 Expression and purification of His-G*

Bacteria containing the His – G* vector were plated on an ampicillin plate and a single colony was picked. The bacteria were then tested for the expression of His – G* by IPTG induction. The bacteria were grown in 5 ml LB media, and after induction for 3 hours at 37°C, the cells were pelleted down, lysed by sonication, and run on 10% SDS – PAGE. The protein was purified according to the manufacturer's instructions (Novagen). 500 ml of LB media were then inoculated with 50 ml of culture grown overnight that expressed the recombinant protein. At 0.6 OD_{600}, inductions were done by adding 0.5mM IPTG. Induction was carried out for 3-4 hours at 37°C. Bacteria were pelleted down and washed with STE buffer (50 mM Tris pH 7.4, 150 mM NaCl, 1 mM EDTA.). Pellets were resuspended in TBS buffer (50 mM Tris pH 8, 450 mM NaCl) and incubated for 30 min with 100 μg/ml of lysozyme and 5 mM βME at 4°C. To that, 1% sarkosyl and 1 mM PMSF were added and cells were lysed by three cycles of French press at 4°C. After centrifugation at 12000*g* for 30 min at 4°C, the supernatant was collected. The supernatant was then incubated with Ni-NTA agarose beads for 1 hr at 4°C. The beads were loaded into a 5 cm X 0.5 cm column, and washed with 20 column volumes of TBS containing 20 mM imidazole and 0.1% Triton X 100. Elution was done with 250 mM imidazole in TBS buffer. His-G* was concentrated by passing it through a spin filter with a 10kDa cutoff and further purified by passing it through sephadexG-150. Purity of the His fusion protein

was determined by SDS PAGE, and protein concentration was estimated by the BCA assay. The purified protein was then stored in 15% glycerol at -20°C.

2.10 Expression and purification of TEV protease

TEV was purified according to the methods of Lucast *et al.* (2001). The process is described here in brief. 500 ml of NZY media were inoculated with 50 ml of culture grown overnight at 20°C. At 0.8 OD_{600}, induction was done by adding 0.5 mM IPTG. Induction was carried out overnight at 20°C. Bacteria were pelleted down and washed with STE buffer (50 mM Tris pH 7.4, 150 mM NaCl, 1 mM EDTA.). Pellets were resuspended in TBS buffer (50 mM Tris pH8 and 300 mM NaCl) and incubated for 30 min with 500 μg/ml of lysozyme and 5 mM βME at 4°C. To that, 1 mM PMSF was added and cells were lysed by three cycles of French press. After centrifugation at 12000*g* for 30 min, the supernatant was collected and then incubated with Ni-NTA agarose beads for 1 hr at 4°C. The beads were then loaded into a column 5 cm tall and 0.5 cm in diameter and washed with 20 c.v. of TBS containing 20 mM imidazol, 5 mM βME, 10% glycerol, and 0.1% Triton X 100. Elution was done with 250 mM imidazol in TBS buffer containing 10% glycerol and 5 mM βME. The protein was immediately dialyzed against 50 mM Tris pH 7.4, 150 mM NaCl, 50% glycerol, and 1 mM EDTA.

2.11 TEV cleavage

The GST – TEV – G* was cleaved with TEV protease according to the methods of Mondigler and Ehrmann (1996). 20 µl of GSH beads bound to the GST fusion protein were washed with TEV cleavage buffer (50 mM Tris pH 8, 150 mM NaCl, 5 mM DTT, 0.5 mM EDTA). 20 µg of TEV protease were added to that and incubated at 30°C for 3 hours. After the reaction was completed, the protein was resolved by SDS-PAGE and bands were visualized by coomassie brilliant blue staining.

2.12 Maintenance of mammalian cells

BHK21 cells were grown in high glucose Dulbecco's medium (HGD) containing 5% fetal bovine serum (FBS) or 10% calf serum (CS), 1% penicillin/ streptomycin, and 2% L – glutamine. The medium containing all the supplements was pre-warmed at 37°C, and frozen cells were directly poured into 10 ml of medium in a 100-mm plate. The cells were gently mixed and allowed to grow in a 5% CO_2 incubator at 37 ^{0}C for two to three hours. Once the cells adhered to the plate, the medium was removed and replaced with fresh medium. For passaging, the cells were allowed to grow up to 85-95 % confluence. After removing the medium, the cells were washed with PBS. To that 0.5 ml of trypsin – EDTA solution was added and incubated for 1-2 min.; trypsin treatment removes the

cells from the plate. 10 ml of HGD containing serum were added immediately to stop further trypsin digestion. The cells were then pipetted several times to break any clumps and small aliquots of this mixture (0.5-1 ml) were added to a new 100-mm plate containing fresh medium. Cells were allowed to grow at 37°C in 5%CO_2 until they reached 80-95% confluence.

For long-term storage, cells were grown until they were 80-90% confluent in 150-mm plates. The cells were washed with PBS and trypsinized, and 5 ml of freezing medium containing HGD, 5% FBS, and 10%(v/v) DMSO were added. The cells were pipetted several times to break any clump formation, and were then stored in 1-ml aliquots in Nalgene cryovials at -70°C.

2.13 Virus preparation

VSV Indiana was grown in a BHK 21 cell line in 150-mm plates. BHK 21 cells were grown up to 80% confluence, and then cells were infected with 0.1 m.o.i. of virus in HGD medium without serum for one hour at 37°C. The medium was aspirated off and fresh DMEM with 5% serum (FBS/ CS) was added and incubated overnight at 37°C. Cell debris was removed by centrifugation at 1250*g* for 5 min. Viruses were then pelleted by centrifugation at 25K r.p.m. for one hour at 4°C through 20% sucrose solution in NTE buffer (10 mM Tris pH 7.2, 1 mM EDTA, 150 mM NaCl) using an SW 27 rotor in a Beckman L8-70M

ultracentrifuge. Pellets were dissolved in NTE buffer by allowing them to stand in the buffer for one hour on ice. The viruses were purified by repeated ultracentrifugation at 36K r.p.m. for one hour at 4°C through a 20% sucrose cushion using an SW 50 rotor. Pellets were then allowed to stand on ice for 3 hours in NTE buffer. The viruses were then resuspended in NTE buffer while gently mixing with a round-bottom glass rod. The virus suspension was aliquoted and stored at -80°C.

For viral stock preparation, 80% confluent BHK 21 cells in 100-mm plates were infected with 0.1 m.o.i. of viruses. Infection was done in serum-free HGD media for one hour at 37°C. After one hour, cells were allowed to incubated in HGD media containing 5% serum (FBS/CS) at 37°C until the cells became rounded. The plates were then kept on ice to stop further viral growth. Cell debris was removed by centrifugation at 1200*g*. The supernatant was then aliquoted and stored at -80°C.

2.14 G protein purification

Purification of the G protein was done according to the methods of Carneiro *et al.*(2001). In brief, purified VSV (1 mg/ml) was incubated with 1% octylglucoside in 20 mM MES, 30 mM Tris, 100 mM NaCl, pH 7.4 for one hour at room temperature. Supernatant containing the G protein was collected after

ultracentrifugation at 36K r.p.m. for 1.5 hours using a Beckman SW-50 rotor at 4°C. The supernatant was then dialyzed overnight against 50 mM HEPES pH 7.4 and 150 mM NaCl to remove the detergent. The protein was concentrated by spin filtration through a 30kDa cutoff filter (Pall filter). The protein was then aliquoted and stored at -20°C with 15% glycerol. Protein concentration and purity were determined by the BCA assay and SDS- PAGE electrophoresis, respectively.

2.15 Trypsin digestion of VSV G

5 µl of VSV (2 mg/ml) were added to the required amount of trypsin digestion buffer (20 mM MES, 30 mM Tris, 100 mM NaCl). 10% Triton X 100 was added to make a final concentration of 1%. Trypsin (TPCK treated) was added to the reaction mixture at varying protein to trypsin ratios (VSV: trypsin). The reaction volume was restricted to 30 µl. The reaction mixture was incubated as mentioned in the specific experiments. To stop the reaction, 5 mM PMSF were added and the samples were analyzed by running on SDS PAGE. To determine the structural change of Gs, the Gs protein was incubated with trypsin (15:1; protein: trypsin) at 37°C for 30 min. in the presence of 1% Triton X 100 at pH 7.4 and 5.4. The activity of trypsin at pH 5.4 was tested by adding 0.9% SDS into the reaction mixture.

2.16 Digestion of VSV G with other protease

5 μg of VSV (2 mg/ml) in 20 mM MES, 30 mM Tris, and 150 mM NaCl (at indicated pH) buffer were incubated with varying ratios of different proteases for different time intervals at 37°C in the presence or absence of 1% Triton X 100. The reaction was stopped by adding protease inhibitor. Trypsin and subtilisin were inhibited by 5 mM PMSF, chymotrypsin and bromelain were inhibited with 2 mM TPCK, and Thermolysin was inhibited with 5 mM EDTA. Aliquots were taken and samples were analyzed by resolution through 8% SDS-PAGE.

2.17 Purification of Gs

VSV (0.3 mg/ml) was incubated with 1.5% octylglucoside in 20 mM MES, 30 mM Tris, 100 mM NaCl, pH 5.4 buffer for 30 minutes at 37°C, with trypsin (TPCK treated, at 15:1 protein to trypsin ratio). The reaction was stopped with soybean trypsin inhibitor (twice the amount of trypsin). Residual particles were removed by ultracentrifugation at 36K r.p.m. for 1.5 hours using a Beckman SW 50 rotor at 4°C. The Gs protein thus obtained was concentrated using a PALL MICROSEP 30K OMEGA filter. The protein was further purified and buffer exchanged to neutral pH buffer by passing through a 30cm X 0.9cm sephadex G – 200 column at a flow rate of 0.15 ml/min; the sample volume was restricted to 1% of the column volume. The column was pre-equilibrated with 50mM HEPES, pH7.4, and 150 mM NaCl buffer or PBS buffer and 1ml fractions were collected. The

protein was generally collected at fraction numbers 6, 7, and 8. All fractions were pulled and passed through benzamidine sepharose beads. The protein was again concentrated by spin filtration (ultra filtration), and the purity and concentration were determined by SDS PAGE gel electrophoresis and BCA assay, respectively. The protein was stored at -20°C in 15% glycerol.

2.18 Cross linking

Cross linking of VSV G and Gs was done according to the methods of Lyles *et al.* (1990), 10 µl of VSV G / Gs (5 µg total protein) were added to 20 µl of 50 mM HEPES pH 7.4 and 150 mM NaCl buffer. pH was adjusted to 5.4 with precalibrated 0.5M Na-Acetate buffers. 500 µM of DTSSP (Dithiobis-[sulfosuccinimidyl propionate]) were added and incubated for 30 min on ice. The reaction was quenched for 15 min with 1M Tris (final concentration 20-50 mM). 15 µl of the sample were aliquoted and run on 8% non-reducing SDS PAGE. Bands were visualized by western blotting.

2.19 SDS – Polyacrylamide gel electrophoresis

The SDS – PAGE was done according to the methods of Laemmli (1970). Gels were cast and run on a Bio – Rad electrophoresis apparatus. For each polyacrylamide gel, the resolving gel was prepared by mixing double-distilled

waster, 30% acrylamide mix (biscrylamide : acrylamide; 1:29), 1.5M Tris pH 8.8,10% SDS, 10% ammonium-persulfate and TEMED. The mixture was immediately poured into the gel mold and overlaid with water to form a uniform surface. After the resolving gel was solidified, the stacking gel was poured with a comb. For the stacking gel, a mixture was made of double-distilled water, 30% acrylamide mix, 1.0 M Tris pH 6.8, 10% SDS, 10% ammonium persulfate, and TEMED. After the gel solidified, unpolymerized acrylamide was removed by washing with water. The sample was boiled for 3 minutes in sample loading buffer and carefully loaded into the wells. The gel was electrophoresed at 150V in running buffer (25 mM Tris, 250 mM glycine, 0.1% SDS) until samples reached the bottom. The gel was then stained with coomassie blue stain and then distained with 45% water, 45% methanol, and 10% acetic acid.

2.20 Western blotting

A nitrocellulose membrane was cut and soaked for 2 min in water and then in transfer buffer (25 mM Tris, 192 mM glycine, 20% methanol). A transferring system was set up according to the manufacturer's instructions. A "sandwich" was made with SDS PAGE and the membrane between two pieces of 3MM Whatman paper. The transfer was done at 100V for one hour. After this time, the membrane was washed once with TBS-TNT buffer (0.9% NaCl, 20 mM Tris pH 7.6, 0.3% Tween 20, 0.2% NP-40, 0.05% Triton X 100) to remove the methanol and then blocking was done overnight in blocking buffer (TBS-TNT buffer + 3%

nonfat milk) at 4°C. The membrane was then incubated with 1:3000 times diluted primary antibody in blocking buffer for one hour at room temperature. After washing the membrane three to four times with TBS-TNT buffer, the membrane was incubated for one hour with HRP – conjugate anti-rabbit IgG. Bands were visualized by chemiluminescence according to the manufacturer's (Perkin Elmer) instructions.

2.21 Lipid binding assay

0.25 μg of phosphatidylserine (PS) and 0.25 μg of phosphatidylcholine (PC) were dissolved in chloroform and evaporated under nitrogen to produce a film. The film was resuspended in 20 mM Tris pH 7.4 and 150 mM NaCl at a concentration of 1 mg/ml. The suspension was vortexed vigorously for 5 min, frozen in liquid nitrogen, and then thawed under tap water. These steps were repeated three times. Small unilamellar vesicles (SUV) were formed by sonication in a bath sonicator (Cole Palmer) containing ice, until suspension became clear. 200μg of liposome were incubated with 50 μg of purified G or Gs protein for 30 min in the indicated pH at 37°C. The final volume was maintained at 500 μl. An 80% sucrose solution in 20 mM MES, 30 mM Tris and 100 mM NaCl (pH 7.4 or pH 5.4 as indicated in the experiment) was added to it, to make a final concentration of 50% sucrose. It was then overlaid with 2 ml of 20% sucrose solution and 1 ml of 5% sucrose in pH 7.4 or pH 5.4 buffer (as indicated in the experiment). The

gradients were run at 50,000 r.p.m. for 2 hours at 4°C using a Beckman SW-50 rotor. 500 µl of sample were collected and analyzed by running on a 10% SDS-PAGE.

2.22 Lipid mixing assay for liposome fusion

The resonance energy transfer method was employed to measure lipid mixing, as described by Struck *et al.* (1981) and Hoekstra and Düzgünes (1993). In brief, SUV was prepared by mixing an equimolar amount of PC and PS. The labeled liposome was made by mixing NBD – PE and Rh – PE at 2 mol% of total lipid. The SUV was prepared as described in section 2.22. Experiments were done by mixing 50 µM of unlabeled and 5.5 µM of labeled SUV in 2 ml of 10 mM HEPES pH 7.4 and 145 mM NaCl buffer. The NBD fluorescence was measured at an excitation wavelength of 465 nm and an emission wavelength of 530 nm in a Photon technology international spectrofluorometer (Dr. David Andrews, McMaster University). The required concentration (as indicated for each experiment) of virus or protein was added and fluorescence was measured. The pH was adjusted to the required value (as indicated in each experiment) with pre-determined amount of 0.1M citric acid. Triton X 100 was added at the end to read 100% lipid mixing. The percentage fusion was calculated by $(F_t - F_o) / (F_m - Fo)$ X 100, where F_t is the increase in NBD fluorescence, F_o is the initial

fluorescence, and F_m is the maximum fluorescence. The data obtained were then plotted using Sigma Plot.

2.23 Leakage assay

Leakage of liposomal vesicles was investigated as described by Ellens *et al.* (1985) and Talbot *et al.* (1997). The liposome was made by mixing an equimolar amount of PC: PS in chloroform. The lipid mixture was dried by N_2 to make a film; the film was further dried under a vacuum for two hours with liquid nitrogen. The film was then resuspend in a stock solution of 12.5 mM ANTS, 45 mM DPX, 68 mM NaCl, 5 mM HEPES, 5 mM MES pH7.0. The osmolarity of the stock solution was adjusted to 300 mosm with NaCl using a Wescor Inc. 5100C vapor pressure osmometer (Dr. Christopher M. Wood, McMaster University). The mixture was then vortexed, frozen, and thawed three to four times. SUV was made by sonicating the lipid mixture in a Cole Parmer Ultrasonicator, until the solution became clear. The un-entrapped material was removed by passing the SUV through a Sephadex G – 75 column (10 x 1 cm) that was pre – equilibrated with 5 mM HEPES, 5 mM MES, and 150 mM NaCl pH7; osmolarity was adjusted to 300 mosm. In a typical experiment, 150 μM SUVs were added to 2 ml pH 7 buffer in a quartz cuvette with a magnetic stirrer, to which the required amount of fusion glycoproteins was added, and the pH was bought down to 5.4 with pre – determined amount of 0.1 M citric acid. Fluorescence was recorded at an

excitation wavelength of 360 nm and an emission wavelength of 530 nm for 400 – 500 seconds using a Photon Technology International spectrofluorometer. The maximum leakage was determined with 20 µl of 10% triton X 100. The leakage was also tested with protein storage buffer and glycoprotein at neutral pH as a control. The percentage fusion was calculated by $(F_t - F_o) / (F_m - F_o) \times 100$, where F_t is the increase in ANTS fluorescence, F_o is the initial fluorescence, and F_m is the maximum fluorescence. The data obtained were then plotted using Sigma Plot.

2.24 Mixing of aqueous content

The mixing of aqueous content is based on the principle of collisional quenching of ANTS fluorescence by DPX as described by Düzgünes and Wilschut (1993). An equimolar amount of PC: PS in chloroform was mixed together. The mixture was dried under a stream of nitrogen to make a film. The lipid mixture was further dried under vacuum for 2 hours. The lipid film was then resuspended in a solution of 25 mM ANTS (Aminonapthalenetrisulfonic acid), 90 mM NaCl, 5 mM HEPES, and 5 mM MES, pH7.4, or 90 mM DPX (p – xylene bis (pyridinium)bromide), 50 mM NaCl, 5 mM HEPES, and 5 mM MES, pH 7.4. The osmolarity of the solutions were adjusted to 300 mosm with NaCl by using a Wescor Inc. 5100C vapor pressure osmometer (Dr. Christopher M. Wood, McMaster University). The liposome mixture was vortexed, frozen, and thawed

five times to produce a suspension. The SUV was made by sonication in a bath sonicator (Cole Parmer Ultrasonicator) with ice. The un-entrapped material was removed by passing the SUVs through a sephadex G 75 column (10 x 1 cm), equilibrated with 5 mM HEPES, 5 mM MES, and 150 mM NaCl pH 5.4 (the osmolarity of the pH 5.4 buffer was adjusted to 300 mosm). To 2 ml of pH 5.4 buffer containing 250 μM DPX and 50 μM ANTS SUVs were added. Fluorescence was recorded at an excitation wavelength of 360 nm and an emission wavelength of 530nm using a Photon Technology International spectrofluorometer. The required amount of glycoprotein was added, and quenching of ANTS fluorescence was measured. For scattering control, DPX SUVs were replaced with SUV containing pH 5.4 buffer with out ANTS or DPX. The relative fluorescence was calculated by (F_t / F_{max}) X 100, where F_t is the fluorescence at any time t and F_{max} is the maximum fluorescence.

2.25 Light scattering measurement to determine Gs aggregation

The aggregation of Gs was measured by right angle light scattering using a Photon Technology International fluorometer with emission and excitation monochromators both set at 280 nm. Gs protein at a final concentration of 45μg/ml was added to 2 ml of 10 mM HEPES pH 7.4 and 150 mM NaCl. Prior to this, the baseline was established with buffer alone. The pH was gradually

lowered with a pre-calibrated amount of 0.1M citric acid, and light scattering was measured.

2.26 Circular dichroism spectroscopy

The CD spectra of Gs protein at different pH (7.4, 6, 5.8, 5.4, 5.2, and 5) were recorded using an AVIV model 215 instrument (Dr. Richard M. Epand, McMaster University). For CD spectra, the protein was purified in PBS pH 7.4. The concentrated protein was then added to different pH buffers at a final concentration of 300μg/ml. The CD data were recorded between 260 – 200 nm at 25°C using a 1-mm quartz cell. To determine the CD spectra of Gs in presence of liposome, the Gs was incubated with liposome for 5 min and CD data were recorded at 25°C. The obtained data were then converted to molar ellipticity [θ] as follows:

$$[\theta] = OD \times (\text{Weight in mg/ml} / \text{Mol Wt.} \times \text{No of a.a residue})^{-1}$$

$$[\theta] = [\text{deg.cm}^2 / \text{dmole}]$$

The [θ] obtained was plotted against wavelength using Sigma Plot. Secondary structure content was determined by CDPro software using the CONTINLL program (Sreerama 1999).

3. RESULTS

The structural changes of the VSV G protein at fusion active pH and the mechanisms of fusion is not yet understood. Until now, investigations have mostly concentrated on the characterization of G protein by mutation and biochemical studies. The initial characterization of the VSV G protein suggests that it extends through the envelope and a portion of it can be cleaved by chymotrypsin (Taube and Braun 1982). Biochemical studies with soluble G protein released in VSV infected cells and cathepsin D released fragment suggest that the Gs protein lacks the C – terminal transmembrane domain, with an apparent molecular weight of 62 – 58 kDa (Chatis and Morrison 1983, Crimmins *et al.* 1983, Garries - Wabnitz and Kruppa 1984, Irving and Ghosh 1982). Sedimentation analysis indicated that the Gs is monomeric in the intact virus (Crimins *et al.* 1983, Crise *et al.* 1989). Chemical crosslinking experiments suggest that the VSV G protein exists in a dynamic equilibrium between monomer and trimer at neutral and fusion active pH (Crise *et al.* 1989, Lyles *et al.* 1990, Zagouras and Rose 1993). However, stability of the trimer increases at low pH (Doms *et al.* 1987). Fluorescence spectroscopic studies were conducted to determine the conformational change of Gs at fusion active pH (Crimmins *et al.* 1983), but no further studies were carried out to verify the biological activity and structure of Gs either at neutral or fusion active states. Later studies were mostly directed towards understanding the function of different domains of VSV

G in membrane fusion. The conservation of amino acid sequences in the H2 (118 – 136) region among VSV serotypes suggested that this region might serve as a possible fusion peptide domain (Oshnishi *et al.* 1988). An additional N-linked oligosaccharide at residue 117 of VSV G, was defective in the low-pH induced membrane fusion, suggesting that the uncharged amino acid sequence may be involved in fusion activity (Whitt *et al.* 1990). Linker insertion mutation at residue 122, 194, 409 and 415 generated four fusion defective mutants H2, H5, H10 and A4 (Li *et al.* 1993). The H2 mutation is present with in the uncharged amino acid sequence, which was located at the putative fusion peptide region. Other regions like H5 and H10/A4 region were located 70 amino acids and 300 amino acids downstream of H2, respectively (Li *et al.* 1993). Site-directed mutagenesis in conserved uncharged sequence (a.a 118-137) alters the fusion activity of the VSV G protein (Fredericksen and Whitt 1996, Zhang and Ghosh 1994). Replacement of amino acids at G124L, F125A, F125D, F125Y, A133K, E139R, P127G, D137N and E139L results in inhibition of membrane fusion. Involvement of residues 118 – 136 in membrane fusion was verified by photolabeling experiments conducted by Durrer *et al.* (1995). Analysis of the labeled protein showed that only amino acid residues between 58 – 221 directly interact with the membrane during fusion. The P2-like peptide (a.a 137 - 168), which can bind to phosphatidylserine, can also induce membrane fusion in a pH-dependent manner (Coll 1997, Carneiro *et al.* 2003). Therefore, it is most likely that the region containing amino acid 80 – 161 is directly involved during membrane

fusion (Coll 1997). Other regions, like H10 / A4 (a.a 395 – 410), also play a critical structural role during membrane fusion (Shokralla *et al.* 1999, 1998). It has been observed that membrane proximal domain preceding the membrane anchoring domain is conserved in the G protein of vesiculoviruses (Bhella *et al.* 1998, Coll 1995). Jeetendra *et al.* (2003) showed that the juxtamembrane region (a.a 440 – 461) is essential for the membrane fusion activity of VSV G. Deletion mutation at GΔ9 (lacking a.a 453 – 461), GΔ13 (lacking a.a 449 – 461) and ΔF 440 – N 449 (lacking a.a 440 – 449) could not induce syncytium formation at fusion active pH (Jeetendra *et al.* 2003). However, it was observed that oligomerization and transport of glycoprotein to the cell surface was not affected by this deletion mutation (Jeetendra *et al.*2003). Substitution of transmembrane domain of VSV G protein with GPI anchor inhibits the membrane fusion activity, which suggests that anchoring to the membrane through transmembrane domain is essential for VSV G mediated membrane fusion (Odell *et al.* 1997). The bromelain cleaved fragment of the influenza HA glycoprotein (BHA) has been found to interact with the liposomal membrane and undergoes a similar kind of conformational change as that of the intact HA molecule (Wharton *et al.* 1988, Skehel *et al.* 1982, Harter *et al.* 1988, Durrer *et al.* 1996). It was reported that GPI-anchored HA fusion glycoprotein induced lipid mixing but could not induce complete transfer of soluble content (Kemble *et al.* 1994). However, influenza virus HA ectodomain expressed (FHA2) in *E.coli* could induce lipid mixing and a small amount of content mixing in model liposome (Epand *et al.* 1999).

Therefore, our objective was to determine whether the ectodomain of VSV G can induce membrane fusion on its own. Membrane fusion can be studied either by studying lipid mixing by resonance energy transfer (RET) assay or by studying aqueous content mixing. Lipid mixing assay could be carried out with a system which exhibits content leakage, in contrast content mixing requires a system which is non-leaky. To further understand the VSV G mediated membrane fusion we studied the conformational change of the soluble ectodomain of G (Gs) at different pH by spectroscopic analysis.

3.1 Generation of soluble ectodomain of VSV G

The ectodomain of VSV G can be generated in two ways. The first approach is to clone the ectodomain in a suitable expression system, and the second approach is to generate the soluble ectodomain by limited proteolysis. The FHA2 fragment (containing the first 127 amino acid residues of HA2 ectodomain) expressed in *E.coli* BL21 strain showed a significant amount of membrane fusion activity (Epand *et al.* 1999). Also, cDNA of the NDV surface glycoprotein was cloned and expressed in mammalian cells for crystallization (Chen *et al.* 2001). Therefore, cDNA of the VSV G ectodomain containing Asn37 – Ser463 was cloned by Yao (2001) in pGEX-2TTEV and pProEX-HTb vectors containing TEV cleavage sites. The proteins were expressed in *E. coli* BL21 strain by IPTG induction, which produced GST-G* and His-G* fusion peptides. Cells were grown up to 0.6 OD

and then induced with 0.5 mM IPTG for 3 hours at 37°C. The cells were lysed in STE or TBE buffer containing 1% sarkosyl by three cycles of French press, and the cell debris was removed by centrifugation at 12,000*g* for 30 min. (Frangioni and Neel 1993). The supernatant was incubated with GSH – agarose beads or Ni – NTA agarose beads and the fusion proteins were eluted with glutathione or imidazole, respectively (Fig 5a and 5b). The GST fusion protein (GST – G*) was insoluble in 50 mM Tris pH 7.4 containing 150 mM NaCl and required 0.5% sarkosyl (17mM) for solubilization. The GST – G* can be cleaved with TEV protease when the proteins are bound to GSH beads. Once the GST moiety is removed, the G* protein precipitates, and is difficult to resolubilize even with 1% sarkosyl . All attempts to purify the cleaved ectodomain were unsuccessful. The His – G* was successfully purified in soluble form with 1% sarkosyl. The His – G* eluted from Ni – NTA agarose beads required 0.5% sarkosyl to remain soluble. The His tag cannot be removed with TEV protease, as TEV is inactive in the presence of sarkosyl. Both the fusion peptides were unable to induce any membrane fusion (no other detergents were tested for G* purification).

Another approach to generate soluble VSV G ectodomain (Gs) is by using proteolytic digestion. Previously, soluble ectodomains of the TBE E and SFV E1 glycoproteins were generated by limited proteolytic cleavage (Heinz *et al.* 1991, Wengler *et al.* 1999). Crimmins *et al.* (1983) were able to purify the soluble G

Fig.5: SDS polyacrylamide gel of purified fusion protein, GST – G* and His – G*. The proteins were expressed in *E – coli* by IPTG induction for 3 – 4 hours at 37°C. The GST – G* and His – G* proteins were purified by GSH – Agarose and Ni- NTA agarose beads respectively in the presence of 0.5% sarkosyl. GST fusion proteins were eluted with reduced glutathione and His fusion protein was eluted with imidazole. Sample from each steps were collected and analyzed on a SDS-polyacrylamide gel. Protein was visualized by coomassie blue staining. a and b represent the purification of GST-G* and His-G* fusion proteins, respectively. The proteins were further purified by passing through sepadex G150 column (c).

a.

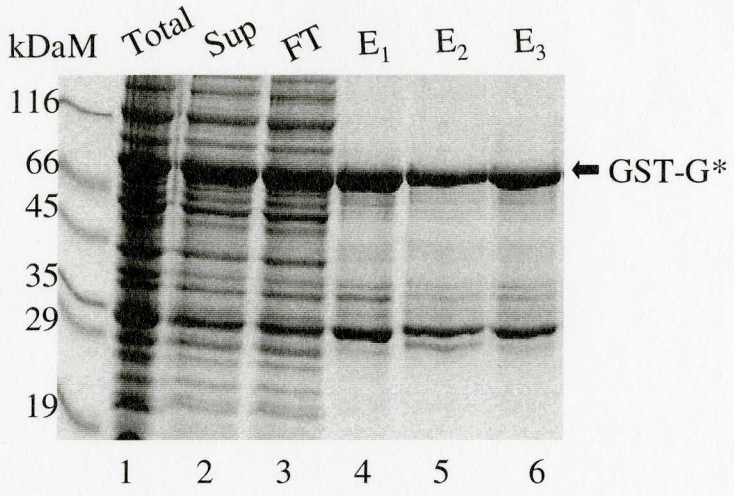
kDaM
Total
Sup
FT
E1
E2
E3
116
66
45
35
29
19
GST-G*
1
2
3
4
5
6

b.

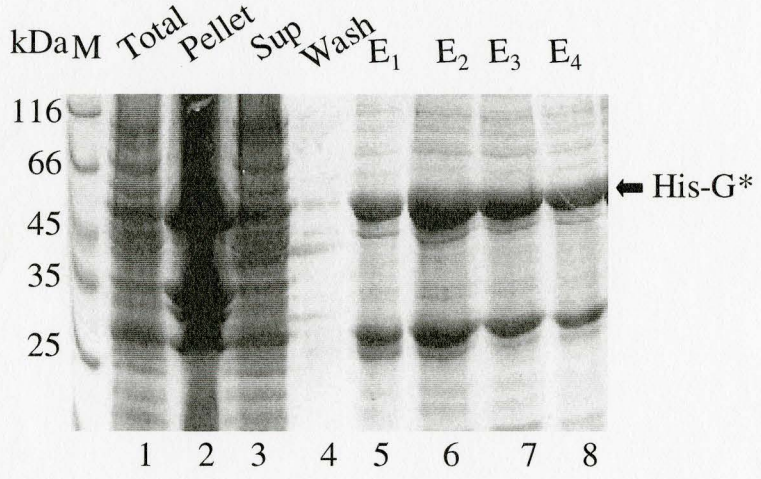
kDa M
Total
Pellet
Sup
Wash
E1
E2
E3
E4
116
66
45
35
25
His-G*
1
2
3
4
5
6
7
8

c.

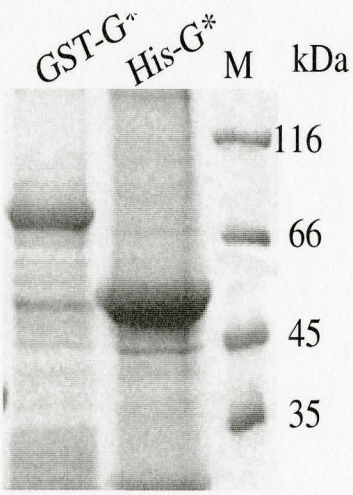
GST-G*
His-G*
M
kDa
116
66
45
35

protein by cathepsin D digestion of VSV G protein at low pH. Therefore, VSV G was subjected to trypsin (tolylsulfonyl phenylalanyl chloromethyl ketone treated) digestion under different conditions, including varying trypsin to protein ratios, time of digestion and the pH of incubation (Fig. 6). Effects of neutral detergents were also tested. When VSV was treated with trypsin at pH 7.4, the G protein was completely digested by trypsin in presence of Triton X – 100. However, in the absence of Triton X – 100, the G protein was resistant to trypsin digestion (Fig. 6a). It seems therefore that Triton X – 100 is required for the trypsin digestion. It was observed that at pH 5.4, the G protein was resistant to trypsin digestion even in the presence of Triton X – 100 (Fig. 6b). Analysis of the digested protein on 8% SDS-PAGE showed that VSV G was not completely resistant to trypsin digestion; instead, it released a shorter fragment (Gs) with an approximate molecular weight of 62 kDa (Fig. 6c). Trypsin completely digested the G protein at pH 5.4 in the presence of 0.9% SDS, which suggests that the low molecular fragment was generated by limited trypsin digestion. Gs obtained by Cathepsin D digestion (Crimmins *et al.* 1983), or the soluble Gs released in the culture medium after infection with VSV (Irving and Ghosh 1982, Wabnitz and Kruppa 1984, Chatis and Morrison 1983) also has molecular weight of about 60 – 62 kDa and lacks the COOH – terminal membrane spanning domain. It has been observed that VSV G was also resistant to trypsin digestion when incubated at pH7.4 for one hour on ice (Fig. 6d). The 62 kDa fragment was also generated by

Fig. 6: Generation of soluble ectodomain of VSV G by limited trypsin digestion. a) VSV was digested with trypsin at 25:1 of protein to trypsin ratio (lanes1, 4 and 5) and 5:1 ratio (lanes 2 and 3) at pH 7.4 at 37°C in the presence and absence of Triton X 100 (lanes 1 and 2 and lanes 3, 4 and 5, respectively) for 30 min (lanes 1, 2, 3, and 4) and One hour (lane 5). The reaction was stopped with PMSF. b) Trypsin digestion of VSV at pH 5.4 with 25:1 and 5:1 of protein to trypsin ratio (lanes 2, 3, 6 and 7 and lanes 1, 4 and 5, respectively) at 37°C for 30 min. in presence and absence of Triton X 100 (lanes 1, 2, 3 and 4 and lane 5, 6 and 7, respectively). c) Trypsin digestion of VSV at pH 5.4 with 25:1 (lane 2), 15:1 (lane 3) and 5:1 (lane 4) of protein to trypsin ratio at 37°C for 30 min. in the presence of Triton X 100. The activity of trypsin at pH 5.4 was tested by adding 0.9% SDS to the reaction mixture (lane 5). Samples were resolved in 8% SDS PAGE. d) Trypsin digestion of VSV at pH7.4 with 25:1 of protein to trypsin ratio on ice for 1hr (Lane 3) and 2hr. (lane 4) in the presence of Triton X 100 (lane 3 and 4) for one hour (lane 1) and two hours (lane 2). Digestion of M protein by trypsin suggests that the trypsin is active at that temperature.

a.

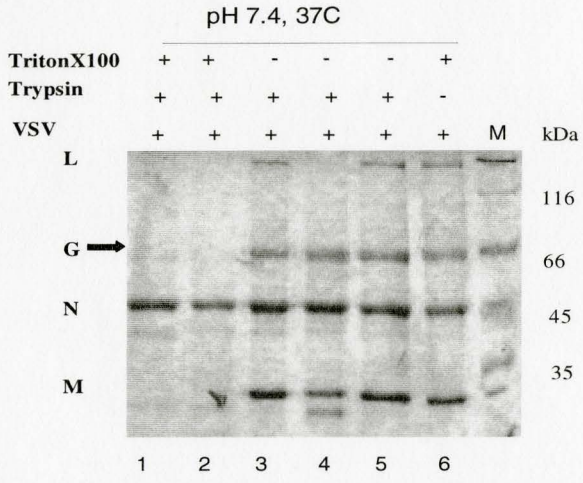
pH 7.4, 37C
TritonX100 + + - - - +
Trypsin + + + + + -
VSV + + + + + + M kDa
L
G
N
M
116
66
45
35
1 2 3 4 5 6

b.

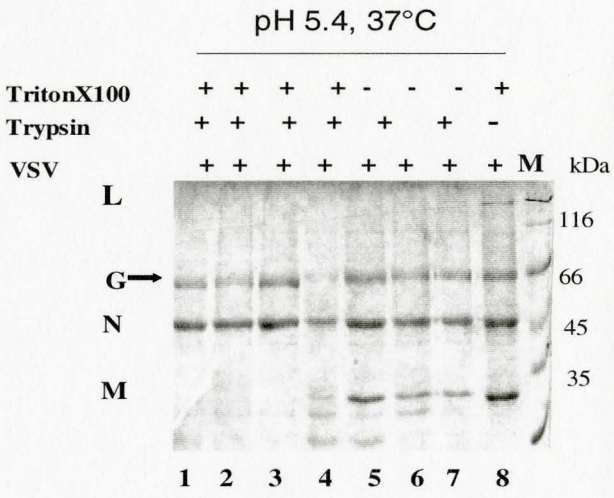
pH 5.4, 37°C
TritonX100 + + + + - - - +
Trypsin + + + + + + -
VSV + + + + + + + + M kDa
L
G
N
M
116
66
45
35
1 2 3 4 5 6 7 8

c.

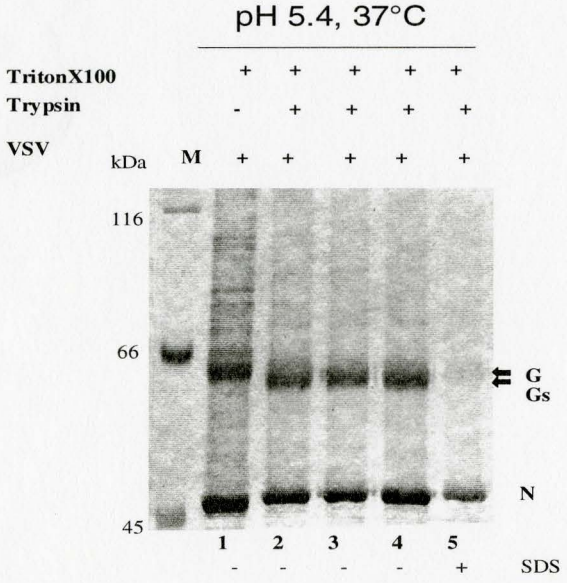
pH 5.4, 37°C
TritonX100 + + + + +
Trypsin - + + + +
VSV + + + + +
kDa M
116
66
45
G
Gs
N
1 2 3 4 5
- - - - + SDS

d.

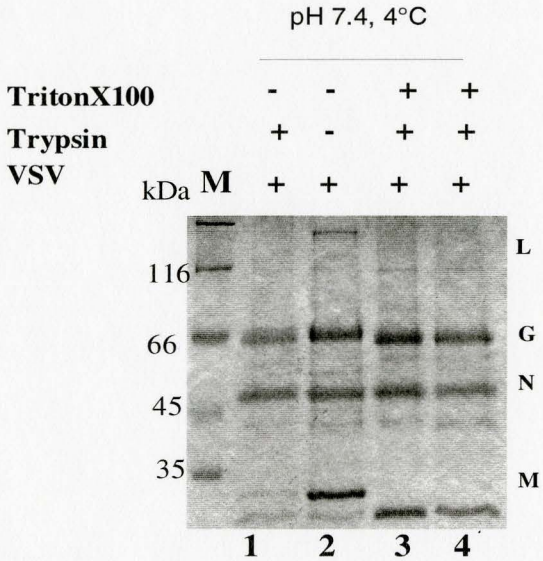
pH 7.4, 4°C
TritonX100 - - + +
Trypsin + - + +
VSV + + + +
kDa M
116
66
45
35
L
G
N
M
1 2 3 4

Fig.7: SDS polyacrylamide gel electrophoresis of trypsin digested VSV in the presence of 1% octylglucoside. The VSV was digested with trypsin at 25:1 of protein to trypsin ratio at pH 7.4 (lane 2) and pH 5.4 (lane 4) at 37°C for 30 minute. The activity of trypsin at pH 5.4 was shown by digestion of VSV in the presence 0.9% SDS.

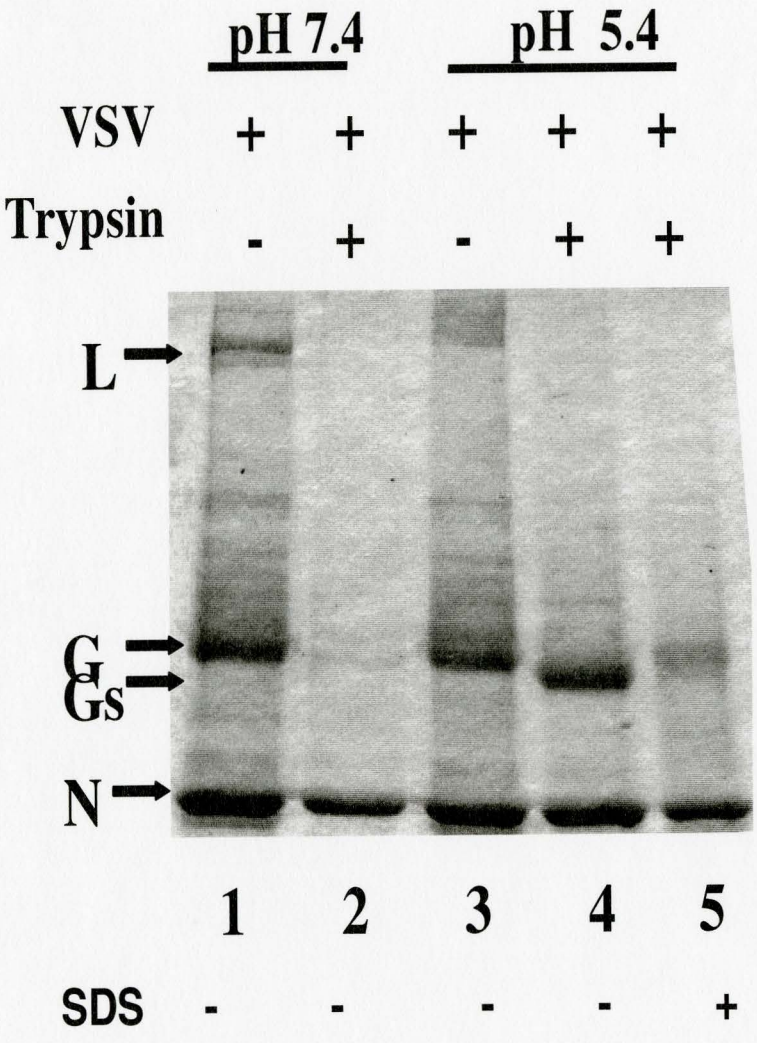
pH 7.4
pH 5.4
VSV + + + + +
Trypsin - + - + +
L
G
Gs
N
1 2 3 4 5
SDS - - - - +

Fig.8: Digestion of VSV with a) trypsin, chymotrypsin, subtilisin and thermolysin ,b) bromelain and c) pronase. VSV was digested at 37°C with trypsin (15:1; protein: trypsin, 30min.), chymotrypsin (15:1, 30min.), subtilisin (10:1, 30min.), thermolysin (10:1, 1hr.), bromelain (8:1, 30 min) and pronase (10:1, 30 min.) at pH 7.4 and pH 5.4 in presence of 1% Triton X 100. The reaction was stopped with 5mM PMSF for trypsin and subtilisin, 2mM TPCK for chymotrypsin and bromelain and 5mM EDTA for thermolysin, respectively. The gels are representative of two separate experiments.

a.

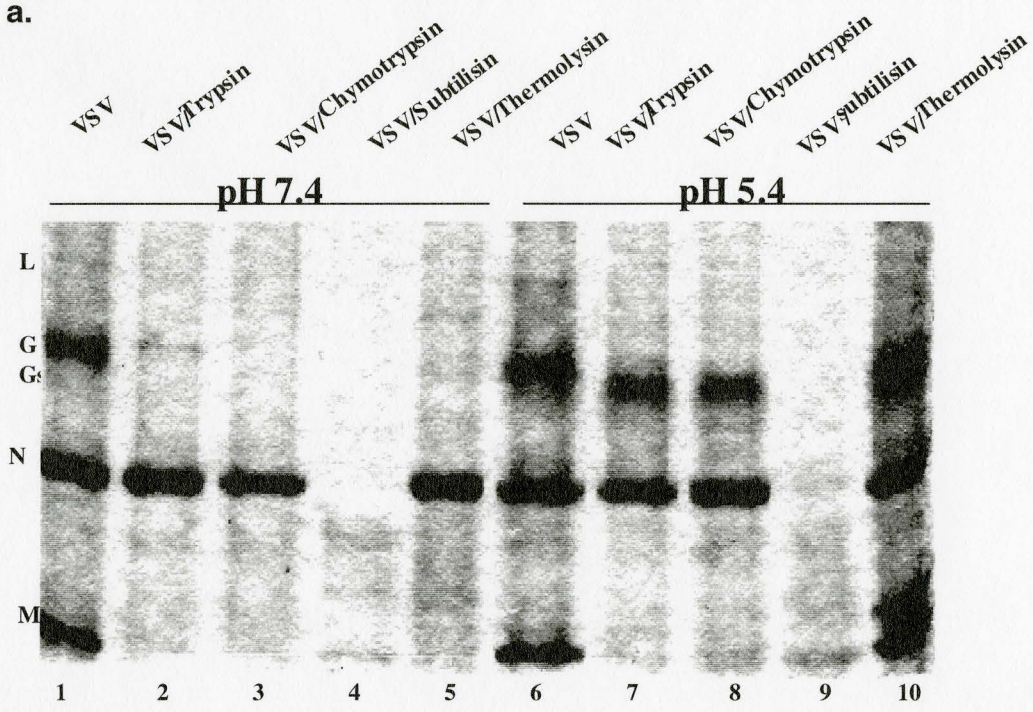
VSV
VSV/Trypsin
VSV/Chymotrypsin
VSV/Subtilisin
VSV/Thermolysin
VSV
VSV/Trypsin
VSV/Chymotrypsin
VSV/subtilisin
VSV/Thermolysin
pH 7.4
pH 5.4
L
G
Gs
N
M
1 2 3 4 5 6 7 8 9 10

b.

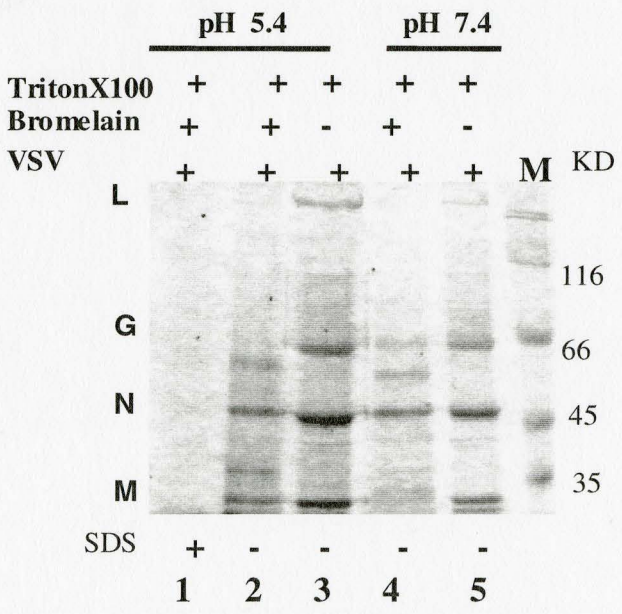
pH 5.4
pH 7.4
TritonX100 + + + + +
Bromelain + + - + -
VSV + + + + +
M
KD
L
G
N
M
116
66
45
35
SDS + - - - -
1 2 3 4 5

c.

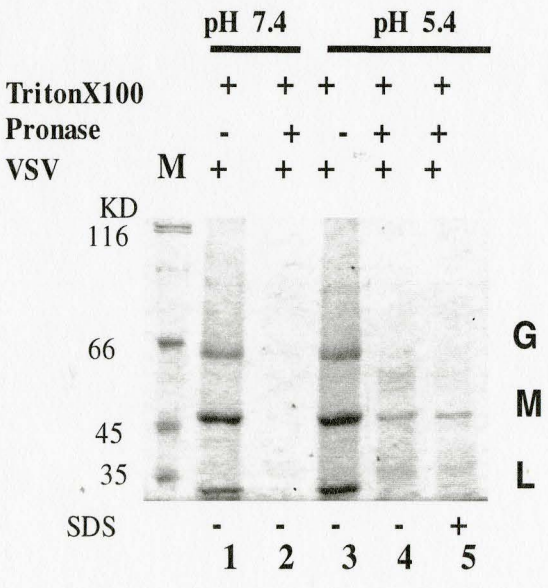
pH 7.4
pH 5.4
TritonX100 + + + + +
Pronase - + - + +
VSV
M + + + + +
KD
116
66
45
35
G
M
L
SDS - - - - +
1 2 3 4 5

trypsin digestion at pH5.4 in the presence of octylglucoside (Fig. 7). Octylglucoside was used because this detergent could be easily removed by dialysis or gel filtration due to the high CMC of the detergent (20-25 mM) (Lorber *et al.* 1990).

To check whether other proteases can generate similar soluble fragments, VSV G was subjected to proteolytic digestion with bromelain, chymotrypsin, pronase, thermolysin, and subtilisin in the presence of detergent at 37°C. After incubation for the required time interval, subtilisin was inhibited with 5 mM PMSF, chymotrypsin and bromelain were inhibited with 2 mM TPCK, and thermolysin was inhibited with 5 mM EDTA. Aliquots were taken and run on 8% SDS-PAGE. VSV G was completely digested by all other proteases except thermolysin and chymotrypsin (Fig. 8a,b,c). VSV G was resistant to chymotrypsin and thermolysin digestion at pH 5.4. The thermolysin, which is a metaloenzyme, is inactive at pH 5.4, but chymotrypsin is active at pH 5.4 and could generate a low molecular weight fragment of approximately 61 – 62 kDa.

3.2 Purification of Gs

The soluble ectodomain of VSV G was obtained by limited trypsin digestion at pH 5.4. For large scale Gs production, trypsin was selected over cathepsin D because trypsin is more economical than cathepsin D (Crimmins *et al.* 1983).

Fig.9: Purification of Gs. a) SDS PAGE analysis of purified Gs. VSV was digested with trypsin (15:1of protein to trypsin ratio) in presence of 1.5% octylglucoside at pH 5.4 at 37°C for 30 min. The reaction was stopped with trypsin inhibitor. The Gs was collected in the supernatant after ultra-centrifugation at 36k r.p.m in a SW 50 rotor in Beckman L8-M ultracentrifuge and concentrated by passing through 30 kDa cutoff filter and further purified through sephadex G 200. The residual trypsin activity was removed by passing the Gs through benzimidine sephadex column. b) Sephadex G 200 elution profile of Gs. The Gs protein obtained in the supernatant after ultracentrifugation in pH 5.4 buffer was buffer exchanged to pH 7.4 buffer by passing through 30 cm x 0.9 cm sephadex G 200 column, equilibrated with pH 7.4 buffer, at flow-rate of 0.15 ml/min. The fractions containing Gs were combined and passed through a benzimidine sephadex column.

a.

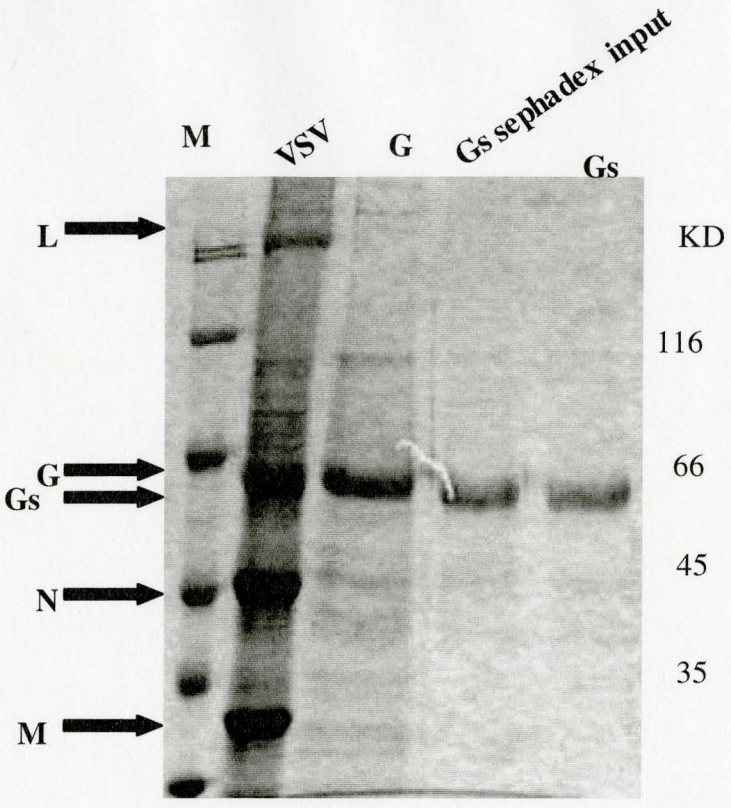
M
VSV
G
Gs sephadex input
Gs
L
G
Gs
N
M
KD
116
66
45
35

b.

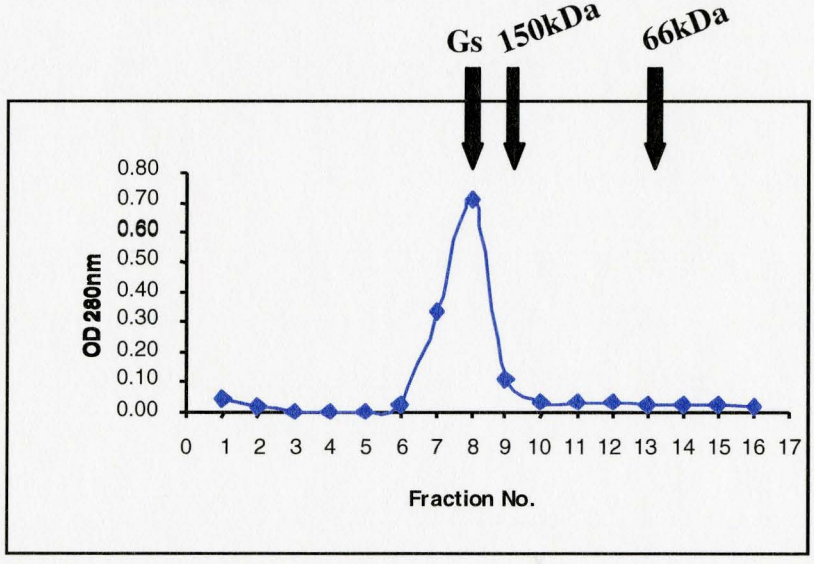
Gs
150kDa
66kDa
OD 280nm
0.80
0.70
0.60
0.50
0.40
0.30
0.20
0.10
0.00
0 1 2 3 4 5 6 7 8 9 10 11 12 13 14 15 16 17
Fraction No.

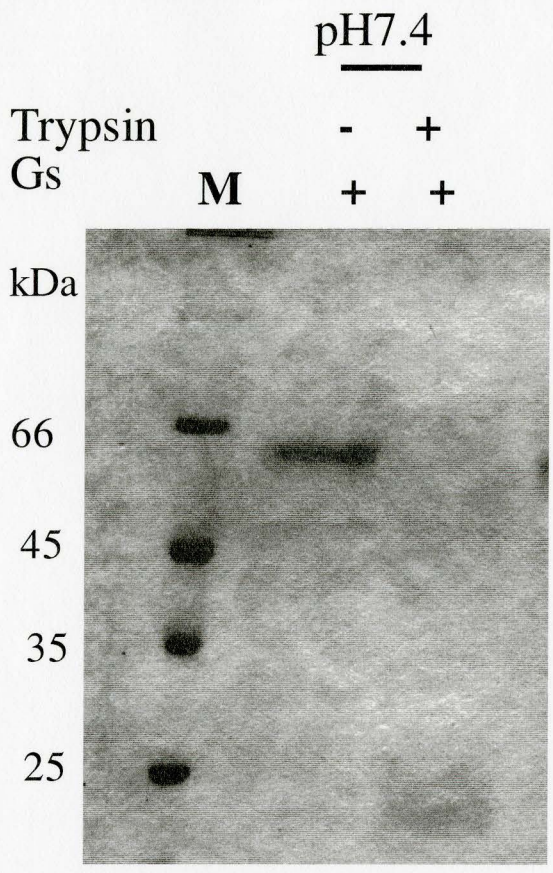

Fig. 10: Reversibility of structure of Gs at pH 7.4. 10 μg of Gs was incubated with 0.5μg of trypsin (TPCK treated) at 37°C for 30 min. in the presence of Triton X 100. The reaction was stopped with 1mM PMSF. Samples were analyzed on a 10% SDS–PAGE and protein was visualized by coomassie blue staining. The gel shown is representative of two separate experiments.

Therefore, we tried trypsin digestion of VSV G to generate Gs for possible crystallization. The reaction was carried out at pH 5.4. VSV was treated with trypsin at a ration of 15:1 (protein: trypsin ratio) in the presence of 1.5% octylglucoside in pH 5.4 buffer at 37°C for 30 min. The reaction was stopped with soybean trypsin inhibitor. The supernatant containing Gs was collected after ultracentrifugation at 36K r.p.m. in a SW-50 rotor in Beckman L8-M ultracentrifuge for 1.5 hours. The Gs was then concentrated through a 30 kDa cutoff PALL filter and further purified and the buffer was exchanged by passing through a sephadex G 200 column equilibrated with pH 7.4 buffer. The fractions containing Gs were pooled, and the residual trypsin was removed by passing through a benzimidin-sephadex column. The protein was collected as a single band and recovery was nearly 60% (Fig 9a and b).

VSV G protein undergoes reversible conformational change when exposed to low pH and should revert back to its native conformational state at neutral pH (Crimimins *et al.* 1983, Clague *et al.* 1990, Blumenthal *et al.* 1987, Puri *et al.* 1988). The protein was tested for its structural reversibility at neutral pH from acidic pH by trypsin sensitivity assay. Trypsin completely digests the VSV G protein at pH 7.4 and the protein becomes resistant to trypsin digestion at acidic pH (Shokralla *et al.* 1998, Odell *et al.* 1997). When Gs was subjected to trypsin digestion, it was observed that trypsin completely digests Gs at pH 7.4, which

Fig. 11: Liposome binding assay to determine the interaction of G and Gs with lipid vesicles. VSV G and Gs were incubated with liposome made up of equimolar amount of PC and PS for 30 min. at pH 7.4 (a, b, c and d) and pH 5.4 (e and f) at 37°C. To the reaction mixtures 80% sucrose solution in respective pH buffer was added to make up to 50% sucrose solution, which was then over layered with 20% and 5% sucrose solution respectively. Gradients were spun for 2 hours at 50K r.p.m. in a SW-50 rotor in Beckman L8-M ultracentrifuge. Eight fractions of 0.5 ml were collected from each set and sample from each fractions were resolved on 10% SDS-PAGE. Gels were visualized after staining with coomassie blue stain.

a. VSV G pH 7.4

b. Gs pH 7.4

c. VSV G + LIPOSOME pH 7.4

d. Gs + LIPOSOME pH 7.4

e. VSV G + LIPOSOME pH 5.4

f. Gs + LIPOSOME pH 5.4

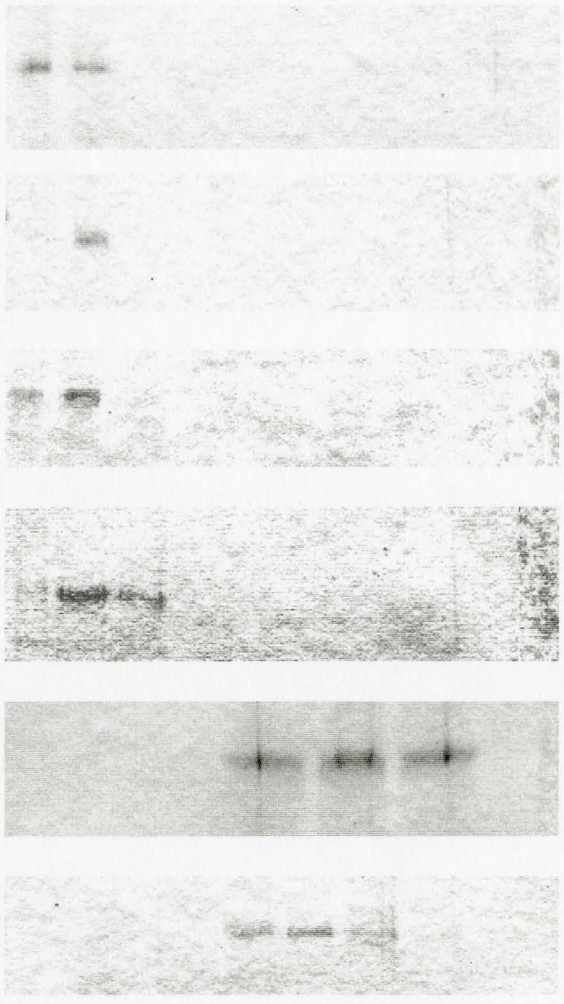

Fraction No. 1 2 3 4 5 6 7 8

BOTTOM TOP

indicates that Gs has reverted back to its native conformation at neutral pH (Fig. 10).

3.3 Lipid binding assay

The biological activity of Gs was determined by studying its membrane interactions at both neutral and fusion-active pH. The VSV G protein interacts with artificial membrane vesicles in a pH-dependent manner (Carneiro *et al.* 2001, Pak *et al.*1997, Capone 1983). Therefore, we investigated whether purified Gs can bind to the artificial membrane vesicle at low pH by using the membrane flotation assay. The VSV G and Gs were incubated at pH 7.4 or pH5.4 with liposome (SUV) made up of phosphatidylserine and phosphatidylcholine (1:1) for 30 min at 37°C. 80% sucrose solution (in pH 7.4 or 5.4 buffer) was added to the reaction mixture to make solution of 50% sucrose. It was then overlaid with 20% and 5% sucrose solutions (in pH 7.4 or 5.4 buffer). The gradients were run at 50 K r.p.m for 2 hours at 4°C using Beckman SW-50 rotor. 500-µl fractions were collected and samples were run on SDS-PAGE (Fig. 11). The G and Gs proteins were collected in the bottom fraction when incubation was done at pH 7.4 in the presence or in the absence of liposomes. This indicates that G or Gs does not bind to liposomes at neutral pH. In contrast, G and Gs were collected in the top fraction when they were incubated with liposome at pH 5.4. The results suggested that G and Gs can bind to liposomes at fusion-active pH.

3.4 Cross linking experiment to determine the oligomeric state of Gs

VSV G and Gs protein released into infected cells form dimers and trimers. They exist in a dynamic equilibrium between the monomer and trimer at both neutral and fusion-active pH (Wilcox *et al.* 1992, Crise *et al.* 1989, Zagouras and Rose 1993, Lyles *et al.* 1990). Soluble TBE E protein forms dimers at neutral pH, but it cannot form trimers at fusion-active pH in the absence of membrane (Stiasny *et al.* 2002). It was suggested that either the stem anchor region or membrane may be required for trimer stability. Therefore, we attempted to determine whether Gs released by limited trypsin digestion can form trimers by chemical cross – linking with DTSSP (dithiobis[sulfosuccinimidylpropionate]). DTSSP bridges two interacting proteins by reacting with the free amino group in the protein, with subsequent release of a hydroxyl succinimide ester (Lomant and Fairbanks 1976, Carlsson *et al.* 1978). The cross linking of VSV G and Gs was done as described by Lyles *et al.* in 1990. VSV G and Gs were added to HEPES buffer and pH was adjusted to 5.4 with pre-determined amount of 0.5M Na -acetate buffer. DTSSP was then added and incubated for 30 min on ice and the reaction was quenched with 1M Tris. The proteins were resolved through 8% SDS-PAGE and proteins were visualized by Western blotting (Fig. 12). It was observed that both VSV G and Gs formed dimers and trimers at neutral and acidic pH. No oligomerization was observed in the absence of the cross linker. Trimer formation by Gs was also supported by the elution profile at neutral pH (Fig.

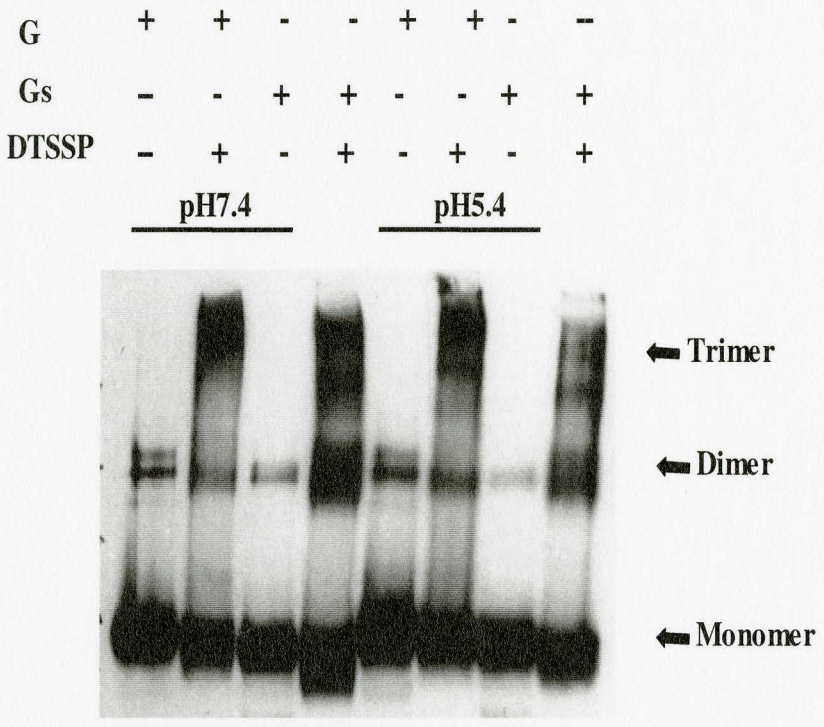

Fig. 12: Oligomarization of VSV G and Gs with the crosslinking agent DTSSP at pH 7.4 and pH 5.4. 10μg of VSV G or Gs was added to 20 μl of 50mM HEPES pH 7.4, 150 mM NaCl buffer. The pH was adjusted to 5.4 with precalibrated amount of 0.5 M Na acetate buffer. 500μM of DTSSP was added to the samples and incubated for 30 min. on ice. The reaction was quenched for 15 min. with 1 M Tris. The protein bands were visualized by western blotting. The western blot shown is representative of three separate experiments.

10b). When Gs was passed through Sephadex G 200, it eluted just one fraction ahead of the 150kDa fragment, indicating that Gs may exist as trimer at neutral pH.

3.5 Aggregation of Gs at low pH

Aggregation of Gs with a decrease in pH was examined by light scattering measurements. Carneiro *et al.* (2001) showed that VSV G starts to aggregate between pH 7.5 and 6. The increase in light scattering of Gs (30 μg/ml) was measured in a spectrofluorometer by setting excitation wavelength and emission wavelength at 280 nm. The pH was gradually adjusted to the required value with pre-determined amount of 0.1M citric acid. It was observed that acidification promotes aggregation of Gs protein and the aggregation gradually increased with decreasing pH until it reached pH 5 (Fig. 13). The Gs protein aggregates possibly due to interactions between the hydrophobic regions that are exposed during conformational change (Carneiro *et al.* 2001). As VSV G does not exist in a metastable conformation, a larger complex of a G protein trimer may be required to drive the fusion process (Yao *et al.* 2003). Unlike the TBE E protein, for the G protein it seems that oligomerization and aggregation do not require the transmembrane region, and the Gs protein can form trimers independent of liposomal membranes (Crise *et al.* 1989).

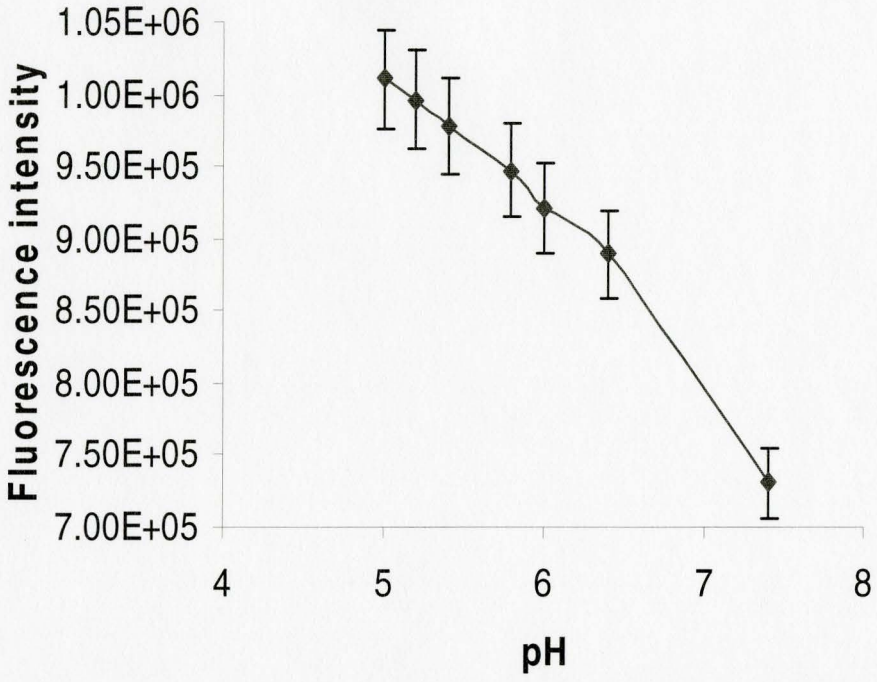

Fig. 13: Aggregation of Gs at low pH. The aggregation of Gs was measured by right angle light scattering using a Photon technology international fluorimeter with emission and excitation monochromators both set at 280nm. Gs protein at a final concentration of 45μg/ml was added to 2ml of 10mM HEPES pH 7.4 and 150mM NaCl. The pH was gradually lowered by adding pre-calibrated amount of 0.1M citric acid and light scattering was measured. Average data and standard deviation of 10 data points are shown.

3.6 Lipid mixing assay

The lipid-binding assays suggested that the VSV G and Gs protein can interact with liposomal membranes in a pH-dependent manner. Blumenthal *et al.* (1987) and Carneiro *et al.* (2001) showed that the purified VSV G protein can also induce liposome fusion, but at a much reduced rate than the intact virus. The FHA2 fragment containing the influenza virus HA2 ectodomain could induce membrane fusion (Epand *et al.* 1999). Therefore, a resonance energy transfer (RET) assay as described by Struck *et al.* (1981) and Hoekstra and Düzgünes (1993), was used to study the fusion activity of the Gs protein. The RET assay is based on the principle of fluorescence energy transfer between a donor fluorophore and the acceptor fluorophore. If the emission wavelength of the donor fluorophore overlaps with the excitation wavelength of the acceptor molecule, and if the two probes are in close physical proximity to each other, then excitation of donor probe will result in transfer of excited state energy to the acceptor. This results in quenching of the donor fluorescence and subsequent increase in the acceptor fluorescence. Labeled liposomes were made up of two fluorophores, NBD – PE (donor, λ_{ex} 465 nm and λ_{em} 530 nm) and Rh – PE (acceptor, λ_{ex} 530 nm and λ_{em} 590 nm). Mixing of NBD – PE and Rh – PE results in quenching of the NBD fluorescence. When labeled liposomes are fused with unlabeled liposomes, the apparent distance between donor and acceptor fluorophores increases, resulting in increased NBD fluorescence because no

Fig. 14: Lipid mixing by resonance energy transfer (RET) assay. 50μmoles of unlabeled liposome and 5.5 μmoles of labeled liposome containing equimolar amounts of PC and PS were incubated with different amounts of VSV (a), VSV G (b) and Gs (c). The pH was lowered with pre calibrated amount of 0.1 M citric acid and the increase in NBD fluorescence was measured at excitation wavelength of 465nm and emission wavelength of 530nm. The 100% fusion was determined by adding 10% Triton X 100. a) Kinetics of liposome fusion with 10 μg/ml (1), 20 μg/ml (2), 40 μg/ml (3) and 80 μg/ml (4) of VSV at pH 5.4 and 37°C. b) Kinetics of liposome fusion with 0.06 μmoles (1), 0.116 μmoles (2), 0.232 μmoles (3) and 0.5 μmoles (4) of VSV G proteins at pH 5.4 and 37°C. c) Kinetics of liposome fusion with 0.06 μmoles (1), 0.116 μmoles (2), 0.232 μmoles (3) and 0.5 μmoles (4) of Gs proteins at pH 5.4 and 37°C. The plots are representative of two independent experiments.

a. VSV

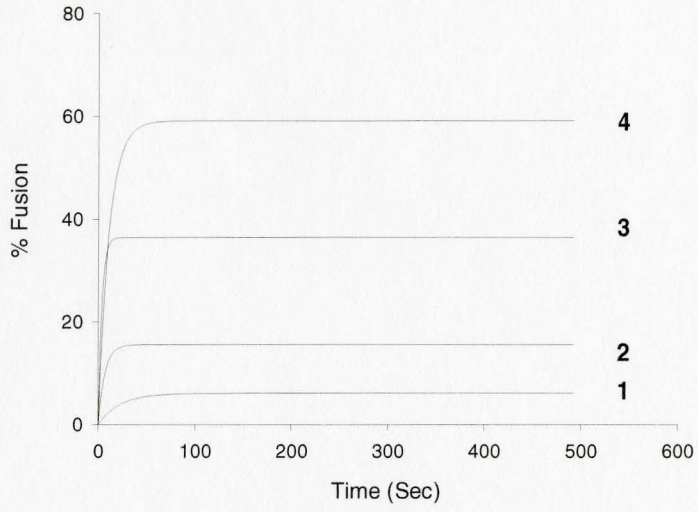
80
60
40
20
0
% Fusion
0
100
200
300
400
500
600
Time (Sec)
4
3
2
1

b.

G

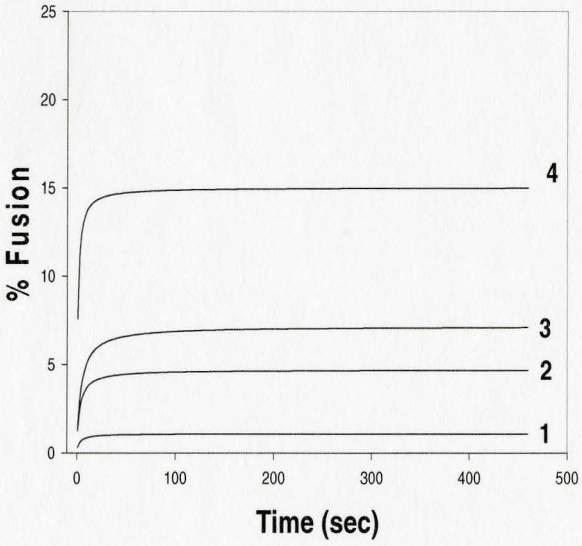
25
20
15
10
5
0
% Fusion
0
100
200
300
400
500
Time (sec)
4
3
2
1

c.

Gs

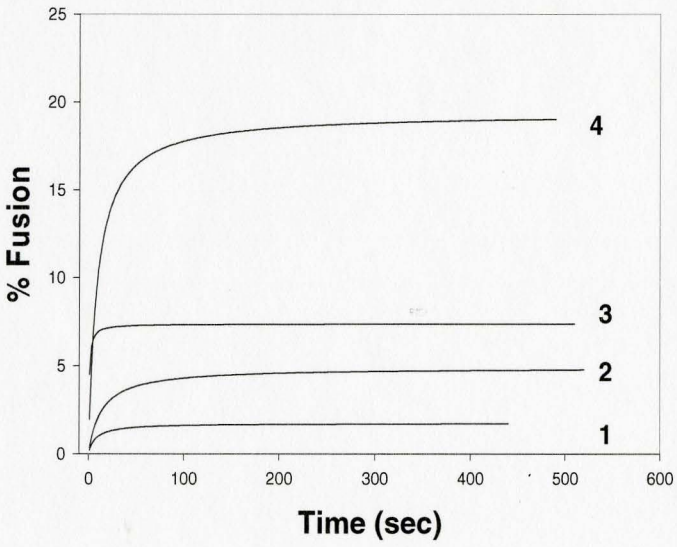
25
20
15
10
5
0
% Fusion
0
100
200
300
400
500
600
Time (sec)
4
3
2
1

Fig. 15: Determination of optimum pH of liposome fusion for VSV G (a) and Gs (b) by resonance energy transfer (RET) assay. 50μmoles of unlabeled liposome and 5.5 μmoles labeled liposome was incubated with VSV G and Gs at pH 7.4 at 37 °C. The pH was adjusted to 7.4, 6.4, 5.8, 5.2 or 5 with pre- calibrated amount of 0.1M citric acid. The increase in NBD fluorescence was measured at excitation wavelength of 465nm and emission wavelength of 530nm. The 100%fusion was determined by adding 10% Triton X 100 to the sample.

a.

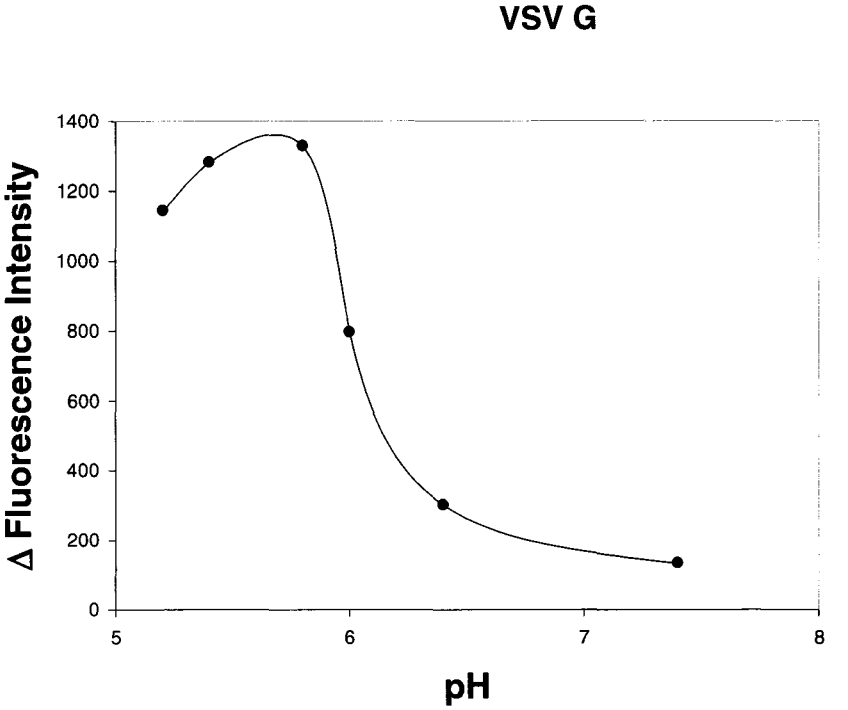
VSV G
Δ Fluorescence Intensity
1400
1200
1000
800
600
400
200
0
5
6
7
8
pH

b.

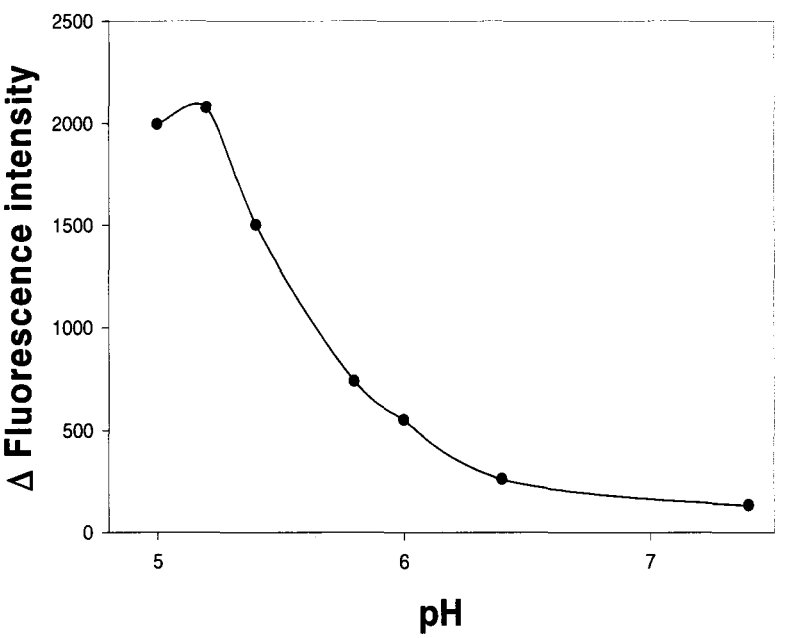
Gs
Δ Fluorescence intensity
2500
2000
1500
1000
500
0
5
6
7
pH

resonance energy transfer can take place between NBD – PE to Rh – PE. Liposome fusion kinetics are generally measured by determining the increase in NBD fluorescence. In a typical experiment, labeled and unlabeled liposomes were mixed in 1:9 ratios and varying amounts of the fusion proteins or virus was added. VSV G and VSV were used as positive controls, and the effects of the protein storage buffer and the detergent used in it were also tested. The amount of fusion protein was kept comparable in all experiments. For VSV, it was considered that 25% of the total viral protein was G protein. The pH was lowered to the required value with pre-determined amount of 0.1 M citric acid, 10% Triton X – 100 was added for complete mixing of the liposome. The results showed that there was no increase in NBD fluorescence with the buffer alone at low pH. It was observed that VSV could induce up to 60% fusion with increasing protein concentration (Fig. 14a), whereas VSV G and Gs induced nearly 16% and 19% fusion, respectively (Fig. 14b,c). Because of the relatively high CMC of octylglucoside, it is easily removed by gel filtration (Lorber *et al.* 1990). However, some trace amounts of detergent might be still present in the protein sample. Therefore, octylglucoside was also tested for its fusion activity. It was observed that octylglucoside (0.15mM final conc.) could not induce membrane fusion in a pH-dependent manner. When fusion kinetics was studied with VSV G and Gs at different pH, it was observed that the optimum fusion pH shifted towards the more acidic side in the case of Gs (Fig 15).

Fig. 16: Effect of PEG on lipid mixing induced by VSV G and Gs proteins. 50μmoles of unlabeled liposome and 5.5 μmoles of labeled liposome made up of equimolar amount of PC and PS was incubated with VSV G (a) and Gs (b) with 1% PEG, 2.5% PEG and 5% PEG. The pH was lowered by adding pre-calibrated amount of 0.1 M citric acid and increase in NBD fluorescence was measured at excitation wavelength of 465nm and emission wavelength of 530nm. The 100% fusion was determined by adding 10% Triton X 100. Effect of 5% PEG on liposome fusion kinetics was also tested. The plots are representative of two independent experiments.

a.

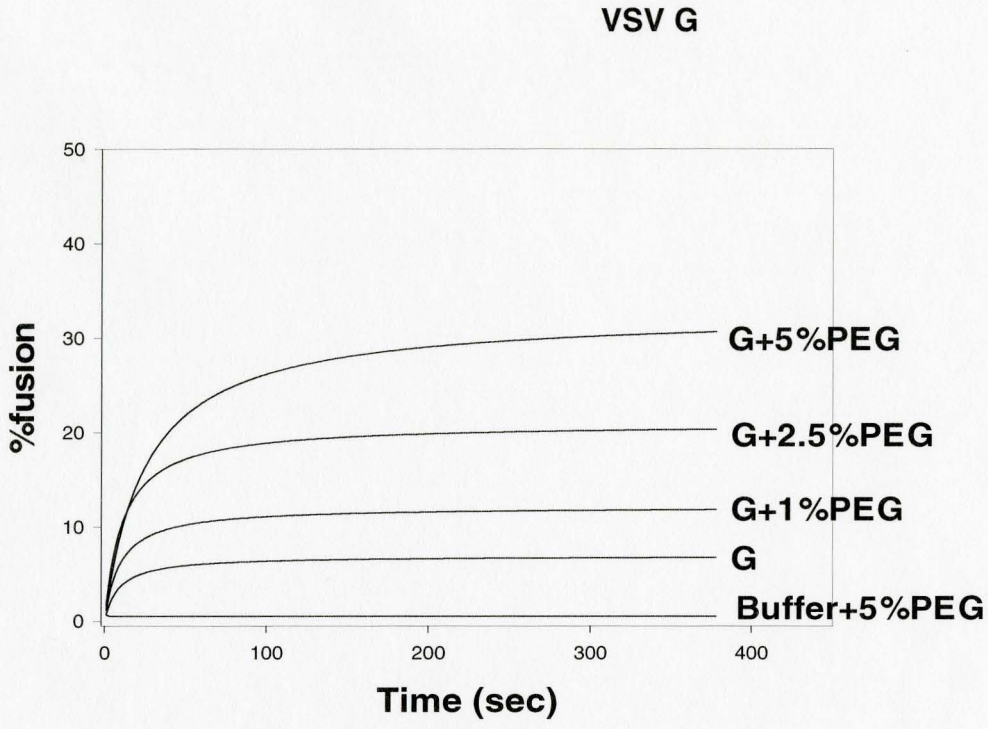
VSV G
%fusion
50
40
30
20
10
0
0
100
200
300
400
Time (sec)
G+5%PEG
G+2.5%PEG
G+1%PEG
G
Buffer+5%PEG

b.

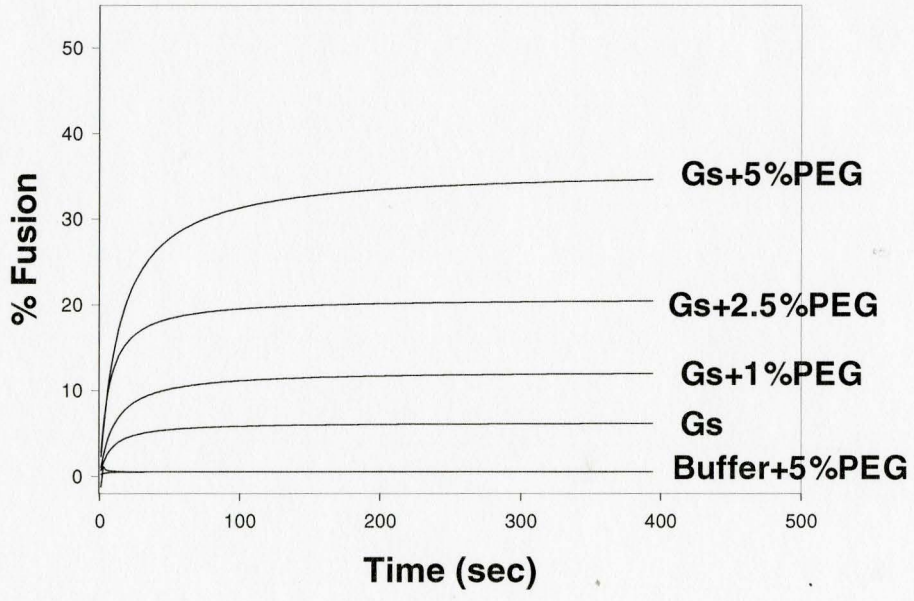
Gs
% Fusion
50
40
30
20
10
0
0
100
200
300
400
500
Time (sec)
Gs+5%PEG
Gs+2.5%PEG
Gs+1%PEG
Gs
Buffer+5%PEG

The extent of liposome fusions induced by VSV G and Gs are nearly similar, but is much less compared to that induced by VSV. It is possible that the G protein anchored to the membrane is essential for efficient membrane fusion. During HA mediated membrane fusion the fusion peptide binds to the target membrane and brings the opposing membrane in close proximity, thereby facilitating the hemifusion (Hernandez *et al.* 1996). Odell *et al.* (1997) showed that anchoring to the membrane is required for fusogenic activity of the VSV G protein. To overcome the energy required for membrane fusion, the G protein may require a bigger fusion complex made up of a large number of trimers of the fusogenic glycoproteins acting in a concerted manner (Gaudin 2000, Yao *et al.* 2003). In the case of VSV G and Gs, the percentage of fusion is determined by the collisional frequency of the interacting liposomes. When the G proteins are not bound to the liposomes, they may not form the large fusogenic complex limiting their fusion activity. Therefore, it was thought that increasing the aggregation of liposomes might improve the fusion efficiency of the protein. Polyethyleneglycol (PEG) is known for enhancing cell – cell fusion and is extensively used for aggregation of biomaterial during protein purification (Durieu and Ochatt 2000). PEG can also induce membrane fusion of SUVs made up of PC when used in significantly high concentration (approx. 25 – 30% (v/v); Talbot *et al.* 1997). However, presence of a small amount of PEG (approx. 1 – 15% v/v) could induce aggregation of liposomes but not membrane fusion. It has been observed that peptides corresponding to transmembrane domain of VSV G could induce

membrane fusion in the presence of 5% PEG (Dennison *et al.* 2002). Therefore, the effects of increasing concentration of PEG (1 – 5% v/v) on membrane fusion were studied to determine if the aggregation of liposomes could improve the efficiency of membrane fusion. It was observed that the aggregation of liposomes increased the fusion efficiency of both VSV G and Gs (Fig. 16A, B). PEG alone could not induce any membrane fusion in a pH-dependent and independent manner. It was observed that at 5% (v/v) PEG concentration, VSV G and Gs induced approximately 30% fusion. These results therefore indicate that the VSV G and Gs could induce lipid mixing and the efficiency of the fusion could be increased by increasing the aggregation of liposome.

3.7 Leakage assay

In general, virus-induced membrane fusion should not be leaky. However, it has been observed that influenza virus-induced membrane fusion is leaky and induces hemolysis (Shangguan *et al.* 1996). Bailey *et al.* (1984) reported that the VSV could induce hemolysis in a pH-dependent manner, which means VSV induced membrane fusion is also leaky. As the rate of content mixing and content leakage are in competition with each other, it was important to measure the content leakage by Gs. The leakage of SUV was measured as described by Talbot *et al.* (1997) and Ellen *et al.* (1985). The leakage of liposomes was

Fig. 17: Vesicle leakage induced by VSV G and Gs proteins. 150μmoles of SUV containing equimolar amount of PC and PS were added to 2ml pH 7 buffer, to that 0.232μmoles or 0.5μmoles of VSV G (a) and Gs (b) fusion glycoproteins were added and pH was bought down to 5.4 with pre – calibrated amount of 0.1M citric acid. Increased in ANTS fluorescence was recorded at excitation wavelength of 360nm and emission wavelength of 530nm. The maximum leakage of vesicles was determined by adding 20μl of 10% Triton X 100 to the sample. The leakage of lipid vesicles was also measured with protein storage buffer. The plots are representation of two independent experiments.

a.

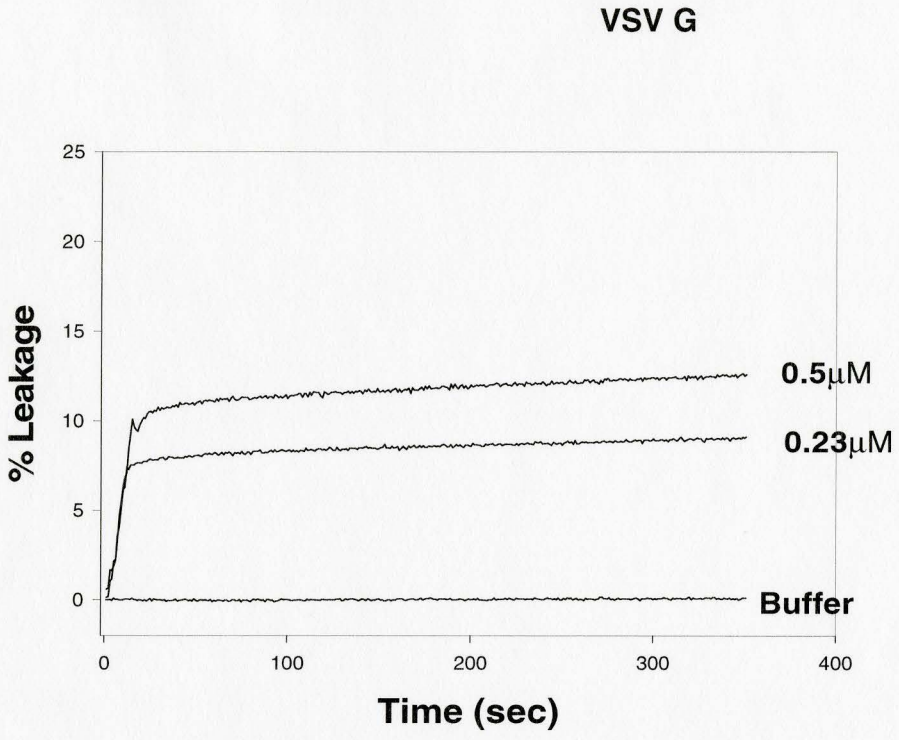
VSV G
% Leakage
25
20
15
10
5
0
0
100
200
300
400
Time (sec)
0.5μM
0.23μM
Buffer

b.

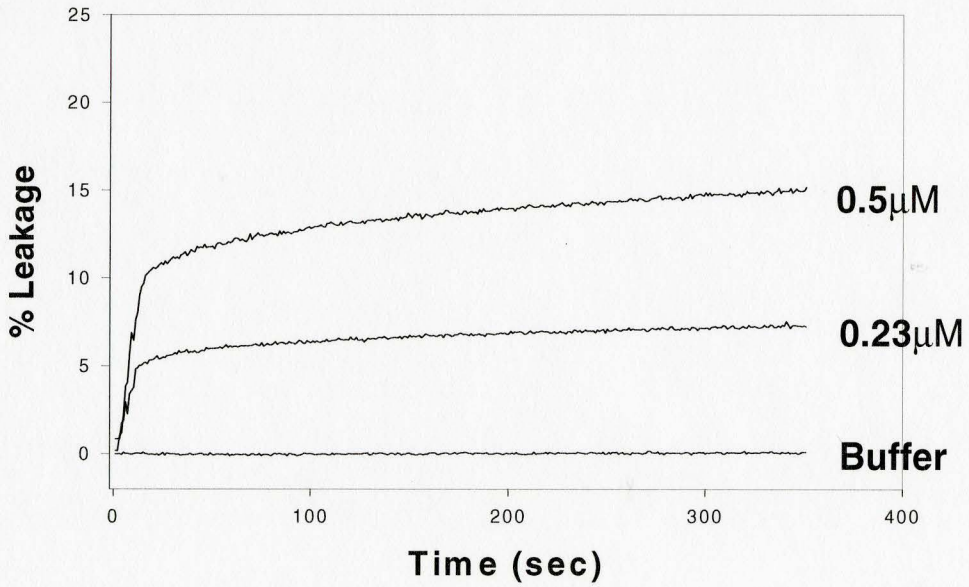
Gs
% Leakage
25
20
15
10
5
0
0
100
200
300
400
Time (sec)
0.5μM
0.23μM
Buffer

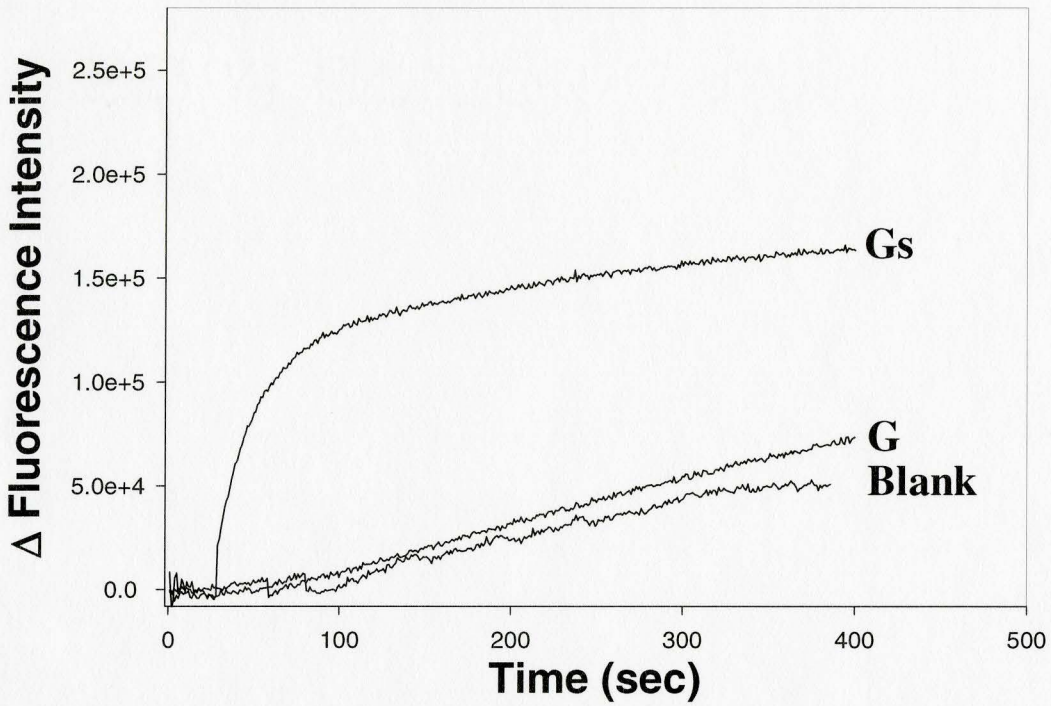

Fig. 18: Mixing of aqueous contents by Gs. ANTS entrapped SUV containing equimolar amount of PC and PS were mixed with five times excess of DPX entrapped SUV in 2ml of pH 5.4 buffer. ANTS fluorescence was recorded at excitation wavelength of 360nm and emission wavelength of 530nm using Photon technology international spectrofluoremeter. To that 0.5 μmole of VSV G or Gs was added and quenching of ANTS fluorescence was measured. The curves are representation of two independent experiments.

measured by the ANTS / DPX assay, which is based on the principle of collisional quenching of ANTS fluorescence by DPX. If ANTS and DPX are in close physical proximity to each other, the ANTS fluorescence is quenched by DPX. The ANTS and DPX were encapsulated in the same SUV, which resulted in quenching of ANTS fluorescence. After addition of fusion peptide the pH was lowered with 0.1 M citric acid. Leakage of liposome would result in dequenching of ANTS fluorescence, as the effective distance between ANTS and DPX will increase. The increase in ANTS fluorescence was measured at λ_{ex} 360 nm and λ_{em} 530 nm. 10% Triton X – 100 was added to induce 100% leakage. It was observed that both VSV G and Gs induced a considerable amount of liposome leakage and that the percentage of leakage increased with an increase in the protein concentration. The rate of leakage was extensive during the first 100 seconds (Fig. 17). The results indicate that VSV G and Gs mediated membrane fusion is leaky.

3.8 Mixing of aqueous content

Membrane fusion occurs through two main steps; in the first step hemifusion occurs, where the outer leaflets mix, which ultimately leads to a complete mixing of the aqueous content (Hernandez *et al.* 1996). It was observed from the RET assay that VSV G and Gs can induce lipid mixing, but it was not clear whether Gs is able to induce complete mixing of the material. It was also observed that

both VSV G and Gs exhibited rapid and extensive leakage of liposomes. As the rate of content mixing competes with vesicle leakage, it is unlikely that they will show any content mixing. The intermixing of aqueous content was measured by the ANTS / DPX assay. The ANTS and DPX were encapsulated in different population of SUV (Düzgünes and Wilschut 1993). The mixing of aqueous content will result in the interaction of ANTS and DPX, which will cause the dequenching of ANTS fluorescence. The SUVs containing ANTS were mixed with five times excess of DPX-entrapped SUV and allowed to fuse with VSV G or Gs; the decrease in ANTS fluorescence was then measured. It was observed addition of VSV G and Gs results in increase in ANTS fluorescence, which suggests that both VSV G and Gs could not induce any content mixing (Fig. 18). The nature of VSV G and Gs curves were different, it is possible due to the fact that VSV G might induce a very small amount of content mixing initially for a very brief period of time which results in slower increase in ANTS fluorescence.

3.9 Change in secondary structure

The VSV G protein undergoes reversible conformational change at low pH (Crimimins *et al.* 1983, Clague *et al.* 1990, Blumenthal *et al.* 1987, Puri *et al.* 1988). The conformational change of VSV G was attributed to the fact that the G protein becomes resistant to trypsin digestion at low pH (Fredericksen and Whitt 1996, Yao *et al.* 2003). To understand the extent of change in the conformation

of Gs at low pH, Gs was subjected to trypsin digestion at neutral and at fusion-active pH. The reaction was stopped with PMSF and samples were analyzed by SDS-PAGE. It was observed that trypsin completely digested Gs at neutral pH, but at fusion-active pH, Gs was resistant to trypsin digestion (Fig. 19). The digestive activity of trypsin at pH 5.4 was confirmed in the presence of 0.9% SDS. It was observed that trypsin cleaved Gs protein at pH 5.4 in the presence of SDS, indicating that resistance to trypsin digestion is actually due to pH-dependent conformational change of Gs.

Circular dichroism spectra at different pH were measured at 260 – 200 nm to determine the change in the secondary structure of Gs. The G protein exists in different conformations at neutral pH, at acidic pH in the absence of liposomes, and at acidic pH in the presence of liposomes (Pak *et al.* 1997). Therefore, CD spectra of Gs were determined both in the presence and in the absence of liposomes. The secondary structural content was calculated using the CONTINLL program (Sreerama 1999). Acidification resulted in significant changes in the CD spectrum of Gs in the presence and also in the absence of liposomes (Fig 20). The α– helix content increased with a decrease in pH, and it was observed that at pH 6, Gs had maximum helix content (Fig. 21). These results indicate that Gs protein undergoes structural rearrangement between pH 6.4 and 5. Cirular dichroism of VSV G protein showed that the VSV G protein undergoes structural rearrangement between pH 7.5 and 5 (Carneiro *et al.*

2001). Difference in CD spectra of VSV G at pH 7.5 and 5 indicates that the protein probably acquires a different conformation. To better understand the structure, we attempted to crystallize the Gs protein, but were unable to obtain any crystals (see addendum).

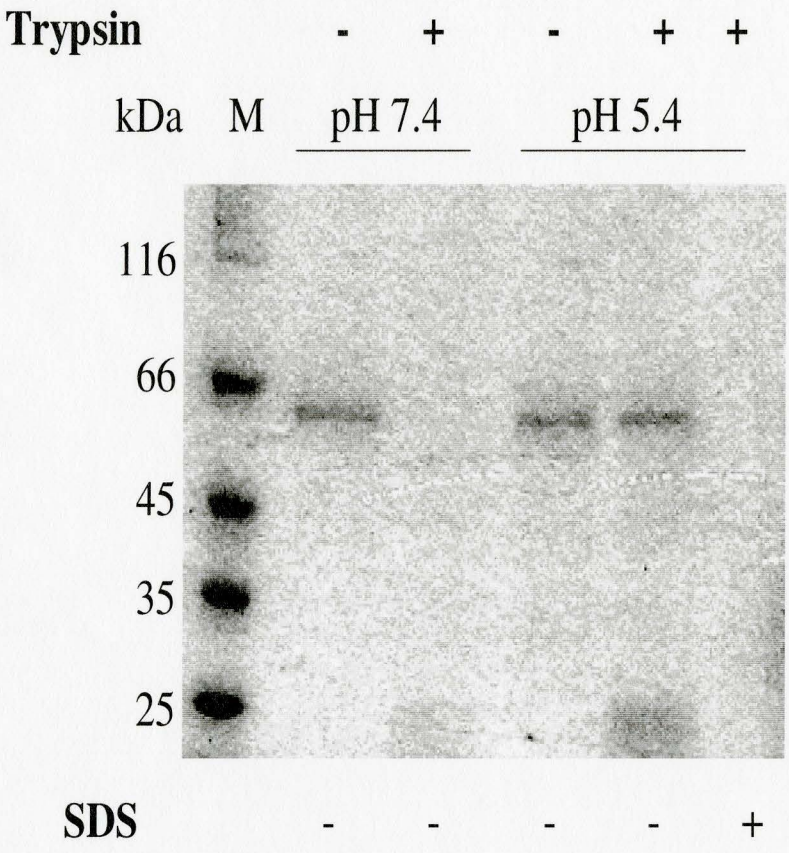

Fig. 19: Trypsin sensitivity assay to determine the structural change of Gs protein at acidic pH. Gs protein was incubated with trypsin (15:1; protein: trypsin) at 37°C for 30 min. in presence of 1% TritonX100 at pH 7.4 or 5.4. The activity of trypsin at pH 5.4 was tested by adding 0.9% SDS into the reaction mixture. The reaction was stopped with 5mM PMSF. The samples were analyzed on 10% SDS PAGE and protein bands were visualized after staining with coomassie blue stain. The gel is representative of two independent experiments.

Fig. 20: Effect of pH on circular dichroism spectra of Gs. CD spectra of Gs in presence of liposome containing equimolar amount of PC and PS (a) and in absence of liposome (b) was recorded at 25°C using a 1mm quartz cell at pH 7.4 (black), 6 (blue) or 5 (red). The Gs was diluted to 300μg/ml in phosphate buffer of respective pH. The plots are representative of two independent experiments.

a.

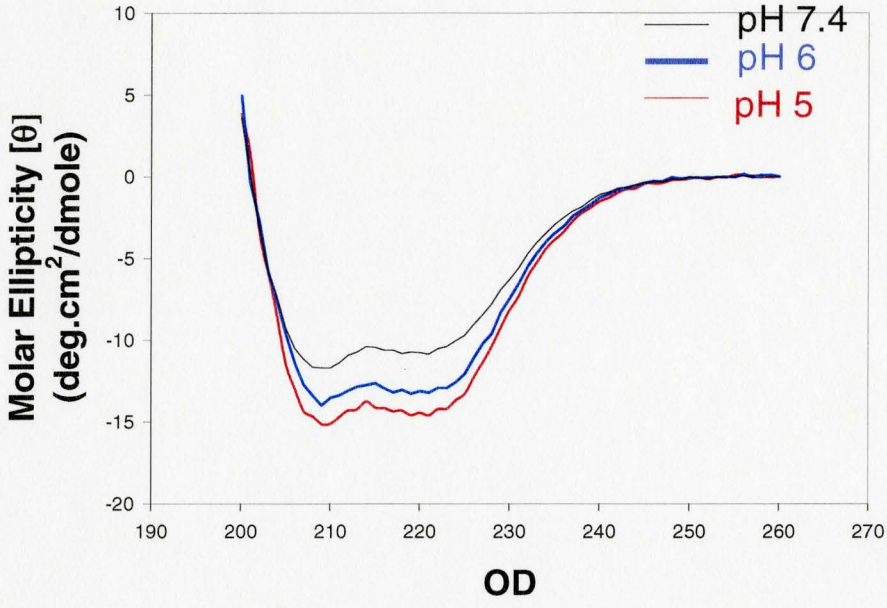
pH 7.4
pH 6
pH 5
Molar Ellipticity [θ]
(deg.cm²/dmole)
10
5
0
-5
-10
-15
-20
190
200
210
220
230
240
250
260
270
OD

b.

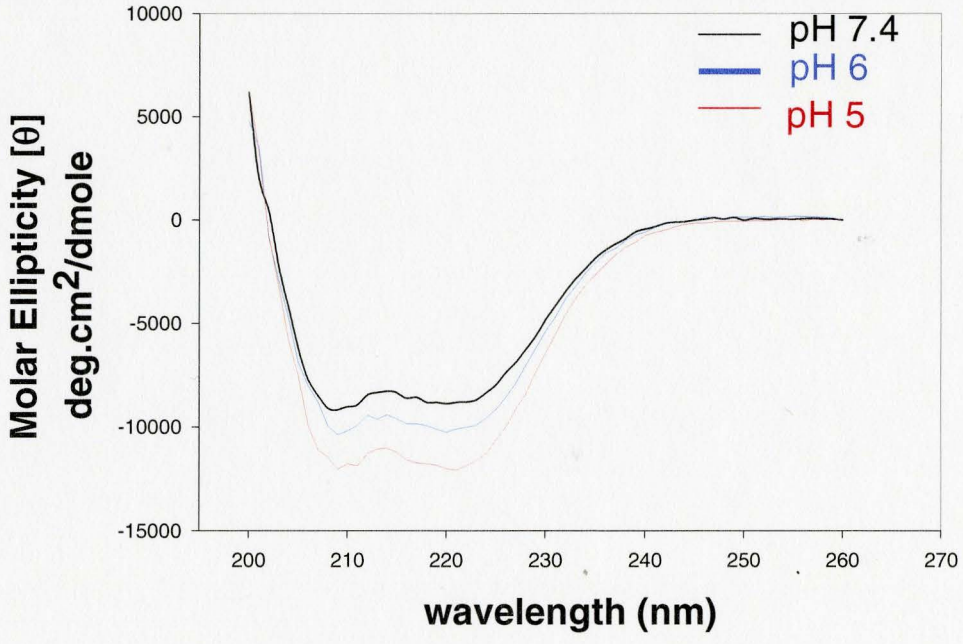
pH 7.4
pH 6
pH 5
Molar Ellipticity [θ]
deg.cm²/dmole
10000
5000
0
-5000
-10000
-15000
200
210
220
230
240
250
260
270
wavelength (nm)

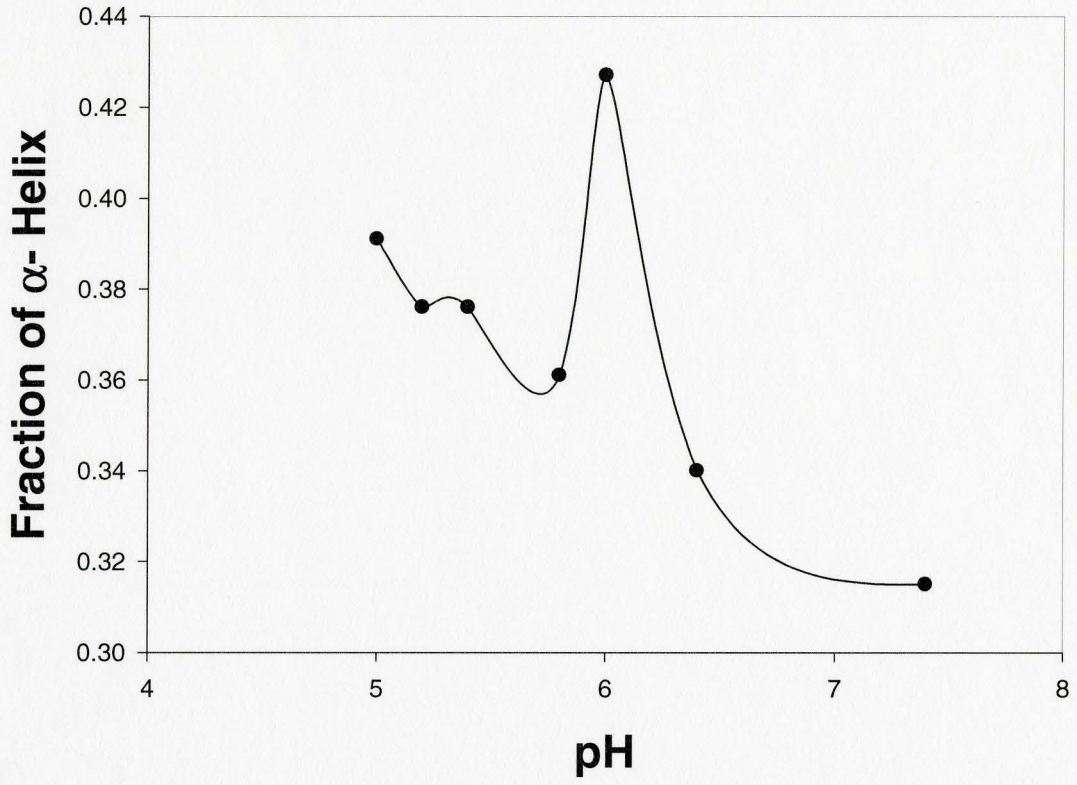

Fig. 21: Effect of pH on α – helix content of Gs protein. The CD spectra for Gs were determined at different pH at 25°C. The secondary structure was determined by CD Pro software using CONTINLL program (Sreerama 1999). Final concentration of protein was maintained at 300μg/ml.

4. DISCUSSION

Vesicular stomatitis virus glycoprotein G is the single viral membrane surface protein responsible for receptor binding and membrane fusion activity of VSV. Although impressive progress has been made to understand the structural bases of the acid induced fusion mechanisms of the influenza virus HA fusion peptide, TBE E, and SFV E1 glycoprotein, very little is known about the 3-D structure of VSV G glycoprotein. For influenza virus hemagglutinin (HA), 3-D structure of the neutral and acid pH forms have been solved (Wilson *et al.* 1981, Bullough *et al.* 1994). The influenza virus HA fusion peptide undergoes irreversible structural change at fusion active pH (Ruigrok *et al.* 1986, Carr *et al.* 1997). A coiled – coil mechanism has been proposed for the HA fusion peptide (Carr and Kim 1993), but no coiled – coil structure was predicted for the VSV G protein (Zhang and Ghosh 1994). Unlike all other fusion peptides, the VSV G protein does not have any hydrophobic fusion peptides; rather, the fusion peptide is neutral. However, the most striking difference between VSV G and other fusion proteins is its reversible structural change at low pH (Crimimins *et al.* 1983, Clague *et al.* 1990, Puri *et al.* 1988, Blumenthal *at al.* 1987). Membrane fusion is an energetically unfavorable process, and the energy is compensated by irreversible structural change from a metastable fusion inactive state to an energetically more stable form (Carr *et al.* 1997, Durrer *et al.* 1996, Skehel *et al.* 1982, Gaudin 2000). For VSV G, no kinetically trapped high energy metastable state has been reported;

rather, the fusion peptide conformational change is fully reversible (Yao *et al.* 2003, Crimimins *et al.* 1983). The thermal stability of G determined by Trp fluorescence and CD spectroscopy indicates that VSV G is equally stable at neutral and acidic pH (Yao *et al.* 2003). It has been suggested that about five trimers aggregate to form a big fusion complex, which may be required for the fusion process (Bundo – Morita *et al.* 1988). VSV has a class III fusion peptide (Yao *et al.* 2003), however, the VSV G protein shares many common features with other class II fusion proteins; for example, it has an internal fusion peptide, and the protein does not undergo any proteolytic maturation. Crystal structure indicates that most of the class II fusion proteins have a predominantly β– sheet structure (Rey *et al.* 1995, Lescar *et al.* 2001). However, like the influenza virus fusion protein, the VSV G protein exists as a trimer at neutral pH (Crise *et al.* 1989, Lyles *et al.* 1990). All these facts indicate that VSV G might employ a distinct fusion mechanism (Class III) from that of Class I and Class II fusion peptide (Gaudin 2000).

To further our understanding of VSV G mediated membrane fusion, the structure and function of the soluble ectodomain of VSV G has been studied. The soluble ectodomain of the VSV G glycoprotein (Gs) was generated by limited trypsin digestion. The soluble Gs obtained by cathepsin D digestion or Gs released in the VSV infected cells has a molecular weight 5000Da to 6000Da less than the mature molecule (Crimmins *et al.* 1983, Irving and Ghosh 1982, Chatis and

Morrision 1983). Tryptic fingerprinting analyses indicate that Gs lacks the C – terminal transmembrane domain (Irving and Ghosh 1982). The Gs protein obtained by limited trypsin digestion of VSV has an apparent molecular weight of 62kDa, whereas the intact G has a molecular weight of 67kDa. If we assume that the average molecular weight of an amino acid residue is 120Da, then the protein fragment released as indicated by SDS-PAGE would have nearly 48 amino acids less than the intact VSV G. Therefore, it is most likely that trypsin has possibly cleaved at Lys_{462}, a potential trypsin cleavage site near the transmembrane domain. The Gs was purified in milligram quantity, after treating the virus with trypsin at pH 5.4 in presence of 1.5% octylglucoside. The reversibility of the Gs protein structure at neutral pH was determined by trypsin digestion. The Gs protein was completely digested by trypsin at neutral pH, which suggests that the Gs protein has reverted back to its native conformation.

The biological activity of Gs protein was determined by monitoring its lipid binding property and its ability to induce membrane fusion. The biological activity and the accompanying structural change of the Gs protein have not been reported yet. The VSV G protein is responsible for the binding to the cellular receptor prior to infection. It has been reported that phosphatidylserine (PS) may play the role of receptor (Schlegel *et al.* 1983, Yamada and Ohnishi 1986). Atomic force spectroscopy experiments and inhibition of membrane binding at high ionic strength indicates that the interaction between G and PS is electrostatic in nature

(Carneiro *et al.* 2002). It has been suggested that negatively charged phospholipids in the cellular membrane are responsible for the initial binding of VSV G protein to the target membrane (Carneiro *et al.*2002). Increase in PS content of the liposomes increased the fusion efficiency remarkably; however, it did not change the binding profile of VSV G to the membrane. Therefore, for all experiments liposomes (SUV) were made up of phosphatidylserine (PS) and phosphatidylcholine (PC). It has been observed in liposome binding experiments that the Gs protein binds to the membrane in a pH-dependent manner. Although the Gs protein can bind to the membrane surface by electrostatic interaction, it does not penetrate the membrane unless the pH is lowered.

The oligomeric status of VSV G and pH-dependent aggregation has been studied in detail (Carneiro *et al.* 2001, Crise *et al.* 1989, Lyles *et al.* 1990, Zagouras and Rose 1993). It has been reported that the VSV G protein obtained after detergent solubilization or *in vivo*, exists in a dynamic equilibrium between the monomer and the trimer at neutral and low pH. However, the stability of the dimer and trimer increases at low pH. The cross linking of Gs with DTSSP suggests that the protein may exists as a monomer, dimer, and trimer at neutral as well as at fusion-active pH. Aggregation of Gs studied by light scattering showed that the Gs protein aggregates between pH 6.4 and 5. Aggregation of VSV G was observed between pH 6.6 and 5.6, which is mainly due to hydrophobic interactions (Carneiro *et al.* 2001). Increase in bis – ANS binding suggests that

the lowering of pH gradually exposes the hydrophobic domain of the VSV G protein (Carneiro *et al.* 2001). Exposure of hydrophobic residue with structural change for Gs was studied by quenching of the intrinsic Trp fluorescence by cis-PnA (Crimmins *et al.* 1983). Increased quenching of Trp fluorescence by cis-PnA at pH 5 indicates an increase in accessibility of the hydrophobic regions of Gs.

The TBE E protein forms a dimer at neutral pH and changes irreversibly to a trimer at fusion-active pH. Two distinctly different kinds of interactions are involved in stabilizing the dimer and trimer, respectively. The cd loop present at the tip of domain II of the TBE E protein is responsible for the stabilization of the dimer (Rey *et al.* 1995). In contrast, it has been proposed that the stem anchor region of TBE E protein (amino acid residues 400 – 450), which has the potential to form an α – helix structure, might play a critical role during trimerization (Stiasny *et al.* 1996, Allision *et al.* 1999). Based on the pattern of conserved Cys residues and structural characteristics of discontinuous antigenic sites, a similar loop structure at the fusion peptide region (118-136) has been predicted for the VSV G protein (Walker and Kongsuman 1999, Grigera *et al.*1992). A double mutation at F125YD411N and D137NG404A of VSV G protein resulted in a less stable trimer at low pH (Shokralla *et al.* 1999) suggesting that the stem region might be involved in the oligomerization of the G protein. Our results suggest that the Gs protein can form a trimer independently of the liposomal membrane. PHD structure analysis suggests an α – helical structure for the stem region of VSV G

protein between amino acid residues 395 and 482. Circular dichroism spectra in the presence of 2,2,2 – trifluoroethanol and NMR data obtained for the peptide correspond to the stem region (394 – 402) of the rabies virus G protein, suggesting that this region has the potential to form an α – helix structure (Maillard *et al.* 2003). In the case of the HA fusion glycoprotein, the interaction between the coiled - coil stem region from each HA1 subunit is responsible for the trimer stability (Wilson *et al.* 1981). Therefore, it could be possible that a similar kind of interaction between α- helix structures at the stem region (a.a 395 – 482) may be involved for the oligomerization of the VSV G protein.

Resonance energy transfer (RET) assay was employed to determine the membrane fusion activity of Gs. Carneiro *et al.* (2001) showed that the purified G protein could induce liposome fusion, but at a much reduced rate compared to the intact virus. The FHA2 fragment containing the influenza virus HA2 ectodomain could induce membrane fusion (Epand *et al.* 1999). Membrane interaction of the bromelain cleaved ectodomain of influenza virus HA (BHA) is also evident from photolabeling experiments (Harter *et al.* 1988, 1989, Durrer *et al.* 1996). The RET assay suggests that the Gs can also induce membrane fusion, although the extent of fusion is much less than the intact virus-induced membrane fusion. Earlier work done in our laboratory suggests that the G protein requires anchoring to the membrane through any hydrophobic peptide sequence for fusion activity (Odell *et al.* 1997). Replacements of G protein membrane

anchoring by a glycolipid anchor (glycosylphosphatidyl inositol) completely abolished polykarion formation at low pH in cells expressing the G protein, whereas replacement of the G protein transmembrane domain with other membrane-anchoring domains has no effect on membrane fusion activity. Our present results, however, suggest that the soluble ectodomain of the VSV G protein can induce lipid mixing. The RET assay shows that the extent of liposome fusion induced by full length VSV G and Gs are similar but much less compared to that of intact virus. This indicates that anchoring to the membrane is essential for efficient membrane fusion. In the case of influenza virus, HA fusion protein brings the opposing membrane to close proximity to facilitate membrane fusion (Hernandez *et al.* 1996). For VSV G, it has been proposed that a bigger fusion complex composed of large number of trimers of the fusogenic glycoproteins may be required to act in a concerted manner to drive the membrane fusion (Yao *et al.* 2003). Inability of the Gs protein to form a bigger fusion complex could be another limiting factor in determining fusion efficiency. In case of VSV G and Gs, the percentage of fusion also depends on the collisional frequency of the interacting liposomes. Therefore, it was assumed that increasing the aggregation would increase the collisional frequency, which in turn will improve the fusion efficiency. PEG, which is extensively used for cell – cell fusion, is the best candidate for this purpose. It has been reported that PEG could enhance the rate of gp 41 fusion peptide mediated membrane fusion (Haque and Lentz 2002). The peptide corresponding to transmembrane domain of VSV G (462 – 483) could

also induce fusion of PEG aggregated lipid vesicle (Dennison *et al.* 2002). It was observed that the addition of PEG dramatically improved the membrane fusion ability of the VSV G and Gs. In the presence of 5% PEG, the VSV G and Gs induced membrane fusion is comparable to that of the intact virus containing the same amount of G protein. The optimum fusion pH for Gs, however, shifted more towards the acidic side. The VSV G protein induced maximum fusion between pH 5.8 and 5.4, whereas Gs induced maximum fusion between pH 5.2 and 5; the optimum fusion pH for VSV has been reported to be between 5.8 and 5.4 (White *et al.* 1981). It has been reported that substitution of Phe-125 and Asp-137 with Tyr and Asn, respectively in the fusion peptide region, shifts the optimum fusion pH to a more acidic range (Zhang and Ghosh 1994, Fredericksen and Whitt 1996). It has been also observed that mutation in the carboxy terminal region (a.a 385 – 410) of the G protein effects the pH dependent membrane fusion (Shokralla *et al.* 1998). This indicates that the carboxy terminal region of VSV G (a.a 385 – 410) could play an important structural role during pH dependent membrane fusion. Recently, Jeetendra *et al.* (2003) showed that the juxtamembrane region of VSV G protein (a.a 440 – 461) is essential for the membrane fusion activity of VSV G. However, this region is not essential for oligomerization or transport of glycoprotein to the cell surface.

Our results showed that the VSV G and Gs mediated membrane fusion were leaky and none of the fusion glycoproteins could induce content mixing.

However, during content mixing it was observed that VSV G and Gs curve showed different patterns, which is possibly due to the fact that the VSV G protein may induce some content mixing for a very short period of time, resulting in a slow increase in ANTS fluorescence in comparison to Gs. The main limitation of content mixing is mainly the extensive vesicle leakage induced by the glycoprotein, as content mixing and vesicle leakage are in competition with each other. Our results suggest that Gs can induce lipid mixing but cannot induce complete mixing of aqueous contents. Jeetendra *et al.* (2003) reported that the membrane proximal domain (a.a 440-461) may be required for efficient membrane fusion. Requirement of transmembrane domain of VSV G during membrane fusion is evident from the inability of the GPI – anchored protein to induce polykarion formation in cells expressing the hybrid G proteins (Odell *et al.* 1997). The role of the transmembrane domain during membrane fusion is also evident from limited content mixing with the FHA2 fragment and the ability of the GPI – anchor ectodomain of HA to induce only hemifusion (Melikyan *et al.* 1995, Epand *et al.* 1999, Kemble *et al.* 1994).

The structural transition of VSV G depends on the protonation of His residue (Carneiro *et al.* 2003). Resistance to trypsin digestion at acidic pH suggests that the Gs protein undergoes conformational change at low pH. The trypsin cleavage sites, which were earlier- exposed at neutral pH, were no longer available at acidic pH. The structural change of Gs with decreasing pH was also evident form

the CD spectroscopy. It was observed that the helicity of the structure increased considerably with a decrease in pH. The maximum amount of α – helix content was observed at pH 6, which suggests that a structural rearrangement occurs at that pH. The change in conformation at this step possibly exposes the fusion peptide for the first time; otherwise, it is buried inside the molecule. A similar structural rearrangement has been reported for the VSV G between pH 6.4 and 6 (Carneiro *et al.* 2001).

Although all viral fusion peptides perform the same function, they have different structural features. An increasing amount of evidence suggests that the VSV G glycoprotein might adopt a completely different mechanism from that of known Class I and Class II fusion peptides and could therefore be classified as a Class III fusion glycoprotein. More detailed structural study of this protein will help us to understand the VSV G mediated fusion mechanism. Mutation experiments done in our laboratory and elsewhere suggest that the conserved uncharged residue between 117 – 139 might be involved in membrane fusion (Fredericksen and Whitt 1996, Li *et al.* 1993, Zhang and Ghosh 1994). Photolabeling experiments further suggest that the residue between amino acids 59 – 221of the G protein is involved in membrane fusion (Durrer *et al.* 1995). The synthetic fusion peptide designed against putative fusion peptide region of VSV G could interact with the artificial membrane in a pH dependent manner but no fusion activity of this peptide has been reported (Hall *et al.* 1998). However, a similar fusion peptide

did not show any membrane fusion activity, possibly due to the absence of the conserved Pro and Cys residue in the fusion peptide (Carneiro *et al.* 2003). It has been reported that the region between amino acid residues 145 – 168 of VSV G could be involved in the membrane fusion. Again fusion peptide designed corresponds to transmembrane domain (a.a 462 – 483) of VSV G protein could induce membrane fusion (Dennison *et al.* 2002, Langosch *et al.* 2001). It has been suggested that the transmembrane domain could act at the later step of membrane fusion (Langosch *et al.* 2001). Therefore, to obtain further insight into the role of the structural domain directly involved during membrane fusion, detailed structure and function studies should be carried out with different fragments of the VSV G ectodomain, particularly near the N – terminal region. Elucidation of the high resolution structure of the VSV G protein will be significant in understanding its fusion mechanism.

5. REFERENCES:

Allison S.L, Stiasny K, Stadler K, Mandl C.W and Heinz F.X. (1999). Mapping of functional elements in the stem- anchor region of Tick-borne encephalitis virus envelope protein. J. Virol. 73, 5605 – 5612.

Bailey C.A, Miller D.K and Lenard J. (1984). Effects of DEAE – dextran on infection and hemolysis by VSV evidence that nonspecific electrostatics interaction mediate effective binding of VSV to Cells. Virology 133, 111-118

Bailey M.J, McLeod D.A, Kang C and Bishop D.H.L. (1989). Glycosylation is not required for the fusion activity of the G protein of vesicular stomatitis virus in insect cells. Virology 169, 323 – 331.

Ball L.A and White C.N (1976). Order of transcription of genes of vesicular stomatitis virus. Proc. Natl. Acad. USA 73, 442 – 446.

Barbey-Martin C., Gigant B., Bizebard T., Calder L.J., Wharton S.A, Skehel J.J. and Knossow M. (2002). An antibody that prevent the hemagglutinin low pH fusion transition. Virology 294, 70 – 74.

Bhella R.S, Nichol S.T, Wanas E. and Ghosh H.P. (1998). Structure expression and phylogenetic analysis of the glycoprotein gene of Cocal virus. Virus Res. 54, 197 – 205.

Blumenthal R, Bali-Puri A, Walter A, Covell D. and Eidelman O. (1987). pH dependent fusion of vesicular stomatitis virus with vero cells. Measurement by dequenching of octadecyl rhodamine fluorescence. J. Biol. Chem. 262, 13614 – 13619.

Bullough P.A, Hughson F.H, Skehel J.J and Wiley D.C. (1994) Structure of influenza hemagglutitinin pH of membrane fusion. Nature 371, 37-43.

Bundo – Morital K., Gibson S. and Lenard J. (1988). Radiation inactivation analysis of fusion and hemolysis by vesicular stomatitis virus. Virology 163, 622 – 624.

Capone J, Leblance P, Gerber G.E. and Ghosh H.P. (1983). Localization of membrane proteins by the use of a photoreactive fatty acid incorporated in vivo into vesicular stomatis virus. J. Biol. Chem. 258, 1395-1398.

Capone J. and Ghosh H.P. (1984). Association of the nucleocapsid protein N of vesicular stomatitis virus with phospholipid vesicle containing the matrix protein M. Can J. Biochem Cell Biol. 62 , 1174 – 1180.

Capone J., Toneguzzo F. and Ghosh H.P. (1982). Synthesis and assembly of membrane glycoprotein membrane anchoring COOH-terminal domain of vesicular stomatitis virus envelope glycoprotein G contains fatty acids. J. Biol. Chem. 257, 16-19.

Carlsson J., Drevin H., and Axen R. (1978). Protein Thiolation and reversible protein-protein conjugation N-succinimidyl 3-(2-pyridyldithio) propionate, a new heterobifunctional reagent. Biochem. J. 173, 723-737.

Carneiro F.A, Ferradosa A.S and Da Poian A.T. (2001) Low pH induced conformational changes in vesicular stomatitis virus glycoprotein involve dramatic structure reorganization. J. Biol. Chem. 276, 62-67.

Carneiro F.A, Stauffer F, Lima C.S, Juliano M.A Juliano L and Da Poian A.T. (2003). Membrane fusion induced by vesicular stomatitis virus dependent on Histidine protonation. J. Biol. Chem 278, 13789-13794.

Carneiro F.A. Bianconi M.L, Weissmüller G., Stauffer F. and Da Poian A.T. (2002). Membrane recognition by vesicular stomatitis virus involves enthalpy- driven protein lipid interactions. J. Virol. 76, 3756-3764.

Carr C.M and Kim P.S (1993). A spring loaded mechanism for the conformational change of influenza hemagglutinin. Cell 73, 823 – 832.

Carr C.M., Chaudhry C. and Kim P.S. (1997). Influenza hemagglutinin is spring- loaded by a metastable native conformation. Proc. Natl. Acad. USA 94, 14306-14313.

Chan D.C, Fass D, Berger J.M. and Kim P.S. (1997). Core structure of gp41 from the HIV envelope glycoprotein. Cell 89, 263 – 273.

Chatis P.A. and Morrison T.G. (1983). Characterization of the soluble glycoprotein released from vesicular stomatitis virus infected cell. J. Virol. 45, 80-90.

Chen L., Colman P.M, Cosgrove L.J, Lawrence M.C, Lawrence L.J, Tulloch P.A and Gorman J.J. (2001). Cloning, expression and crystallization of the fusion protein of Newcastle disease virus. Virology 290, 290 – 299.

Chernimordik L.V, leikina E., Frolov V., Bronk P. and Zimmerberg J. An early stage of membrane fusion mediated by the low pH conformation of influenza hemagglutinin depends upon membrane lipids. J. Cell Biol. 136, 81-93.

Chernomordik L., Kozlov M.M., and Zimmerberg J. (1995). Lipids in biological membrane fusion. J.Membrane Biol. 146, 1-14.

Clague M.J, Knutson J.R, Blumenthal R and Herrmann A (1991). Interaction of influenza hemagglutinin amino terminal peptide with phospholipids vesicle: a fluorescence study. Biochemistry, 30, 5491 – 5497.

Clauge M.J, Schoch C, Zech Loren and Blumenthal R. (1990). Gating kinetics of pH activated membrane fusion of vesicular stomatitis virus with cells: stopped flow measurements by dequenching of octadectlrhodamine fluorescence. Biochemistry 29, 1303 – 1308.

Coll.J.M. (1995). The glycoprotein of rhabdoviruses. Arch Virol. 140, 827-851.

CollJ.M (1997). Synthetic peptide from the heptad repeats of the glycoproteins of rabies, vesicular stomatitis and fish rhabdovirus bind phosphatidylserine. Arch Virol 142, 2089-2097.

Crennell S, Takimoto T, Portner A and Taylor G. (2000). Crystal structure of the multifunctional paramyxovirus hemagglutinin neuraminidase. Nature struc. Biol. 7, 1098 – 1074.

Crimmins D.L, Mehard W B., and Schlesinger S. (1983) Physical properties of a soluble form of the glycoprotein of vesicular stomatitis virus at neutral and acidic. Biochemistry 22, 5790-5797.

Crise B., Ruusala A., Zagouras, P., Shaw, A. and Rose, J.K. (1989). Oligomerization of glycolipid- anchored and soluble forms of the vesicular stomatitis virus glycoprotein. J. Virol 63, 5328-5333.

Daniel P.S, Jeffries S, Yates P, Schild G.C, Rogers G.N, Paulson J.C, Wharton S.A, Douglas A.R, Skehel J.J. and Wiley D.C. (1987). The

receptor binding and membrane-fusion properties of influenza virus variants selected using anti-hemagglutinin monoclonal antibody. EMBO 6 ,1459 – 1465.

Dennison S.M, Greenfield N, Lenard J. and Lentz B.R. (2002). VSV transmembrane domain (TMD) peptide promotes PEG-mediated fusion of liposome in a conformationally sensitive fashion. Biochemistry 41, 14925 – 14934.

Doms R.W,Keller D.S, Helenius A. and Balch W.E. (1987). Role for adenosine triphosphate in regulating the assembly and transport of vesicular stomatitis virus G protein trimers. J. Cell Biol. 105, 1957 – 1969.

Durrer P, Galli C, Hoenke S, Corti C, Gluck R Vorherr Tand Brunner J. (1996). H^+ induced membrane insertion of influenza virus hemagglutinin involve the HA2 amino terminal fusion peptide but not the coiled coil region. J. Biol. Chem. 271, 13417 – 13421.

Durrer P., Gaudin Y, Ruigrok R.W.H., Graf R., Brunner J. (1995). Photolabeling identifies a putative fusion domain in the envelope glycoprotein of rabies and vesicular stomatitis viruses. J. Biol. Chem. 270, 17575-17581.

Durieu P. and Ochatt S.J. (2000). Efficient intergeneric fusion of pea (Pisum sativum L.) and grass pea (Lathyrus sativus L.) protoplast. J. Exp. Bot. 51, 1237 – 1242.

Düzgünes N and Wilschut J. (1993). Fusion assay monitoring intermixing of aqueous content. Method enzymology 220, 2 – 14.

Eckert D.M. and Kim P.S. (2001). Mechanism of viral membrane fusion and its inhibition. Ann. Rev. Biochem. 70, 777-810.

Ellen, H, Bentz, J and Szoka F.C (1985). H^+ and Ca^{2+} induced fusion and destabilization of liposomes. Biochemistry 24, 3099 – 3106.

Epand R.F, Macosko J.C, Russell C.J, Shin Y.and Epand R.M. (1999). The ectodomain of HA2 of influenza virus promotes rapid pH dependent membrane fusion. J.Mol.Biol 286, 489-503.

Epand R.M, Epand R.F, Marin I and Ruysschaert J.M. (2001). Membrane interaction of mutant form of the influenza fusion peptide. Biochemistry 40, 8800-8807.

Frangioni J.V and Neel B.G. (1993). Solubilization and purification of enzymatically active Glutathione S –Transferase (pGEX) fusion protein. Biochemistry 210, 179-187.

Fredericksen B.L and Whitt M.A . (1996). Mutation at two conserved acidic amino acids in the glycoprotein of vesicular stomatitis virus affect pH- dependent conformational changes and reduce the pH threshold for membrane fusion. Virology 217, 49-57.

Freed E.O and Martin M.A. (1995). The role of human immunodeficiency virus type 1 envelope glycoprotein in virus infection. J.Biol. Chem 270, 23883 – 23886.

Freed E.O, Myers D and Risser R. (1990). Characterization of fusion domain of the human immunodeficiency virus type 1 envelope glycoprotein gp41. Proc. Natl. Acad. USA 87, 4650 – 5654.

Garreis – Wabnitz C. and Kruppa J. (1984). Interacellular appearance of glycoprotein in VSV – infected BHK cells lacking the membrane – anchoring oligopeptide of the viral G – protein. EMBO J. 3, 1469 – 1476

Gaudier Martin, Gaudin Y, and Knossow M. (2002). Crystal structure of vesicular stomatitis virus matrix protein. EMBO J. 21, 2886-2892.

Gaudin Y, Ruigrok R.W.H and Brunner J. (1995). Low pH induced conformational changes in viral fusion proteins: implications for the fusion mechanism. J.Gen. Virol. 76, 1541-1556.

Gaudin Yves. (2000). Reversibility in fusion protein conformational changes the intriguing case of Rhabdovirus- induced membrane fusion. Subcell. Biochem. 34, 379-408.

Gething M.J, Doms R.W, York D and White J. (1986). Studies on the mechanism of membrane fusion: site-specific mutagenesis of the Hemagglutinin of influenza virus. J. Cell Biol. 1986 102, 11-23.

Gibbons D.L, Ahn A., Chatterjee P.K and Kielian M. (2000) Formation and characterization of the trimeric form of the fusion protein of semliki forest virus. J. Virol. 74, 7772-7780.

Gibbons D.L. and Kielian M. (2002). Molecular dissection of the semilki forest homotrimer reveals two functionally distinct region of the fusion protein. J.Virol. 76, 1194-1205.

Grigera P.R, Walter K, and Wagner R.R. (1992). Disulphide – bond discontinuous epitope on the glycoprotein of vesicular stomatitis virus (new jersey serotype). J.Virology 66, 3749-3757.

Hall M.P, Burson K.K. and Huestis W.H. (1998). Interaction of Vesicular stomatitis virus G protein fragment with phosphatidylserine: NMR and fluorescence studies. Biochemica at Biophysica Acta 1415 10-113.

Han X, Bushweller J.H, Cafiso D.S and Tamm L.K (2001). Membrane structure and function – triggering conformational change of the fusion domain from influenza hemagglutinin. Nature stru. Biol 8, 715 – 720.

Haque M.E. and Lentz B.R. (2002). Influence of gp 41 fusion peptide on the kinetics of poly(ethylene glycol)- mediated model membrane fusion. Biochem. 41, 10866 – 10876.

Harter C, Bachi T, Semenza G and Brunner J.(1988). Hydrophobic photolabeling identifies BHA2 as the subunit mediating the interaction of bromelain soluble influenza virus hemagglutinin with liposome at low pH. Biochemistry 27, 1856 – 1864.

Harter C, James P, Bachi T, Semeha G and Brunner J. (1989). Hydrophobic binding of the ectodomain of influenza hemagglutinin to membrane occurs through the fusion peptide. J. Biol. Chem 264, 6459 – 6464.

Heinz F.X and Allison S.L. (2000). Structure and mechanisms in flavivirus fusion. Adv. Virus Research 55, 231 – 269.

Heinz F.X and Allison S.L. (2001). The machinery for flavivirus fusion with host cell membranes. Curr. Opinion. Microbiol. 4, 450 – 455.

Heinz F.X, Mandl C.W, Holzmann H, Kunz C, Harris B.A, Rey Felix and Harrison S.C. (1991). The flavi virus envelope protein E: isolation of

a soluble form from tick born encephalitis virus and its crystallization. J. Virology 5579-5583.

Hernandez L.D, Hoffman L.R, Wolfsberg T.G and White J.M. (1996). Virus cell and cell-cell fusion. Annu. Rev. cell Dev. Biol. 12, 627-661.

Hoekstra D. and Düzgünes N (1993). Lipid mixing assay to determine fusion in liposome systems. Methods in Enzym. 220, 15-19.

Hoekstra D. and Düzgünes N. Lipid mixing assay to determine fusion in liposome systems. Methods in Enzym. 220, 15-19.

Hughson F.M. (1999). Membrane fusion: structure snared at last. Curr Biol 9, 49 – 52.

Irving R.A and Ghosh H.P. (1982). Shedding of vesicular stomatitis virus glycoprotein by removal of carboxy-terminal peptide. J.Virol. 42, 322-325.

Irving R.A, Toneguzzo F, Rhee S.H, Hofmann T., and Ghosh H.P. (1979) . Synthesis and assembly of membrane glycoprotein: Presence of leader peptide in nonglycosylated precursor of membrane glycoprotein of vesicular stomatitis virus. Proc. Natl. Acad. 76, 570-574.

Jeetendra E, Ghosh K, Odell D, Li j, Ghosh H.P and Whitt M. A. (2003). The membrane proximal region of vesicular stomatitis virus glycoprotein G ectodomain is critical for fusion and virus infection. J. Virology 77, 12807 – 12818.

Jeetendra E, Robison C.S, Albritton L.M and Whitt M.A. (2002). The membrane proximal domain of vesicular stomatitis virus G protein functions as a membrane fusion potentiator and can induce hemifusion. J. Virol. 76, 12300 – 12311.

Kemble G.W, danieli T. and White J.M. (1994). Lipid anchored influenza hemagglutinin promotes hemifusion, not complete fusion. Cell 76 383 – 391.

Kielian M (1995). Membrane fusion and the alphavirus life cycle. Adv. Virus Research 45, 113 – 149.

Kim G.N, Choi W.Y, Park M. and Kang C.Y. (2002). Replication and transcription of viral RNA by recombinant L proteins of New Jersey Serotype of vesicular stomatitis virus. 90, 347 –364.

Korte T, Epand R.F, Epand R.M and Blumenthal R. (2001). Role of the Glu residue of the influenza hemagglutinin fusion peptide in the pH dependence of fusion activity. Virology 289, 353 – 361.

Kreis T.E and Lodish H.F. (1986). Oligomerization is essential for the transport of vesicular stomatitis virus glycoprotein to cell surface. Cell 46, 929 – 937.

Krug R.M (1989). The influenza virus. New York: plenum press.

Laemmli U.K. (1970). Cleavage of structural proteins during the assembly of the head of bacteriophage T4. Nature 227, 680 – 685.

Langosh D, Brosig B. and Pipkorn R. (2001). Peptide mimics of the vesicular stomatitis virus G protein transmembrabne segment drive membrane fusion in vitro. J.B.C. 276, 32016 – 32021.

Lear J.D and deGarado W.F (1987). Membrane binding and conformational propertied of peptides representing the NH_2 terminus of influenza HA2. J. Biol. Chem 262, 6500 – 6505.

Lefrancois L. and Lyles D.S (1982). The interaction of antibody with the major surface glycoprotein of vesicular stomatitis virus. Virology 121, 157-167.

Lescar J. Roussel A., Wien M.W., Navaza J., Fuller S.D, Wengler G., Wengler G. and Rey F.A. (2001). The fusion glycoprotein shell of semliki forest virus: an icosahedral assembly primed for fusogenic activation at endosomal pH. Cell 105, 137-148.

Li Y, Drone C, Sat E and Ghosh H.P. (1993). Mutation analysis of the vesicular stomatitis virus glycoprotein G for membrane fusion domains. J.Virol. 67, 4070-4077.

Lomant A.J and Fairbanks G. (1976). Chemical probes of extended biological structures: synthesis and properties of the cleavable protein cross-linking reagent [^{35}S] Dithiobis(succinimidyl propionate). J.MolBiol. 104, 243-261.

Lorber B, Bishop J.B and DeLucas J.L (1990). Purification of octyl β–D-glucopyranoside and reestimation of its micellar size. Biochimica et Biophysica Acta 1023, 254-264.

Lu M, Blackow S.C and Kim P.S (1995). A trimeric structural domain of HIV – 1 transmembrane glycoprotein. Nature Struct. Biol 2, 1075 – 1082.

Lucast L.J., Batey R.T., and Doudna J.A. (2001). Large scale purification of a stable form of recombinant tobacco etch virus protease. Biotechniques 30, 544-554.

Lyles D.S., Varela V.A and Parce J.W. (1990). Dynamic nature of the quaternary structure of the vesicular stomatitis virus envelope glycoprotein. Biochem. 29, 2442-2449.

Maillard A, Domanski M, Brunet P, Chaffotte A, Guittet E and Gaudin Y (2003). Spectroscopic characterization of two peptides derived from the stem of rabies virus glycoprotein. Vitus resh 93, 151-158.

Melikyan G.B., White J.M. and Cohen F.S. (1995). GPI – anchored influenza Hemagglutinin induces hemifusion to both red blood cell and planer bilayer membrane. J. Cell Biol. 131, 679 – 691.

Mondigler M. and Ehrmann M. (1996). Site – specific proteolysis of Escherichia coli SecA protein In Vivo. J. Bacteriology 178, 2986 – 2988.

Moore J.P, McKeating J.A, Weiss R.A and Sattentau Q.A. (1990). Dissociation of gp 120 from HIV – 1 virion induced by soluble CD4. Science 250, 1139 – 1142.

Odell D, Wanas E, Yan J. and Ghosh H.P. (1997). Influence of membrane anchoring and cytoplasmic domains on the fusogenic activity of vesicular stomatitis virus glycoprotein G. J. Virol 71, 7996-8000.

Ohnishi S. (1988). Fusion of viral envelopes with cellular membrane. Curr. Top. Memb. Transp. 32: 257 – 296.

Pak C.C, Puri A, and Blumenthal R. (1997). Conformational changes and fusion activity of vesicular stomatitis virus glycoprotein: [^{125}I] Iodonaphthyl azide photolabeling studies in biological membranes. Biochemistry 36, 8890-8896.

PHD structure prediction program (2000). http://www.embl-heidelberg.de/predictprotein/predictprotein.html

Puri A, Winick J, Lowy R.J, Covell D, Eidelman O. and Walter A. (1988). Activity of vesicular stomatitis virus fusion with cells by pretreatment at low pH. J.B.C 263, 4749 – 4753.

Puri A, Grimaldi S and Blumenthal R. (1992). Role of viral envelope sialic acid in membrane fusion mediated by the vesicular stomatitis virus envelope glycoprotein. Biochemistry 31, 10108-10113.

Paternoster M.T, Lowy R.J. and Blumenthal R. (1989). pH dependent fusion of reconstituted vesicular stomatitis virus envelopes with vero cells. Measurement by dequenching of fluorescence. FEBS Lett. 243, 251 – 258.

Qiao H, Armstrong R.T, Melikyan G.B, Cohen F.S and White J.M. (1999). A specific point mutation at position 1 of the influenza Hemagglutinin fusion peptide displays a hemifusion phenotype. Mol. Biol. Cell 10, 2759-69.

Rafalski M., Ortiz A, Rockwell A, Ginkel L.C, Lear J.D., DeGrade W.F and Wilschut J. (1991). Membrane fusion activity of the influenza virus hemagglutinin: interaction of HA2 N- terminal peptide with phospholipids vesicles. Biochemistry 30, 10211 – 10220.

Rey F.A, Heinz F.X, Mandl C., Kunz C and Harrison S.C. (1995). The envelope glycoprotein from tick- born encephalitis virus at 2Åresolution. Nature 375, 291-298.

Ruigrok R.W.H., Martin C., Kunz C and Harison S.C. (1986). Conformational change in the hemagglutinin of influenza virus which accompany heat-induced fusion of virus with liposomes. Virology 155, 484-497.

Schlegel R, Tralka T.S., Willingham M.C., Pastan I. (1983). Inhibition of VSV binding and infection by phosphatidylserine: is phosphatidylserine a VSV binding site. Cell 32, 639-646.

Schnell M.J, Buonocore L., Borit E., Ghosh H.P Chernish R., and Rose J.K. (1998). Requirement for a non specific glycoprotein cytoplasmic domain sequence to drive efficient budding of vesicular stomatitis virus. EMBO J. 17, 1289-1296.

Shangguan T, Alford D and Bentz J (1996). Influenza virus liposome lipid mixing is leaky and largely insensitive to the material properties of the target membrane. Biochemistry 35, 4956-4965.

Shokralla S, Chernish R, and Ghosh H.P. (1999). Effects of double-site mutations of vesicular stomatitis virus glycoprotein G on membrane fusion activity. Virology 256, 119-129.

Shokralla S, He Y, Wanas E and Ghosh H.P. (1998). Mutations in a Carboxy-terminal region of vesicular stomatitis virus glycoprotein G that affect membrane fusion activity. Virology 242, 39-50.

Skehel J.J, Bayley P.M., Brown E.B, Martin S.R, Waterfield M.D, White J.M, Wilsin I.A and Wiley D.C. (1982). Changes in the conformation of influenza virus hemagglutinin at the pH optimum of virus-mediated membrane fusion. Proc. Natl. Acad. 79, 968-972.

Sreerama. N. (1999), CD Pro software. http://www.CDPro.html

Stegmann T, Delfino J.M, Richards FM and Helenivs A (1991). The HA2 subunit of influenza hemaglutinin inserts into the target membrane prior to fusion. J. Biol. Chem 266, 18404 – 18410.

Stiasny K, Allison S.L, Marchler – Bauer A, Kunz C and Heinz F.X. (1996). Structural requirements for low – pH induced rearrangements in the envelope glycoprotein of tick – born encephalitis virus. J. Virol 70, 8142 – 8147.

Stiasny K., Allison S.L, Mandl C.W. and Heinz F.X. (2001). Role of metastability and acidic pH in membrane fusion by tick born encephalitis virus. J. Virol. 75, 7392-7398.

Stiasny K., Allison S.L., Schalich J., and Heinz F.X. (2002). Membrane interactions of the tick borne encephalitis virus fusion protein E at low pH. J. Virol. 76, 3784-3790.

Struck D.K, Hoekstra D and Pagano R.E. (1981). Use of resonance energy transfer to monitor membrane fusion. Biochemistry 20, 14093-14099.

Talbot W.A, Zheng L.X and Lentz B.R (1997). Acyl chain unsaturation and vesicle curvature alter outer leaflet packing and promote polyethyleneglycol mediated membrane fusion. Biochemistry 36, 5827 – 5836.

Taube S.E and Braun P.C (1982). Structural study of Vesicular stomatitis virus G protein in the virion envelope. J. Virol 59, 319 – 327.

Toneguzzo F and Ghosh H.P. (1978). *In vitro* synthesis of vesicular stomatitis virus membrane glycoprotein and insertion into membrane. Proc. Natl. Acad. USA 75, 715 – 719.

Tsurudome M., Gluck R, Graf R, Falchetto Rocco, Schaller U and Brunner J. (1992). Lipid interaction of the hemagglutinin HA2 NH_2 – terminal segment during influenza virus induced membrane fusion. J. Biol Chem. 267, 20225 – 20232.

Vandepol S.B., Lefrancois L., and Holland J.J. (1986). Sequences of the major antibody binding epitopes of the Indiana serotypes of vesicular stomatitis virus. Virology 148, 312-325.

Walker P.J. and Kongsuman K. (1999). Deduced structural model for animal rhabdovirus glycoproteins. J.Gen. Virol. 80, 1211-1220.

Wangner R.R (1987). The Rahbdovirus. Plenum Press.

Wangner R.R. and Rose J.K. (1996). Fundamental virology. Raven publishers Phildelphia.

Wanitz G.C and Kruppa J. (1984). Intercellular appearance of a glycoprotein in VSV-infected BHK cells lacking the membrane- anchoring oligopeptide of the viral G-protein. The EMBO J. 3, 1469-1476.

Wengler G, Wengler G and Rey Felix. The isolation of the ectodomain of the alphavirus E1 protein as a soluble Hemagglutinin and its crystal. Virology 257, 472 – 482 (1999).

Wharton S.A, Martin S.R, Ruigrok R.W.H, Skehel J.J and Wiley D.C (1988). Membrane fusion peptide analogues of influenza virus hemagglutinin. J. Gen virol 69, 1847 – 1857.

Wharton S.A, Ruigork R.W.H, Martin S.R, Skehel J.J, Bayley P.M. Weis W and Wiley D.C. (1988). Conformational aspects of the acid-induced fusion mechanism of influenza virus Hemagglutinin. JBC 263, 4474 – 4480.

White J, Matlin K., and Helenius A. (1981). Cell fusion by semliki forest, Influenza and Vesicular stomatitis virus. J. Cell Biol. 89, 674-679.

White J.M (1992). Membrane fusion. Science 258, 917 – 924.

Whitt,M.A, Zagouras P, Crise B, and Rose J.K. (1990). A fusion defective mutant of the vesicular stomatitis virus glycoprotein. J. Virol. 64, 4907 – 4913.

Wilcox M.D, McKenzie M.O, Parce J.W and Lyles D.S. (1992). Subunit interactions of vesicular stomatitis virus envelope glycoprotein influenced by detergent micelles and lipid bilayers. Biochem. 31, 10458-10464.

Wiley D.C (1998). Conformational aspect of the acid induced fusion mechanism of influenza virus hemagglutinin. J. Biol. Chem 263, 4474 – 4480.

Wiley D.C and Skehel J.J (1987). The structure and function of the hemagglutinin membrane glycoprotein of influenza virus. Ann. Rev. Biochem 56, 365 – 94.

Wilson T.A, Skehel J.J and Wiley D.C (1981). Structure of the hemagglutinin membrane glycoprotein of influenza virus at 3Å resolution. Nature 289, 366 – 373.

Yamada S. and Ohnishi S.I. (1986). Vesicular stomatitis virus binds and fuses with phospholipids domain in target cell membranes. Biochem. 25, 3703 – 3737.

Yao Y, Ghosh K, Epand R.F, Epand R.M and Ghosh H.P. (2003). Membrane fusion activity of vesicular stomatitis virus glycoprotein G is induced by pH but not by heat or denaturant. Virology 310, 319 - 332.

Zagouras P and Rose J.K. (1993).Dynamic equilibrium between vesicular stomatitis virus glycoprotein monomers and trimers in the golgi and at the cell surface. J. Virol. 67, 7533-7538.

Zhang L. and Ghosh H.P. (1994). Characterization of the putative fusogenic domain in vesicular stomatitis virus glycoprotein G. J.Virol 68, 2186-2193.

6. ADDENDUM

6.1 Crystallization of soluble Gs

The high-resolution crystal structure of influenza virus HA both at neutral and fusion active pH, TBE E protein, and SFV glycoprotein have helped to understand the fusion mechanism of class I and class II fusion proteins (Bullough *et al.* 1994, Wilson *et al.* 1981, Lescar *et al.* 2001, Rey *et al.* 1995). The CLUSTALW multiple sequence alignment program showed no sequence homology between TBE E and VSV G proteins. The secondary structure of the VSV G glycoprotein, predicted by the PHD program, showed that the β – sheets are the predominating structure, but α – helix structures are also present in substantial amounts, whereas in the case of TBE E glycoprotein, β – sheets are the only predominating structures. To get further insight into the structure of VSV G, we attempted to crystallize the soluble ectodomain of VSV G released by restricted trypsin digestion.

For large-scale virus production, VSV Indiana was grown in BHK 21 cell lines in 36 150-mm plates, and the virus was purified as described in the Materials and Methods (2.13). Large-scale Gs was prepared by trypsin cleavage as described in the Materials and Methods (2.17). Impurities left after the sephadex column were removed by using a Q – Column (Dr. Murray Junop, McMaster University).

The fractions containing Gs obtained from the sephadex column were pooled and adjusted to 0.5% octylglucoside and 100 mM NaCl. The Gs was then loaded onto a 5-ml Q – column (Pharmacia), pre-equilibrated with 50 mM tris pH 8 and 100 mM NaCl containing 0.5% octylglucoside. A small amount of detergent (concentration less than CMC) was required for the efficient elution of Gs from the Q – column. In the absence of detergent, Gs cannot be eluted even with 1M NaCl. Therefore, Gs was eluted by running a linear NaCl gradient containing 0.5% octylglucoside. The protein was eluted between 300 – 350 mM NaCl and also at 500 mM and 1M NaCl concentrations. The fractions collected between 300 – 350mM NaCl were pooled, and the salt concentration was adjusted to 180 mM NaCl. For the initial crystal trial, the protein was concentrated to 4 mg/ml and set for crystal screening at different conditions using HAMSTAN I / II and a Sigma Membrane crystallization kit at 4°C. Detailed crystallization conditions are summarized in Table – I, Table – II, and Table – III. The hanging drop vapor diffusion method was used for the crystallization, as this method has been successfully used for crystallization of other class II fusion proteins. For typical crystal screening, 1 μl of concentrated protein was mixed with 1 μl of screening buffer and set for crystallization. The initial crystal trial did not yield any crystal.

Table – I. Summary of the crystal trial using a Sigma Membrane Kit

Crystal screening buffer	Crystal
1. Na-chloride 0.1M, Na-acetate (pH4.6) 0.1M, 2-methyl-2,4-pentanediol 12%	No
2. Zn-acetate 0.1M, Na- acetate (pH4.6) 0.1M, PEG4000 12%	No
3. NH_4-sulfate 0.2M, Na-acetate (pH4.6) 0.1M, PEG 4000 10%	No
4. Na-chloride 0.1M, Na acetate (pH4.6) 0.1M, 2-propanol 12%	No
5. Na - acetate (pH4.6) 0.1M, PEG4000 12%	No
6.NH_4-sulfate 1M, Na acetate (pH4.6) 0.1M	No
7. Mg-sulfate 1M, Na acetate (pH4.6) 0.1M	No
8. Mg-chloride 1M, Na acetate (pH4.6) 0.1M, PEG 400 18%	No
9. NH_4- dihydrogenphosphate 1M, Li-sulfate 0.1M, Na acetate (pH4.6) 0.1M	No
10. Na-chloride 0.1M, Na acetate (pH4.6) 0.1M, PEG6000 12%	No
11. Mg-chloride0.1M, Na acetate (pH4.6) 0.1M, PEG 6000 12%	No
12. Na-chloride 0.1M, Na-citrate (pH5.6) 0.1M, PEG 400 18%	No
13. Li-sulfate 0.1M, Na-citrate (pH5.6) 0.1M, PEG 4000 12%	No
14. Na-citrate (pH5.6) 0.1M, 2-propanol 10%	No
15. Na-chloride 0.1M, Na-citrate (pH5.6) 0.1M, 2-methyl-2,4-pentanediol 12%	No
16. Mg-sulfate 1M, Na-citrate (pH5.6) 0.1M.	No
17.Na-chloride 0.1M, Na-citrate (pH5.6) 0.1M, PEG 4000 12%	No
18. Li-sulfate 0.1M, Na-citrate (pH5.6) 0.1M, PEG 6000 12%	No
19. Mg-chloride 0.1M, Na-citrate (pH5.6) 0.1M, 2-methyl-2,4-pentanediol 4%	No
20. Na-chloride 0.1M, Na-citrate (pH5.6) 0.1M.	No
21. Li-sulfate 0.1M Na-citrate (pH5.6) 0.1M, PEG 400 4%	No
22. NH_4-sulfate 1M, ADA (pH6.5) 0.1M	No
23. Li-sulfate 0.1M, ADA (pH6.5) 0.1M, 2-propanol 2%, PEG 4000 12%	No
24. NH4-dihydrogenphosphate 1M, ADA (pH6.5) 0.1M	No
25. Mg- chloride 0.1M, ADA (pH6.5) 0.1M, PEG 6000 12%	No
26. ADA (pH6.5) 0.1M, 2-methyl-2,4-pentanediol	No
27. Mg-sulfate1M, Li-sulfate 0.1M, ADA (pH6.5) 0.1M	No
28. Li-sulfate 0.3M, ADA (pH6.5) 0.1M, 2-propanol 2%, PEG 400 4%	No
29. K-,Na-hydrogenphosphateeach 0.5M, NH_4-sulfate, HEPES Na-salt (pH7.5) 0.1M	No
30. Na-chloride 0.1M, , HEPES Na-salt (pH7.5) 0.1M, PEG 4000 10%	No
31. Mg-chloride 0.1M, , HEPES Na-salt (pH7.5) 0.1M, PEG 400 18%	No
32. K-, Na – tartrate 0.1M, HEPES Na-salt (pH7.5) 0.1M.	No
33. NH_4-sulfate 0.1M, , HEPES Na-salt (pH7.5) 0.1M, PEG 400 18%	No

34. NH_4-sulfate 0.1M, , HEPES Na-salt (pH7.5) 0.1M, PEG 4000 10%	No
35 Na-citrate 0.1M, HEPES Na-salt (pH7.5) 0.1M, 2-methyl –2,4-pentanediol 12%.	No
36. Na-citrate 1M, , HEPES Na-salt (pH7.5) 0.1M	No
37. Mg-sulfate 0.6M, , HEPES Na-salt (pH7.5) 0.1M, PEG 400 4%	No
38. Mg-sulfate 0.6M, HEPES Na-salt (pH7.5) 0.1M, 2-methyl-2, 4-pentanediol 4%.	No
39. K-,Na-tartrate 0.1M, Li-sulfate 0.1M HEPES Na-salt (pH7.5) 0.1M	No
40. Na-chloride 0.15M, TRIS-HCl (pH8.0) 0.1M, PEG 6000 12%	No
41. Na –chloride 0.1M, TRIS-HCl (pH8.0) 0.1M, 2-methyl-2,4-pentanediol 12%	No
42. Li-sulfate 0.1M, TRIS-HCl (pH8.0) 0.1M, 2-methyl-2,4-pentanwdiol 12%	No
43. K-,Na-hydrogenphosphate each 0.5M, NH_4-hydrogenphosphate 0.1M, TRIS-HCl (pH8.0) 0.1M	No
44. Na-acetate 0.1M, TRIS-HCl (pH8.0) 0.1M	No
45. Na-chloride 0.1 M, TRIS-HCl (pH8.0) 0.1M	No
46. NH_4-hydrogenphosphate 0.1M, TRIS-HCl (pH8.0) 0.1M, PEG 6000 12%	No
47. K-,Na-tartrate 0.1M, Mg-sulfate 0.4M, TRIS-HCl (pH8.0) 0.1M	No
48. Li-sulfate 0.2M, TRIS-HCl (pH8.0) 0.1M	No
49. NH_4-sulfate 0.5M, TRIS-HCl (pH8.0) 0.1M	No
50. Na-citrate 0.1M, TRIS-HCl (pH8.0) 0.1M, PEG 400 5%	No

Table – II. Summary of crystal trial using Hampton 2 Kit

Crystal screening buffer	Crystal
1. 10% PEG 6000, 2.0M sodium chloride	No
2. 0.5M sodium chloride, 0.1 M CTAB, 0.1M Magnesium Chloride	No
3. 25% ethylene glycol	No
4. 35% Dioxane	No
5. 5% iso-propanol, 2.0M ammonium sulfate	No
6. 1.0M Imidazole pH 7.0	No
7. 10%PEG 1000, 10% PEG 8000	No
8. 10%Ethanol, 1.5M sodium chloride	No
9. 2.0M Sodium chloride, 0.1M Na-acetate (pH 4.6)	No
10. 30% MPD, 0.1M Na-acetate (pH 4.6), 0.2 M Sodium chloride	No
11. 1.0M 1,6 Hexanediol, 0.1M Na-acetate (pH 4.6), 0.01M cobaltchloride	No
12. 30% PEG 400, 0.1M Na-acetate (pH 4.6), 0.1M Cadmium chloride	No
13. 30% PEG MME 2000, 0.1M Na-acetate (pH 4.6), 0.2M Ammonium sulfate	No
14. 2.0M Ammonium sulfate, 0.1M Na-Citrate (pH 5.6), 0.2 M K/Na tartrate	No
15. 1.0M Li-sulfate, 0.1M Na-Citrate (pH 5.6), 0.5M ammonium sulfate	No
16. 2%Polyethyleneimine, 0.1M Na-Citrate (pH 5.6), 0.5M Na-chloride	No
17. 35%tert-butanol, 0.1M Na-Citrate (pH 5.6)	No
18. 10%Jeffamine M-600, 0.1M Na-Citrate (pH 5.6), 0.01M Ferric chloride	No
19. 2.5M1.6 Hexanediol, 0.1M Na-Citrate (pH 5.6)	No
20. 1.6M Mg-sulfate, 0.1M MES pH (6.5)	No
21. 2.0M Na-chloride, 0.1M MES pH (6.5), 0.2 M Na/ K phosphate	No
22. 12% PEG 20,000, 0.1M MES pH (6.5)	No
23 10% Dioxane, 0.1M MES pH (6.5), 1.6M ammonium sulfate	No
24. 30% jeffamine M – 600, 0.1M MES pH (6.5), 0.05M Cs-chloride	No
25. 1.8M Ammonium chloride, 0.1M MES pH (6.5), 0.01M Co-chloride	No
26. 30% PEG MME 5000, 0.1M MES pH (6.5), 0.2M ammonium sulfate	No
27. 25% PEG MME 550, 0.1M MES pH (6.5), 0.01Zn-sulfate	No
28. 1.6 M Na-citrate (pH 6.5)	No
29. 30%MPD, 0.1 M HEPES (pH 7.5), 0.5M ammonium sulfate	No
30. 10% PEG 6000, 0.1 M HEPES (pH 7.5), 5%MPD	No
31. 20% Jeffamine M – 600, 0.1 M HEPES (pH 7.5)	No
32. 1.6 M ammonium sulfate, 0.1 M HEPES (pH 7.5), 0.1M Na-chloride	No
33. 2.0M Ammonium formate, 0.1 M HEPES (pH 7.5)	No
34. 1.0M Sodium Acetate, 0.1 M HEPES (pH 7.5), 0.05M Cd – sulfate.	No
35. 70% MPD, 0.1 M HEPES (pH 7.5)	No

36. 4.3M Na- chloride, 0.1 M HEPES (pH 7.5)	No
37. 10% PEG 8000, 0.1 M HEPES (pH 7.5), 8% Ethylene glycol	No
38. 20% PEG 10,000, 0.1 M HEPES (pH 7.5)	No
39. 3.4M1,6 Hexanediol, 0.1M TRIS-HCl (pH 8.5), 0.2M Mg-chloride	No
40. 25% tert-Butanol, 0.1M TRIS-HCl (pH 8.5)	No
41. 1.0M Li-sulfate, 0.1M TRIS-HCl (pH 8.5), 0.01M Ni(II)-chloride	No
42. 12% Glycerol, 0.1M TRIS-HCl (pH 8.5), 1.5M ammonium sulfate	No
43. 50% MPD, 0.1M TRIS-HCl (pH 8.5), 0.2M ammonium phosphate	No
44. 20% Ethanol, 0.1M TRIS-HCl (pH 8.5)	No
45. 20% PEG MME 2000, 0.1M TRIS-HCl (pH 8.5), 0.01M Ni(II)chloride	No
46. 20% PEG MME 550, 0.1M Bicine (pH 9.0), 0.1 M Na-chloride	No
47. 2.0M Mg-chloride, 0.1M Bicine (pH 9.0)	No
48. 10% PEG 20,000, 0.1M Bicine (pH 9.0), 2% Dioxane.	No

Table – III. Summary of crystal trial using Hampton 1 Kit

Crystal screening buffer	Crystal
1. 30% MPD, 0.1M acetate pH 4.6, 0.02 M Ca- chloride	No
2. 0.4M K, Na tartrate	No
3. 0.4M Ammonium phosphate	No
4. 2.0M ammonium sulfate, 0.1M TRIS-HCl pH 8.5	No
5. 30% MPD, 0.1 M Na HEPES pH 7.5, 0.2 M Na-citrate	No
6. 30% PEG 4000, 0.1M TRIS HCl pH 8.5, 0.2 M Mg-chloride	No
7. 1.4M Na-acetate, 0.1M Na-cacodylate pH 6.5	No
8. 30% iso-propanol, 0.1M Nacacodylate pH 6.5, 0,2M Na- citrate	No
9. 30% PEG 4000, 0.1M Na citrate pH 5.6, 0.2M ammonium acetate	No
10. 30% PEG 4000, 0.1M Na-acetate pH 4.6, 0.2 M ammonium acetate	No
11. 1.0M ammonium phosphate, 0.1 Na citrate pH 5.6	No
12. 30% iso-propanol, 0.1M Na-HEPES pH7.5, 0.2M Mg-chloride	No
13.30%PEG 400, 0.1M TRIS-HCl pH 8.5 , 0.2M Na-citrate	No
14. 28% PEG 400, 0.1 M Na HEPES pH 7.5, 0,2M Ca-chloride	No
15. 30%PEG 8000, 0.1M Na-cacodylate pH 6.5, 0.2M ammonium sulfate	No
16. 1.5 M Li-sulfate, 0.1M Na-HEPES pH7.5	No
17. 30% PEG 4000, 0.1 M TRIS-HCL pH 8.5, 0.2M Li-sulfate	No
18. 20% PEG 8000, 0.1M Na- cacodylate pH 6.5, 0.2 M ma-acetate	No
19. 30% iso-propanol, 0.1M TRIS-HCl pH 8.5, 0.2M ammonium acetate	No
20. 25% PEG 400, 0.1M Na-acetate pH 4.6, 0.2M ammonium sulfate	No
21. 30%MPD, 0.1M Na cacodylate pH 6.5, 0.2M Mg-acetate	No
22. 30% PEG 4000, 0.1M TRIS – HCl pH8.5. 0.2 M sodium acetate	No
23 30% PEG 400, 0.1 M Na HEPES pH 7.5, 0.2 M Mg-chloride	No
24. 20% iso-propanol, 0.1M Na-Acetate pH 4.6, 0.2M Ca-chloride	No
25. 1.0M Na-acetate, 0.1M imidazole pH 6.5	No
26. 30% MPD, 0.1 M Na citrate pH 5.6, 0.2 M ammonium acetate	No
27. 20% iso-propanol, 0.1 M Na HEPES pH 7.5, 0.2 M Na citrate	No
28. 30% PEG 8000, 0.1M Na cacodylate pH 6.5, 0.2 M Na- acetate	No
29. 0.8M K,Na tartrate, o.1M Na HEPES pH 7.5	No
30. 30% PEG 8000, 0.2M ammonium sulfate	No
31. 30% PEG 4000, 0.2M ammonium acetate	No
32. 2.0M ammonium sulfate	No
33. 4.0M Na-formate	No
34. 2.0M Na-formate, 0.1M Na acetate pH 4.6	No
35. 1.6M Na,K phosphate, 0.1M Na HEPES pH 7.5	No
36. 8% PEG 8000, 0.1M TRIS – HCl pH 8.5	No
37. 8% PEG 4000, 0.1 M Na acetate pH 4.6	No

38. 1.4M Na-citrate, 0.1 M Na HEPES pH 7.5	No
39. 2% PEG 400, 0.1M Na HEPES pH 7.5, 2.o M ammonium sulfate	No
40. 20% iso-propanol, 0.1M Na citrate pH 5.6, 20% PEG 4000	No
41. 10% iso- propanol, 0.1M Na-HEPES pH 7.5, 20% PEG 4000	No
42 20%PEG 8000, 0.05M Potassium phosphate	No
43. 30% PEG 1500	No
44. 0.2 M Mg-formate	No
45. 18% PEG 8000, 0.1M Nacacodylate pH 6.5, 0.2M Zn-acetate	No
46. 18% PEG 8000, 0.1M Na cacodylate pH 6.5, 0.2M ca-acetate	No
47. 2.0M ammonium sulfate, 0.1 M Na-acetate pH 4.6	No
48. 2.0M ammonium phosphate, 0.1M TRIS HCL pH 8.5	No
49. 2% PEG 8000, 1.0 Li-sulfate	No
50. 15% PEG 8000, 0.5M Li-sulfate	No